Dissertation zur Erlangung des Doktorgrades
der Fakultät für Chemie und Pharmazie der
Ludwig-Maximilians-Universität München

Advanced mesenchymal stem cell-mediated gene delivery of the theranostic sodium iodide symporter (NIS) in non-thyroidal tumors

Christina Schug

aus

Penzberg, Deutschland

2018

Erklärung

Diese Dissertation wurde im Sinne von § 7 der Promotionsordnung vom 28. November 2011 von Frau Professor Dr. C. Spitzweg betreut und von Herrn Professor Dr. E. Wagner vor der Fakultät für Chemie und Pharmazie vertreten.

Eidesstattliche Versicherung

Diese Dissertation wurde eigenständig und ohne unerlaubte Hilfe erarbeitet.

München, 07.12.2018

Christina Schug

Dissertation eingereicht am	16.10.2018
1. Gutachter:	Prof. Dr. Ernst Wagner
2. Gutachterin:	Prof. Dr. Christine Spitzweg
Mündliche Prüfung am	27.11.2018

Table of contents

1. Introduction

1.1 Cancer

Cancer is the second leading cause of death in the Western world. The four cancer types that are responsible for the largest number of deaths worldwide are lung, liver, stomach and colon, whereas in developed countries, breast, prostate and pancreas carcinoma are a major concern [1, 2].

1.1.1 Cancer biology

Carcinogenesis develops in a multistep process. Malignant tumors are characterized by fast proliferation and the ability to migrate and invade to other tissues. Hanahan and Weinberg defined the hallmarks of cancer describing the capabilities a cell must acquire to undergo the multistep development of tumors. These hallmarks include: advantages in the proliferative behavior of tumor cells, evading growth suppressors and eluding apoptosis, enabling replicative immortality, fostering angiogenesis, enhancing the ability of the tumor to invade and metastasize into other tissues and organs as well as escaping the immune system and deregulating cellular energetics [3]. In addition to these hallmarks, two consequential characteristics were defined: genome instability and mutation, and tumor-promoting inflammation [3].
The resulting tumor mass consists not only of tumor cells, but is also comprised by a variety of normal cells, such as fibroblasts and myofibroblasts, pericytes, epithelial, vascular and immune cells, secreted factors and the extracellular matrix (ECM), which interact with the malignant cells, and are collectively referred to as the tumor stroma [4-6]. Over the last few years, the tumor stroma has emerged as an important target for the development of innovative anticancer strategies. The stroma forms a complex network of signaling and crosstalk between tumor and the tumor-associated cells that help drive cell progression, apoptosis and migration. Various inflammatory cytokines, growth factors and chemokines are key molecules for regulating these cell-cell interactions and are secreted by both the tumor cells and normal cells within the tumor microenvironment. Important factors in this context include the pleiotropic transforming growth factor beta (TGFB), fibroblast growth factor 2 (FGF2) and platelet-derived growth factor (PDGF), which can activate carcinoma-associated fibroblasts (CAFs) as well as foster angiogenesis [7].

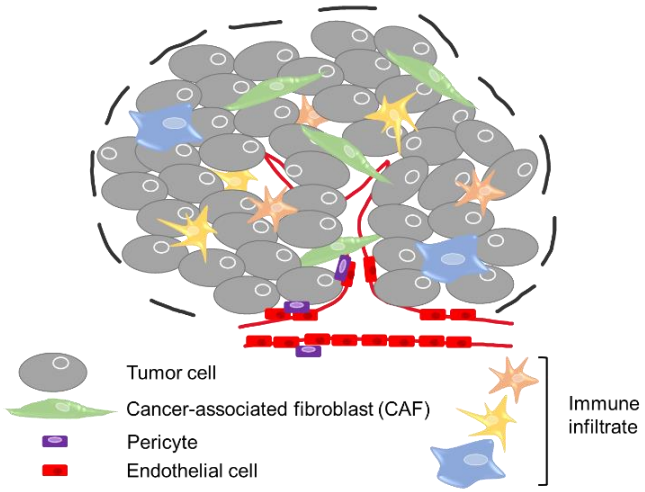

Fig. 1: *Schematic illustration of the tumor stroma consisting of tumor cells, cancer-associated fibroblasts (CAFs), immune cells, vascular endothelial cells and pericytes. All these components interact with the tumor cells and influence tumor growth, progression and angiogenesis (based on Balkwill et al. [8]).*

CAFs originate from local fibroblasts or progenitor cells such as epithelial cells, smooth muscle cells or mesenchymal stem cells [8]. CAFs play different roles within the tumor microenvironment, they can have a mitogenic effect on tumor cells by secreting growth factors such as the hepatocyte growth factor (HGF) or FGF, influence the epithelial-mesenchymal transition (EMT) by secreting TGFB or promote tumor growth due to stromal cell-derived factor 1 (SDF-1) or insulin-like growth factor-1 and -2 secretion [8-10].

An important step in tumorigenesis is the development of new blood vessels, called angiogenesis. A central player in tumor angiogenesis is the vascular endothelial growth factor (VEGF), which is released within the tumor environment as a response to different signals, including hypoxia that helps to induce neovascularization as well as microvascular permeability [7]. Endothelial cells then build blood vessels, which are supported by pericytes to supply the tumor with oxygen and nutrients. The blood vessels of the tumor are heterogenous and differ in their function as compared to normal blood vessels [8]. They are characterized by a leaky structure allowing molecules to travel between the blood capillaries and interstitial space.

Another important component of the tumor stroma are immune cells, which include: B- and T-lymphocytes, neutrophils, neutral killer (NK) and NKT-cells, dendritic cells and tumor-associated macrophages (TAM). These cells are described to have either

a promoting or inhibiting effect on tumor progression, depending on the tumor type and stage of the disease or polarization of the macrophages [8]. TAMs for example express antitumorigenic proteins but also promote tumorigenesis by producing various growth factors (HGF, VEGF and TGFB) or cytokines (tumor necrosis factor alpha (TNFα) and interleukin 8 (IL8)).

Although the tumor stroma is in general composed of the same elements, the amount of stroma varies among different tumor types [4]. Breast, stomach or pancreatic carcinomas are described as desmoplastic carcinomas, where the tumor stroma constitutes about 90 % of the tumor, whereas other cancer types possess only a small stromal compartment [4]. The microenvironment of the tumor is critical for tumor growth and spread and represents a complex and heterogeneous tissue. The biology behind carcinogenesis and its complexities regarding genomic changes, cell signaling, the role of the tumor stroma as well as intra- and interheterogeneity of tumors, has opened new avenues for novel therapeutic approaches.

1.1.2 Anticancer therapy

Traditional anticancer therapies include surgery, chemotherapy and radiotherapy. Surgery, when possible, is considered the most effective technique to eliminate solid tumors. Nearly half of all cancer patients receive radiotherapy as the initial treatment in early stage head and neck tumors, prostate cancer or as adjunct treatment to surgery or chemotherapy [11]. Cytotoxic chemotherapy uses agents that interfere with the process of cell growth. However, chemotherapy is usually associated with significant systemic toxicity [12]. Although these traditional anticancer therapies can be effective, many cancer patients still suffer from negative side effects and poor prognosis due to relapse or metastasis. Due to a better understanding of the biology of carcinogenesis, various novel therapy strategies have been developed or are currently under investigation.

Targeted therapy is based on the biological characteristics of the tumor. The expression patterns of receptors for growth factors or hormones or deregulated signaling pathways can be used to directly target cancer cells or the tumor microenvironment. To date, various therapies have been developed which directly target molecular structures such as receptors, inhibit signal transduction, modulate gene expression, induce apoptosis, inhibit angiogenesis or trigger the immune

system [11, 13]. In the last few decades, great progress has been made in the development of targeted cancer gene therapy. Gene therapy, or gene transfer, is a method used to introduce genetic material into cells to act locally as therapeutic agents. Principles of gene therapy are [14]:

- **Gene re-expression**
  A vector is used to restore gene expression by delivering the functioning version of a mutant gene into the tumor cell.
- **Suicide genes**
  A non-toxic prodrug is administered in combination with the tumor-specific delivery of the prodrug-activating gene. The tumor cell then transforms the prodrug into a toxic metabolite, leading to apoptosis.
- **Immunotherapy**
  To stimulate immune response against tumor cells, genes for specific immunogenic tumor antigens, co-stimulatory molecules or inflammatory cytokines are carried to tumor cells by a vector.
- **Oncolytic viruses**
  Oncolytic viruses specifically replicate in tumor cells and are characterized by tumor cell-specific toxicity.
- **Therapeutic RNA interference**
  Synthetic double-stranded short interfering RNA (siRNA) or short hairpin (shRNA) (expressed by a vector) bind an oncogene RNA resulting in inhibition of the oncogene translation or RNA cleavage and thus in cell apoptosis.

To date, most gene therapy approaches are focused on vehicle administration for local gene delivery to reach sufficient transgene expression in tumors. However, metastatic disease requires systemic vector application to reach not only the primary tumor but also tumor metastases throughout the body. Success and effectiveness of these gene therapy strategies rely on the choice of the vector, especially if systemic delivery is the goal. The genetic material must be sufficiently protected against degradation before it is released selectively in the tumor cells. To date, various viral and non-viral vectors are available to deliver therapeutic genes to cancer cells or their environment.

Recombinant viruses such as adenoviruses, retroviruses, lentiviruses or measles viruses have shown to be efficient therapeutic transgene delivery systems to carcinomas. Replication incompetent adenoviruses have been used to deliver the herpes simplex virus thymidine kinase (HSV-TK) gene to tumors to induce tumor cell death upon treatment with the prodrug ganciclovir [15]. This method is currently being used in experimental trials for cancer treatment and in clinical treatment of brain tumors [16]. Limiting factors for viral vectors is their immunogenicity as well as the possibility of insertional mutagenesis [14]. In addition to viral systems, non-viral gene transfer methods have been extensively investigated to circumvent safety issues of viral vectors. Synthetic vectors, such as polymers (polyplexes after DNA complexation), cationic liposomes (lipoplexes after DNA complexation) or peptides, have been successfully used to deliver DNA to tumor cells [17]. Nanoparticles as vectors (lipoplexes or polyplexes) can extravasate through gaps between endothelial cells of the blood vessels and accumulate in the tumors due to the enhanced permeability and retention (EPR) effect [14].

Another class of gene delivery vehicles are biological non-viral vectors, such as transgene-expressing bacteria or genetically engineered mesenchymal stem cells (MSCs), which naturally target tumors. In addition to a suitable vector system for therapeutic transgene delivery, the therapeutic gene itself plays a crucial role in the effectiveness of an anticancer therapy. One highly promising candidate gene for cancer gene therapy combines diagnostic and therapeutic properties: the sodium iodide symporter (NIS).

1.2 The sodium iodide symporter (NIS)

1.2.1 General characteristics

The transmembrane glycoprotein NIS consists of 643 amino acids and actively transports iodide from the blood stream into thyroid follicular cells (Fig.2). One iodide (I^-) is transported across the basolateral membrane in exchange for two sodium ions (Na^+). The sodium gradient that drives the co-transport of Na^+ and I^- ions is generated by a 3 Na^+/2 K^+ adenosine triphosphatase (ATPase).

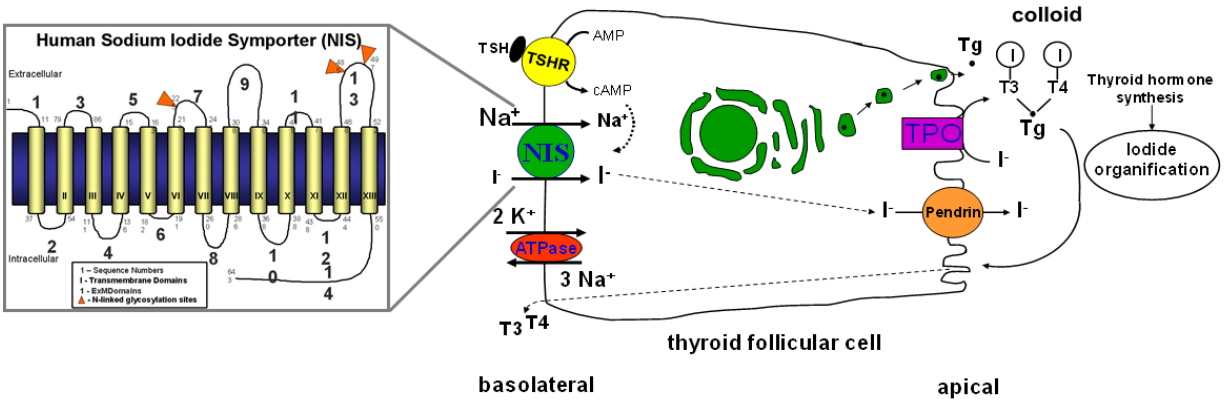

Fig. 2: *Protein structure of the transmembrane human sodium iodide symporter (NIS) (left) and schematic illustration of the iodide uptake in a thyroid follicular cell and the processes of thyroid hormone synthesis (right). Adapted from Spitzweg et al., J Clin Endocrinol Metab, 2001.*

In addition to iodide transport, the NIS protein is also capable of transporting other ions such as thiocyanate (SCN^-), nitrate (NO_3^-), bromide (Br^-), chlorate (ClO_3^-), tetrafluoborate (BF_4^-) among others, although with less affinity [18]. A well-known competitive NIS-inhibitor is perchlorate (ClO_4^-).

Iodide is an essential constituent of thyroid hormones. The process of oxidization of iodide to iodine followed by incorporation into thyroglobulin (TG) within the process of thyroid hormone synthesis is known as iodide organification. TG is a precursor protein of the thyroid hormones T3 (3,5,3′-triiodo-L-thyronine) and T4 (3,5,3′,5′-tetraiodo-L-thyronine or thyroxine), whose release into the blood stream is regulated by the thyroid-stimulating hormone (TSH) [19]. Endogenous NIS expression is also present in the stomach, salivary glands and lactating mammary glands, but is not regulated by TSH and is expressed at lower levels compared to the thyroid gland [20].

1.2.2 *NIS* as reporter and therapy gene

The ability of NIS to concentrate iodide in thyroid follicular cells offers the possibility to use NIS for molecular imaging and therapy after application of radionuclides. *NIS* as a reporter gene has been used in different approaches for radionuclide imaging of thyroid carcinomas and metastases using scintigraphy, single photon emission computed tomography (SPECT) (^{123}I, ^{99m}Tc or ^{125}I) or positron emission tomography (PET) imaging (^{124}I or ^{18}F-TFB) [21]. Radionuclide imaging allows the diagnosis of

thyroid cancer patients, the tracking of tumor progression and the detection of metastases. Imaging of tumoral radionuclide accumulation is used to calculate the tumor-absorbed dose prior to a therapeutic application of radionuclides. These calculations allow a personalized adjustment of the applied radionuclide dose (^{131}I, ^{188}Re, ^{211}At) with a maximal therapeutic effect and minimal toxicity [20-23]. The therapeutic effect is achieved by ionizing radiation, which kills cells by breaking DNA and disrupting cellular proteins. In addition, NIS-mediated radioiodide therapy is characterized by a bystander effect resulting from the crossfire effect of the beta-emitter radionuclide ^{131}I. These effects lead to apoptosis of the neighboring cells. Further, the therapeutic radioiodine is organified in thyroid follicular cancer cells, which leads to a prolonged retention time of tumoral iodine resulting in a high tumor-absorbed dose of ^{131}I. The successful and effective radioiodine therapy makes NIS an interesting and promising candidate to develop a cytoreductive gene therapy strategy based on *NIS* transgene delivery to non-thyroidal tumors.

1.2.3 *NIS* gene therapy

An important step in administering *NIS* for imaging and therapy in non-thyroidal tumors was the cloning and characterization of the *NIS* gene [24]. This breakthrough allowed the transfection of non NIS-expressing tumor cells with *NIS* DNA. Shimura *et al.* were the first to demonstrate the successful delivery of ^{125}I for noninvasive gamma camera imaging after transfection of a clonal variant FRLT thyroid cell line with rat *NIS* [25]. The cloning and characterization of *NIS* and the extensive clinical experience in NIS-based diagnosis and treatment of thyroid carcinomas effectively set the stage for the potential introduction of *NIS* into nonthyroidal tumors using diverse gene delivery vehicles including viral and non-viral approaches. The evaluation of *NIS* gene transfer was performed in a series of preclinical studies that demonstrated effective and successful ^{131}I-based therapy in various tumor types including prostate, colon, liver, pancreatic and ovarian carcinomas [26].

The most common vectors used in preclinical and clinical studies are viruses, which have been widely investigated for *NIS* transgene delivery. Pioneering studies of Spitzweg *et al.* used an adenovirus and the cytomegalovirus (CMV) promoter to control *NIS* transgene expression in transfected prostate cancer cells, which was applied intratumorally. This study demonstrated for the first time that *in vivo NIS* gene

transfer to non-thyroidal tumors resulted in a significant therapeutic effect after radionuclide application [27]. Further studies investigated the potential of specific promoters, such as the alpha-fetoprotein (AFP) or a prostate-specific (probasin) promoter to control *NIS* expression after adenovirus-mediated intratumoral delivery in different tumor mouse models for a NIS-mediated radioiodide therapy [28-30]. In human hepatocellular carcinoma (HCC), Geoffrey Grünwald from the laboratory of Christine Spitzweg intratumorally injected a replication-selective adenovirus in which the *E1a* gene (for viral replication) is driven by the alpha-fetoprotein promoter and the *NIS* gene is inserted within the E3 region (thus *NIS* is only expressed in tumor cells where adenoviral replication takes place) (Ad5-E1/AFP-E3/NIS). The combination of targeted oncolytic virotherapy with NIS-mediated radionuclide therapy resulted in an additional reduction in HCC tumor growth as compared to virotherapy alone [30]. This local gene delivery approaches demonstrated effective transgene expression in tumors but is not suitable for the treatment of metastatic disease. To date, relatively few studies have investigated systemic injection of *NIS* transgene delivery vehicles. Systemic application is limited by tumor-specific transduction efficiency and safety issues. Furthermore, the efficiency of *NIS* gene transfer is dependent on the ability of the delivery system to avoid rapid enzymatic degradation of naked *NIS* DNA in the blood and tissue. Thus, it has been necessary to focus on the investigation of potential delivery vehicles that allow effective systemic *NIS* transgene delivery. Initial studies using systemic application of gene delivery vehicles demonstrated an enhanced oncolytic potency of an oncolytic measles virus carrying the *NIS* gene in multiple myeloma after systemic injection of the virus followed by radioiodine application [31]. Goel *et al.* designed a NIS-expressing oncolytic vesicular stomatitis virus (VSV) for systemic application in multiple myeloma [32]. Kathrin Klutz from the laboratory of Christine Spitzweg investigated the potential of a replication-deficient adenovirus with the *NIS* gene linked to the tumor-specific AFP-promoter for systemic injection in mice with subcutaneous liver carcinoma. Systemic application of the adenoviral vector resulted in high specificity and promoter activation in tumors [28]. In collaboration with Prof. Dr. Ernst Wagner, Geoffrey Grünwald coated the replication-deficient adenovirus in which *NIS* is under the control of the CMV-promoter (Ad5-CMV/NIS) and the replication-selective Ad5-E1/AFP-E3/NIS with poly(amido-amine) dendrimers of the fifth generation (PAMAM-G5) to develop a combination of systemic oncolytic virotherapy and NIS-induced radioiodine therapy with improved shielding

and targeting. Intravenous injection of dendrimer-coated Ad5-CMV/NIS resulted in reduced liver toxicity and enhanced transduction efficacy in HCC xenografts [33]. An enhanced oncolytic effect was observed using systemically injected dendrimer-coated Ad5-E1/AFP-E3/NIS, which was further increased by combining this approach with NIS-mediated radioiodine therapy resulting in a significantly prolonged survival [33]. New adenovirus constructs suitable for systemic application were subsequently developed to improve tumor-selective targeting of an adenovirus-mediated *NIS* gene transfer. Viruses containing the *NIS* transgene were coated with PAMAM linked to the peptidic, epidermal growth factor receptor (EGFR)-specific ligand GE11 to specifically target high EGFR-expressing tumor cells. Specific targeting and shielding of the virus led to reduced liver trapping of the virus after systemic application with reduced hepatotoxicity and thereby enhanced transduction efficacy of *NIS* in peripheral tumor cells resulting in a strong therapeutic response [34].

Although viruses demonstrate high transduction efficacy, they are often accompanied by potential risks, such as anti-viral immunity or infection of non-target cells causing unwanted side-effects during therapy [35]. To improve safety and targeting efficacy, synthetic systems such as polymers have been widely investigated and are now seen as promising candidates for systemic *NIS* transgene delivery. In collaboration with Prof. Dr. Ernst Wagner, the laboratory of Christine Spitzweg has further investigated the potential of a NIS-mediated radioiodide-based therapy in non-thyroidal tumors introducing synthetic polymeric vectors. The first generation of vectors were based on oligoethylenimine (OEI)-grafted polypropylenimine dendrimers (G2-HD-OEI) complexed with *NIS* DNA (polyplexes) which were tested in mice harboring subcutaneous syngeneic neuroblastoma tumors and subcutaneous HCC xenografts. In both models the results showed a therapeutically sufficient accumulation of radioiodine resulting in a delay of tumor growth [36, 37]. In further studies, Kathrin Klutz *et al.* of the laboratory of Christine Spitzweg used linear polyethlenimine (LPEI)-based polymers shielded with polyethylenglycol (PEG) to reduce toxicity of LPEI and prolong blood circulation time. In addition, the tumor-specific ligand for EGFR (GE11) was used to specifically target tumor cells for enhanced NIS expression in HCC [38]. LPEI-PEG-GE11/NIS polyplexes were further investigated in clinically more relevant advanced mouse models, an engineered mouse model of endogenous pancreatic ductal adenocarcinoma (PDAC) and a colon cancer metastasis mouse model, which allowed high quality PET imaging of NIS-mediated radioiodine accumulation in

tumors followed by effective ^{131}I therapy in both models with reduced tumor growth and prolonged survival of animals [39, 40].

As LPEI-based polyplexes are accompanied by long-term toxicity and show limited specificity among other disadvantages, novel sequence-defined polymers are under investigation to enhance biocompability, lower immunogenicity and enhance tumor-selective transduction efficiency. They consist of small and well biocompatible polymer backbones with various functional domains, such as cationic (oligoethanoamino) amide cores (for nucleic acid binding), protonatable amino acids (to increase the rate of endosomal escape due to a buffer function), PEG linkers (for surface shielding) and target ligands (for specific cell binding) [41]. These sequence-defined vectors were coupled to a cMET-specific ligand and the resulting cMBP2-PEG-Stp/NIS polyplexes were used *in vivo* for tumor-specific *NIS* transgene delivery in hepatocellular carcinoma resulting in an efficient therapeutic response [41].

These preclinical studies have effectively demonstrated the great potential for image-guided NIS-mediated radionuclide therapy of non-thyroidal tumors. Non-invasive imaging of *NIS* transgene expression allows the determination of vector biodistribution and calculation of radioiodide uptake in every organ and thus offers a safe therapy strategy with individual adjustment of the therapeutic dose. The use of *NIS* as a reporter and therapy gene in the context of non-thyroidal tumor gene therapy studies has advanced to clinical trials: NCT00450814, NCT00788307, NCT01503177, NCT01846091, NCT02068794, NCT02192775, NCT02364713, NCT03017820, NCT03647163. These clinical trials use genetically engineered viruses for tumor-specific *NIS* transfection of various tumor entities such as multiple myeloma, ovarian or hepatocellular carcinoma. Although these studies are highly promising in translating the NIS-mediated radioiodine therapy concept to non-thyroidal tumors, the efficacy of this approach depends on the delivery system. In the field of non-viral vectors, mesenchymal stem cells (MSCs) are being intensively investigated as potential gene delivery vehicles due to their high lineage plasticity, selective tumor homing capacity and minimal ethical concerns with regards to isolation and their use. Thus, MSCs show great potential in improving safe and tumor-specific systemic *NIS* transgene delivery in non-thyroidal tumors.

1.3 Mesenchymal stem cells (MSCs)

1.3.1 MSCs and tumor homing

Mesenchymal stem cells (MSCs) are non-hematopoietic progenitor cells, that have self-renewing potential and possess the ability to differentiate into various cell types including stromal cells, adipocytes, chondrocytes and osteocytes [42]. MSCs are characterized by different surface marker proteins such as CD90, CD73 and CD105, but must lack HLA-DR, CD34, CD45, CD19, CD11b, CD14 and CD79 [43, 44]. They are easy to isolate from bone marrow, adipose tissue and others [42]. Their ability to not only home to inflammatory sites or damaged tissues, but also to tumors, has made them an interesting and widely investigated tool to deliver anti-cancer agents or therapeutic genes to tumor sites (Fig. 3). The mechanisms underlying the directed MSC recruitment toward solid tumors is thought to be driven by processes similar to those seen in chronic wounds, where the release of certain inflammatory factors plays a major role in attracting MSCs [45, 46].

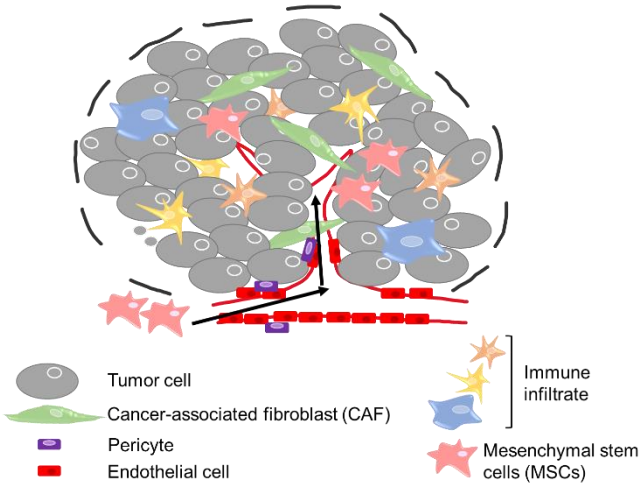

Fig. 3: *Schematic illustration of the tumor homing capacity of mesenchymal stem cells (MSCs) to tumors. Secretion of inflammatory chemokines and growth factors attract MSCs to the tumor microenvironment (based on Balkwill et al. [8]).*

Tumor cells and cells of the tumor environment release diverse factors linked to MSC tumor homing. In addition to growth factors such as PDGF, EGF, FGF2 and VEGF, cytokines and chemokines, including interleukin-6 (IL-6) and the chemokine (C-X-C motif) ligand 12/stromal cell-derived factor 1 (CXCL12/SDF-1), CXCL8 and the

pleotropic growth factor TGFB1/3, play critical roles in the MSC recruitment process [5, 47].

1.3.2 Genetically engineered MSCs

MSCs are reasonably easy to culture and handle for genetic modifications *ex vivo.* Genetically engineered MSCs have been used to specifically target tumors and to deliver diverse therapeutic agents. One advantage of using MSCs as gene delivery vehicles is the ability to use them autologously in patients. As these cells are also hypo-immunogenic they also allow an allogeneic application [48]. Early studies investigated MSCs transfected with interferon β (IFN-β) that were intravenously injected in mice harboring melanoma xenografts which led to decreased tumor growth and prolonged survival [49]. Subsequently, the ability of MSCs to act as gene delivery vehicles was intensively investigated in a variety of settings. MSC-mediated delivery of IFN-γ, IL-12 or IL-24 was shown to inhibit tumor growth, whereas local production of the tumor necrosis factor-related apoptosis inducing ligand (TRAIL) by MSCs within tumors led to the induction of apoptosis [43]. Further, HSV-TK transfected MSCs were shown to actively home to breast, liver and pancreas tumors, and, in combination with ganciclovir, resulted in reduced tumor growth [50-52]. In a phase I study, our collaboration partner Prof. Dr. Peter Nelson investigated genetically modified MSCs in combination with ganciclovir [53]. These MSCs express HSV-TK and were used in combination with ganciclovir for treatment of patients with advanced gastrointestinal adenocarcinoma demonstrating acceptable safety and tolerability in patients. MSCs have also been used to deliver oncolytic viruses to tumors. MSCs engineered by conditionally replicative adenovirus (CRAd) were applied to human glioma, lung metastasis as well as melanoma and breast carcinoma animal models, which resulted in prolonged survival and reduction of metastases [43]. Inhibition of liver carcinoma growth and ovarian cancer was achieved by MSCs infected with the oncolytic measles virus (MV) [43]. Further, approaches to induce tumor cell apoptosis have made use of are engineered MSCs carrying drug-loaded nanoparticles, which are able to directly and slowly release doxorubicin or paclitaxel in tumors [54, 55].

1.3.3 MSC-mediated *NIS* gene delivery

A highly promising approach to systemically deliver the theranostic *NIS* transgene is the use of MSCs as therapy vehicles. Non-invasive tracking of MSCs transfected with an adenovirus construct containing *NIS* under control of a constitutive CMV-promoter was determined by radionuclide imaging experiments and therapy of mice harboring breast cancer [56]. Injection of NIS-MSCs made it possible to track MSC biodistribution as well as *NIS* transgene expression by radioiodine imaging prior to an application of a therapeutic dose of radioiodide. The therapy approach revealed a significant decrease of tumor growth.

The laboratory of Christine Spitzweg in collaboration with Prof. Dr. Peter Nelson have investigated the potential efficacy of MSCs for the delivery of *NIS* into different types of primary tumors as well as metastases. In addition, they have examined a wide range of gene promoters to specifically control *NIS* expression within tumors and their micromilieu (Fig. 4) [57-60].

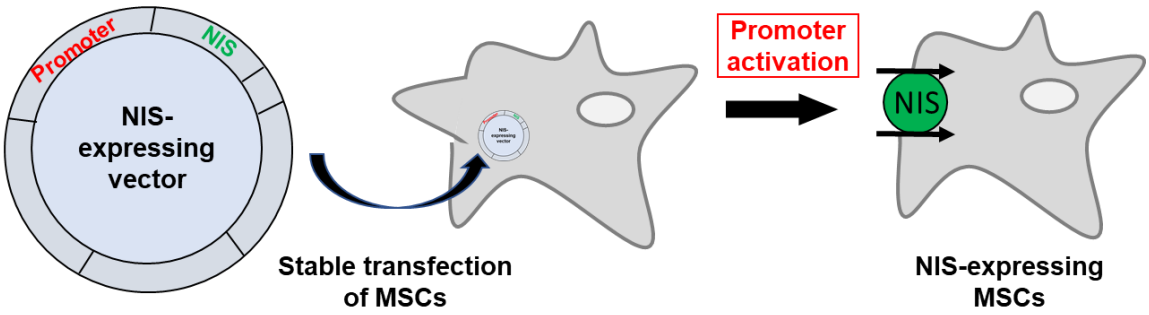

Fig. 4: *Stable transfection of MSCs with a plasmid containing the NIS transgene linked to a promoter to control NIS expression specifically in the tumor. Promoters can be designed to be activated through secreted factors (cytokines, chemokines or growth factors) involved in tumorigenesis, angiogenesis, hypoxia or other processes.*

The first proof-of-principle studies using *NIS*-transduced MSCs made use of the constitutively active CMV-promoter to drive *NIS* expression in MSCs and a subcutaneous mouse model of HCC [57]. Knoop *et al.* demonstrated high tumor-specific radioiodide accumulation *in vivo* as compared to control tumors with wild-type MSCs. Following MSC-mediated NIS-based radioiodine therapy, a significant reduction in HCC tumor growth was observed [57]. To enhance tumor stroma-specific *NIS* expression, various strategies using of tissue-specific gene promoters were

investigated. One approach made use of the regulated on activation, normal T-cell expressed and secreted (RANTES)/CCL5 gene promoter to control *NIS* expression (RANTES-NIS-MSCs). Studies using subcutaneous HCC xenografts revealed an improved radioiodide uptake in tumors in comparison to studies using the CMV-promoter and resulted in an enhanced therapeutic response in animals and prolonged survival [58]. Further, RANTES-NIS-MSCs were applied in a colon cancer liver metastasis model. Even in this aggressive tumor mouse model a strong therapeutic effect was induced after ^{131}I application [59].
In another approach, a synthetic gene promoter that responds to tumor hypoxia was examined in a subcutaneous as well as an orthotopic liver cancer mouse model. MSCs were transfected with a construct containing the *NIS* transgene linked to a hypoxia responsive promoter (HIF-NIS-MSCs) [60]. A significant decrease in tumor growth and prolonged survival was observed using the orthotopic mouse model. Although a stronger activation of the promoter was expected in subcutaneous tumors, as those tumors are more hypoxic than orthotopic ones, it seemed that in this setting MSC migration was the rate-limiting factor. The difference in the migratory behavior of MSCs to subcutaneous and intrahepatic HCC was also described by Garcia *et al.* [61]. This is thought to be based on activation of the surrounding liver cells by the cancer cells to secrete cytokines, chemokines and growth factors implicated in the mechanisms of MSC recruitment [60].

1.3.4 Approaches to improve MSC-mediated *NIS* gene therapy

The aforementioned studies point out the importance of the animal model used to evaluate the efficacy of MSC-based gene delivery. The earliest mouse models were developed by subcutaneous implantation of tumor cells in immune incompetent mice. Subcutaneous xenograft mouse models are easy to establish and a useful first step for evaluation of new therapy strategies. However, these models often fail to predict human response as they poorly reflect cancer heterogeneity, immune response of the host or existing or developed drug resistance [62]. While subcutaneous mouse models are important models for proof-of-principle studies, the next step towards clinical application are orthotopic or genetically engineered mouse models, which endogenously develop tumors and most reliably represent cancer development and features in human cancers. The next step of preclinical development of the MSC-

mediated *NIS* gene therapy concept is therefore the investigation of MSCs-mediated *NIS* gene delivery in advanced and more complex mouse models.

A further strategy, to not only improve *NIS* transgene delivery by MSCs but also enhance flexibility regarding tumor inter- and intraindividual heterogeneity, is the development and evaluation of novel promoters with higher specificity and efficacy to control *NIS* expression within the tumor microenvironment. Taking advantage of tumor characteristics, factors that are overexpressed within the tumor microenvironment can be used to drive *NIS* expression, leading to activation only upon arrival of MSCs in the tumor stroma.

A promising approach offers the combination of *NIS* transgene therapy with existing therapies such as chemotherapy or radiotherapy, which is an important angle to enhance therapeutic outcome with regards to tumor reduction and improvement of survival. A limited number of studies have assessed the potential effect of radiotherapy and tumor homing capacity of adoptively applied MSCs [63-65]. These studies open an exciting aspect to improve MSC-mediated NIS radionuclide therapy. The current thesis investigates the potential of different strategies to enhance the potential of MSC-mediated *NIS* transgene therapy.

2. Aims of this thesis

Mesenchymal stem cells were evaluated for their tumor-homing ability to specifically deliver the *NIS* transgene deep into the tumor environment taking advantage of the dual role of *NIS* as reporter and therapy gene in multiple tumor mouse models. As a next step towards clinical development, the major focus of this thesis was the general improvement of the MSC-based *NIS* gene therapy.

Previous studies have demonstrated successful therapeutic approaches using MSCs as *NIS* gene transfer vehicles. However, clinical transferability of studies in xenograft mouse models without an intact immune system is limited. Therefore, as a first aim of this thesis, the efficacy of systemically applied MSCs was studied in a more clinically relevant and suitable mouse model of advanced endogenous pancreatic ductal adenocarcinoma (PDAC) described as *Ptf1a*$^{+/Cre}$*;Kras*$^{+/LSL\text{-}G12D}$*;Trp53*$^{loxP/loxP}$ *(Kras;p53)*. The *Kras;p53* mouse model endogenously develops PDAC, which strongly reflects the human disease. Murine MSCs stably transfected with *NIS* under the control of the unspecific cytomegalovirus (CMV) promoter (NIS-MSCs) demonstrated high cellular NIS-specific radioiodide uptake. Systemic injection of NIS-MSCs in mice harboring PDAC allowed noninvasive monitoring of NIS expression by ^{123}I-scintigraphy and ^{124}I-PET imaging, as well as examination of the therapeutic potential of the NIS-MSC-based *NIS* gene therapy using ^{131}I in the *Kras;p53* PDAC mouse model.

Considering the high intra- and intertumoral heterogeneity the group of Prof. Dr. Christine Spitzweg in collaboration with the laboratory of Prof. Dr. Peter Nelson has been searching for new ways to express *NIS* more selectively within the tumor and its environment. The use of specifically designed promoters allows control of *NIS* expression specifically within the tumor tissue and to meet the needs of individual tumor types. As the pleiotropic factor TGFB is a central player in carcinogenesis and upregulated in a variety of tumors, a synthetic TGFB1-inducible SMAD-responsive promoter was designed and human MSCs were stably transfected with NIS under the control of this promoter (SMAD-NIS-MSCs) to potentially improve tumor specificity of MSC-dependent NIS gene delivery. SMAD-NIS-MSCs were characterized *in vitro* by radioiodine uptake activity assay using different doses of TGFB1 to stimulate *NIS*

expression in MSCs. The potential improvement of diagnostic and therapeutic application of SMAD-NIS-MSCs in a subcutaneous HuH7 xenograft mouse model was investigated.

The next step towards optimization of the efficacy of MSC-based *NIS* gene therapy was the investigation of the effects of external beam radiation therapy (EBRT) on the tumor-homing capacity of MSCs to radiation pretreated tumors. Currently, there is growing evidence that radiation enhances MSCs recruitment to tumor sites by increasing the secretion of inflammatory cytokines and growth factors. As part of this thesis we investigated the effects of radiation treatment on the biology of the human hepatocellular carcinoma cell line HuH7, as well as of the human breast adenocarcinoma cell line MDA-MB-231, by analyzing the *in vitro* secretion profiles for different inflammatory factors involved in MSC migration. Further, the effect of supernatants of irradiated and non-irradiated tumor cells on MSC migration was examined using a 3D live cell imaging migration assay. To investigate the potential of radiation pretreatment on MSC tumor homing *in vivo*, mice harboring HuH7 xenograft tumors were pretreated with low doses of radiation (0, 2 or 5 Gy) followed by intravenous application via the tail vein of human MSCs expressing *NIS* under the control of the CMV-promoter (CMV-NIS-MSCs) followed by analysis of the tumoral radioiodide uptake by ^{123}I-scintigraphy.

Based on data from the studies outlined above demonstrating EBRT as potent stimulator of MSC homing as well as TGFB as central mediator of the inflammatory response underlying this effect, in the final step radiation tumor pretreatment was combined with the novel tumor stroma-specific SMAD-NIS-MSC therapy approach to evaluate the therapeutic efficacy of increased MSC recruitment and enhanced promoter activity of SMAD-NIS-MSCs in irradiated HuH7 tumors. *In vitro,* effects of stimulation with non-irradiated and irradiated HuH7 cell supernatants on the radioiodide uptake activity of SMAD-NIS-MSCs were determined. Nonirradiated as well as irradiated (using low-dose radiation of 5 Gy) tumors were immunohistochemically stained for their TGFB1 expression levels. The effect of radiation pretreatment on the migratory capacity and the promoter activation through TGFB1 in SMAD-NIS-MSCs was then evaluated *in vivo* using ^{123}I-scintigraphy.

Further, tumors were pretreated using 5 Gy followed by SMAD-NIS-MSC and radioiodine application to evaluate the therapeutic efficacy of this novel approach.

3. Chapter 1: A Novel Approach for Image-guided ^{131}I Therapy of Pancreatic Ductal Adenocarcinoma using Mesenchymal Stem Cell-mediated *NIS* gene delivery

This chapter has been adapted from:

Schug C[1*], Gupta A[2*], Urnauer S[1], Steiger K[3], Cheung PFY[4,5], Neander C[4,5], Savvatakis K[4,5], Schmohl KA[1], Trajkovic-Arsic M[4,5], Schwenk N[1], Schwaiger M[6], Nelson PJ[7], Siveke JT [2,4,5] and Spitzweg C[1], A Novel Approach for Image-guided ^{131}I Therapy of Pancreatic Ductal Adenocarcinoma using Mesenchymal Stem Cell-mediated *NIS* gene delivery. Molecular Cancer Research. 2018 August. [Ebup ahead of print]

[1]Department of Internal Medicine IV, University Hospital of Munich, LMU Munich, Munich, Germany, [2]Department of Internal Medicine II, Klinikum rechts der Isar der Technischen Universität München, Munich, Germany, [3]Institute of Pathology, Klinikum rechts der Isar der Technischen Universität München, Munich, Germany, [4]Division of Solid Tumor Translational Oncology, West German Cancer Center, University Hospital Essen, Essen, Germany, [5]German Cancer Consortium (DKTK), partner site Essen and German Cancer Research Center (DKFZ), Heidelberg, Germany, [6]Department of Nuclear Medicine, Klinikum rechts der Isar der Technischen Universität München, Munich, Germany, [7]Clinical Biochemistry Group, Department of Internal Medicine IV, University Hospital of Munich, LMU Munich, Munich, Germany, *C.S. and A.G. contributed equally

3.1 Abstract

The sodium iodide symporter (*SLC5A5/NIS*) as theranostic gene would allow for non-invasive imaging of functional NIS expression and therapeutic radioiodine application. Genetically engineered mesenchymal stem cells (MSCs), based on their tumor-homing abilities, show great promise as tumor-selective *NIS* gene delivery vehicles for non-thyroidal tumors. Towards this clinical application, tumor specificity and efficacy of MSCs were investigated in an advanced genetically engineered mouse model of pancreatic ductal adenocarcinoma (PDAC). Syngeneic murine MSCs were stably transfected with a *NIS* expressing plasmid driven by the CMV-promoter (NIS-MSC). *In vivo* ^{123}I-scintigraphy and ^{124}I-PET revealed significant perchlorate-sensitive NIS-mediated radioiodide accumulation in PDAC after systemic injection of NIS-MSCs. Active MSC recruitment into the tumor stroma was confirmed using NIS immunohistochemistry (IHC). A therapeutic strategy, consisting of three cycles of systemic MSC-mediated *NIS* delivery, followed by ^{131}I application, resulted in a significant delay and reduction in tumor growth as compared to controls. Further, IHC analysis of α-SMA and Ki67 revealed differences in the amount and behavior of activated fibroblasts in tumors of mice injected with NIS-MSCs as compared to saline treated mice. Taken together, MSCs as *NIS* gene delivery vehicles in this advanced endogenous PDAC mouse model demonstrated high stromal targeting of NIS by selective recruitment of NIS-MSCs after systemic application resulting in an impressive ^{131}I therapeutic effect.

Implications: These data expand the prospect of mesenchymal stem cell-mediated radioiodine imaging-guided therapy of pancreatic cancer using the sodium iodide symporter as a theranostic gene in a clinical setting.

3.2 Introduction

The sodium iodide symporter (NIS) is an intrinsic transmembrane glycoprotein that is responsible for the active transport of iodide into the thyroid gland [20]. As NIS is also expressed in follicular cell-derived differentiated thyroid cancer cells, its expression provides the molecular basis for diagnostic and therapeutic application of radioiodine in thyroid cancer patients [20, 22]. The extensive clinical experience of using *NIS* as theranostic gene in the management of thyroid cancer patients has provided the basis for the development of *NIS* gene-based therapy approaches in nonthyroidal tumors [21, 23]. The *NIS* transgene has been successfully transferred selectively into extrathyroidal tumor cells or cells of the tumor environment using various gene delivery systems where diagnostic use of *NIS* has allowed the direct monitoring and detailed characterization of vector biodistribution, localization and duration of transgene expression within tumors using ^{123}I-scintigraphy and ^{124}I-PET imaging [21, 28, 30, 33, 34, 36-38, 41, 56-60, 66, 67]. The dosimetric calculations derived from the imaging studies allowed the application of an optimized therapeutic dose of radioiodine (^{131}I). Different approaches for systemic *NIS* gene delivery (i.e. polyplexes, mesenchymal stem cells, viral vectors) are currently under evaluation in several experimental settings and in tumor mouse models [28, 30, 33, 34, 36-38, 41, 57-60, 66]. One promising approach has been the use of bone-marrow derived mesenchymal stem cells (MSCs) as tumor therapy vehicles based on their excellent intrinsic tumor-homing capacity [45, 46, 52]. Their active recruitment into growing tumor stroma is mediated by mechanisms that are thought to be similar to those that occur in the context of wound healing [45, 46]. Once MSCs enter the tumor environment, they differentiate into various tumor stroma-associated cell types [68]. These include cells associated with the tumor vasculature and stromal fibroblast-like cells. A series of studies have demonstrated the potential of using adoptively applied MSCs to deliver therapeutic genes into primary tumors as well as to tumor metastases [51, 52, 57-60, 65, 69]. MSC-mediated *NIS* gene delivery in xenograft tumor mouse models has shown successful selective NIS-expression in tumors and metastases as well as a robust therapeutic response after ^{131}I application [57-60]. Although these results are very promising, the studies with implanted xenograft models often suffer from limited correlation to the human situation and are not ideal for clinical translation due to the immune deficient state of tumor carrying animals and

a less than optimal tumor environment [70]. By contrast, genetically engineered mouse models (GEMM) with endogenous tumor development represent a better model system for the evaluation of diagnostic and therapeutic tumor studies due to their heterogeneity on a genetic and morphological level, and their more complex tumor environment that better reflect that seen in cancer patients [70, 71]. Pancreatic ductal adenocarcinoma (PDAC) is the fourth leading cause of cancer deaths in developed countries, and while surgical intervention may be effective in very limited cases, no effective long-term therapeutic strategies are currently available [71, 72]. PDAC development and progression is known to involve genetic and morphological changes such as the activation of the *KRAS* oncogene and inactivation of *TP53*, a tumor suppressor also known as “guardian of the genome”. When these genetic changes occur in concert with the activation and malfunction of diverse growth factor receptors and others, the process eventually manifests as PDAC [73-76].

Several GEMMs of PDAC have been shown to accurately recapitulate key aspects of the human disease, including the *Ptf1a*$^{+/Cre}$*;Kras*$^{+/LSL\text{-}G12D}$*;Trp53*$^{loxP/loxP}$ (*Kras;p53*) model used in the present study [73, 75, 77-79]. These mice develop extremely aggressive PDAC, which leads to quick fatality. The tumors are characterized by strong desmoplasia as well as a dynamic communication between tumor cells and its environment and a complex microarchitecture [75, 80]. Further, PDAC has an extensive tumor stroma consisting of fibroblasts, inflammatory cells and vasculature girded by high amounts of extracellular matrix. These tumors are also able to respond to treatments by remodeling and rearranging the tumor stroma [80].

We investigated the efficacy of adoptively applied murine MSCs as gene delivery vehicles for tumor-selective *NIS* gene transfer in the *Kras;p53* PDAC mouse model, a model that provides an important step towards studying this therapy approach in a clinically more relevant preclinical setting. NIS was used for noninvasive ^{123}I-scintigraphy and ^{124}I-PET imaging to determine MSC localization as well as level and duration of transgene expression. The efficacy of a *NIS* gene ^{131}I therapy approach was further evaluated in this advanced endogenous PDAC mouse model.

3.3 Materials and methods

Mesenchymal stem cells

The MSC cell line used in this study was isolated from the bone marrow of a female $p53^{-/-}$ mouse with Balb/c background (in the following referred to as wild type MSCs) as described previously [81]. MSCs were cultured in RPMI (Sigma-Aldrich, St. Louis, Missouri, USA) supplemented with 10% FBS and 100 U/ml penicillin/100 µg/ml streptomycin. Cells were maintained at 37°C and 5% CO2 in an incubator.

Wild type MSCs (WT-MSC) were stably transfected with the expression vector CMV-NIS-pcDNA3, wherein the full length *NIS* cDNA is coupled to the cytomegalovirus (*CMV*) promoter. The transfection and isolation of clones as well as the screening for iodide uptake levels was performed as described previously [57]. The resulting stably transfected cell line for the following experiments was referred to as NIS-MSCs.

^{125}I uptake assay

Radioiodide uptake of MSCs was determined at steady-state conditions as described previously [66].

Quantitative real-time PCR (qRT-PCR)

Total RNA from MSCs was extracted using the RNeasy Mini Kit with QIAshredder (Qiagen, Hilden, Germany). Reverse transcription and quantitative real-time PCR were conducted using a Mastercycler ep gradientS PCR cycler as described previously (Eppendorf, Hamburg, Germany) [58]. Relative expression levels were calculated from ΔΔCt values normalized to internal β-actin and results are expressed as fold change relative to controls.

Animals

Establishment of the *Kras;p53* (*Ptf1a*$^{+/Cre}$;*Kras*$^{+/LSL\text{-}G12D}$;*Trp53*$^{lox/loxP}$) strain has been described previously and was maintained on a mixed C57BL/6;129/Sv background [39, 73, 82, 83]. Animals were maintained under specific pathogen-free conditions with access to mouse chow and water ad libitum. Both male and female mice at 4-8 weeks of age were used for experiments. Experiments were performed in accordance with institutional guidelines of the Klinikum rechts der Isar, Technische

Universität München and was approved by the regional governmental commission for animals (Regierung von Oberbayern, Munich, Germany).

MSC application and ^{123}I-scintigraphy

Experiments started when mice were about 6-8 weeks of age and tumors were developed. To suppress thyroidal iodide uptake for the imaging study, mice were given 5 mg/ml L-T4 (Sigma-Aldrich) in their drinking water. The first experimental group received NIS-MSCs (n=5) or WT-MSCs (n=2) three times on every second day via the tail vein at a concentration of 5 × 10^5 cells/500 µl PBS. As an additional control, 30 min before radioiodide administration, a subset of mice (n=2) was pretreated with 2 mg of the competitive NIS inhibitor sodium perchlorate (Sigma-Aldrich). 72 h after the last MSC application, mice received 18.5 MBq (0.5 mCi) ^{123}I (GE Healthcare, Braunschweig, Germany) i.p. and radioiodide accumulation was monitored using a gamma camera provided with a low-energy high resolution collimator (e.cam, Siemens, Munich, Germany).

The second group received only one MSC application via the tail vein of 5 × 10^5 cells/500 µl PBS NIS-MSCs (n=5) or WT-MSCs (n=2) followed 48 h later by 18.5 MBq (0.5 mCi) ^{123}I i.p. application and monitoring of radioiodide biodistribution as described above. Also, a subset of mice (n=2) were treated with perchlorate as well 30 min before radioiodide application.

Analysis and Quantification of regions of interest were done using HERMES GOLD (Hermes Medical Solustions, Stockholm, Sweden). Results are expressed as a fraction of the total amount of applied radionuclide per gram tumor tissue (after post mortem weighing) (% ID/g). Radionuclide retention time was examined by serial scanning within the tumors. Dosimetric calculations for ^{131}I were done according to the concept of medical internal radiation dose using the dosis factor of RADARgroup (www.dosisinfo-radar.com).

MSC application and ^{124}I-PET imaging

In order to achieve a better discrimination between uptake in the tumor and the adjacent stomach, a ^{124}I-PET imaging was performed. NIS-MSCs (n=5) or WT-MSCs (n=2) were applied three times for every second day as described above and mice received 10 MBq ^{124}I (Perkin Elmer, Waltham, MA, USA) i.p. 72 h later. 30 min before radioiodide administration, a mouse (n=1) was pretreated with 2 mg of the

competitive NIS inhibitor sodium perchlorate. Using a micro PET system (Inveon, Siemens Preclinical Solutions, Erlangen, Germany) radioiodide biodistribution was monitored by static acquisition 3 h post injection.

Radionuclide therapy study

For inclusion of mice harboring PDAC, a 7T dedicated animal MR scanner was used for monitoring. Therapy started as soon as they fulfilled the inclusion criteria (tumor volume of 100-500 mm^3). To monitor tumor growth, the 7T-MR imaging was done on a weekly basis. Following a L-T4 pretreatment as described above, three groups of mice were established receiving only one systemic NIS-MSCs application followed 48 h later by a therapeutic dose of 55.5 MBq ^{131}I i.p. (NIS-MSCs + ^{131}I, n=10) or, as control, received NaCl (saline) instead of radioiodide, (NIS-MSCs + NaCl, n=9). The therapy cycle consisting of systemic MSC-mediated NIS gene transfer followed by radioiodide was repeated for a total of three times on days 0/2, 4/6 and 7/9. The body conditions of the mice were closely monitored for the whole time of treatment. Mice were sacrificed after reaching one or more endpoint criteria (tumor volume >1000 mm^3, body weight loss >15 %, abnormalities in physical or behavioral criteria).

Immunohistochemical staining

Immunohistochemical NIS staining of paraffin-embedded tissue sections derived from PDAC or non-target organs (liver, lung and spleen) after systemic NIS-MSC or WT-MSC administration was performed as described previously [84]. Quantification of NIS immunohistochemical staining was performed by a highly experienced pathologist. Areas (1 mm^2) of high NIS protein expression were defined as hot spots and the number of NIS-expressing MSCs within a hot spot was quantified.

Immunohistochemistry for all other markers was performed using a Bond RXm system (Leica, Wetzlar, Germany, all reagents from Leica) with primary antibodies against Ki67 (ab16667, abcam, Cambridge UK) and α-SMA (ab124964, abcam, Cambridge UK). Briefly, slides were deparaffinized using deparaffinization solution, pretreated with Epitope retrieval solution 1 (corresponding to citrate buffer pH6) for 20 minutes. For single stainings, antibody binding was detected with a polymer refine detection kit without post primary reagent and visualized with DAB as a dark brown precipitate. For double stainings, after DAB visualization as described above, a second primary antibody was applied, and detected and visualized with a polymer

refine red kit without post primary reagent. Counterstaining was, in all protocols, done with hematoxyline.

Stromal contents were determined by MOVAT pentachrome staining as described previously [80].

Statistical methods

Results are expressed as mean ± SEM, mean-fold change ± SEM or, for survival plots, percent. Statistical significance was tested by two-tailed Student´s *t*-test or, for tumor volumes, using one-way ANOVA followed by Tukey's Honestly Significant Difference test. For Kaplan-Meier plots statistical significance was analyzed by log-rank test. For all tests, *p*-values <0.05 were considered statistically significant (**p*<0.05; ***p*<0.01; ****p*<0.001; n/s not significant).

3.4 Results

Characterization of MSCs stably expressing NIS

After stable transfection of bone marrow derived murine MSCs with a *NIS* expressing plasmid (CMV-NIS-pcDNA3) (NIS-MSC), NIS-MSCs showed a 38-fold increase in NIS-mediated iodide uptake activity as compared to non-transfected wild type MSCs (WT-MSCs) (Fig. 1A). Addition of the NIS-specific inhibitor perchlorate significantly decreased levels of iodide uptake in NIS-MSCs to background levels. No perchlorate-sensitive iodide uptake above background levels could be observed in WT-MSCs.

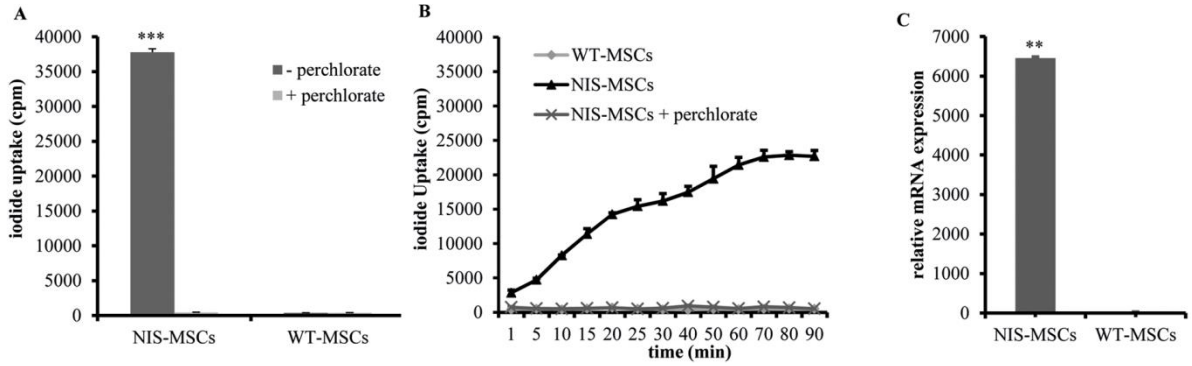

Fig. 1: *Establishment of murine mesenchymal stem cells (MSCs) stably expressing the sodium iodide symporter (NIS). Iodide uptake studies revealed 30-fold higher NIS-specific and perchlorate-sensitive ^{125}I uptake in NIS-MSCs as compared to wild type MSCs, where no perchlorate-sensitive radioiodide uptake above background levels was observed* ***(A)****. A time course experiment of NIS-MSCs and WT-MSCs showed that NIS-MSCs reached half-maximal levels of radioiodide uptake within 15-25 min, obtaining saturation at approximately 50 min* ***(B)****. Confirmation of NIS transgene expression was done using qRT-PCR revealing 6500-fold higher NIS mRNA expression of NIS-MSCs as relatively compared to WT-MSCs* ***(C)****. Data are represented as mean values ± SEM (n=3; two-tailed Student's t-test: *P<0.05; **P<0.01, ***P<0.001).*

A time course of iodide uptake in NIS-MSCs (and WT-MSCs controls) identified half-maximal levels of radioiodide accumulation within 15-25 min, and a saturation of uptake at approximately 50 min in the NIS-MSCs whereas no NIS-specific iodide uptake was observed when cells were treated with perchlorate (Fig. 1B).

The expression levels of steady state *NIS* mRNA in the NIS-MSC and WT-MSCs were validated using qRT-PCR. NIS was significantly higher expressed at relative mRNA levels (approximately 6500-fold) in NIS-MSCs as compared to WT-MSCs (Fig.

1C).

In vivo imaging studies reveal high NIS-mediated radioiodide accumulation in PDAC

To compare the general efficacy of MSC-mediated *NIS* gene delivery and radioiodide uptake activity using ^{123}I-scintigraphy in mice harboring endogenous PDAC with the results of earlier studies in xenograft mouse models, a group of mice received three applications at two-day intervals of NIS-MSCs (5 x 10^5 cells, intravenously (i.v.) via the tail vein) or WT-MSCs, followed by a single radioiodide application (18.5 MBq ^{123}I, intraperitoneally (i.p.)) 72 h later – the application regimen that we had applied in our previous studies. While no radioiodide accumulation above background levels was detected in tumors of mice receiving WT-MSCs (Fig. 2C), significant iodide accumulation was observed in tumors of mice which had received NIS-MSCs (Fig. 2A). Physiologic iodide accumulation was observed in the thyroid and salivary glands (SG), stomach and bladder (Fig. 2A, C). As determined by serial scanning, a maximum of approximately 16.2 ± 2.9 % injected ^{123}I dose per gram (ID/g) tumor was accumulated after three cycles of NIS-MSCs application which showed a biological half-life of 7 h, and a calculated tumor absorbed dose of 136.9 mGy/MBq ^{131}I (Fig. 2I). To confirm that tumoral iodide uptake was NIS-mediated, a subset of mice treated with NIS-MSCs received perchlorate 30 min prior to ^{123}I administration. Perchlorate treatment completely blocked tumoral iodide accumulation as well as iodide uptake in stomach and thyroid gland (Fig. 2B). To assess an optimized, less time intense treatment schedule more applicable in the rapidly growing tumor model, an additional ^{123}I-scintigraphy experiment was performed with only one MSC application (Fig. 2G, H). PDAC harboring mice received only one NIS- or WT-MSC application followed by an injection of 18.5 MBq ^{123}I 48 h later. Radioiodide distribution revealed significant radiodide accumulation in the tumors (Fig. 2G), while no iodide accumulation was detected in tumors of mice receiving perchlorate 30 min prior to ^{123}I administration (Fig. 2H). As determined by serial scanning, a maximum of 16.3 ± 2.3 % ID/g ^{123}I was shown to accumulate after a single NIS-MSC application, with a biological half-life of 4 h, and a calculated tumor absorbed dose of 100.7 mGy/MBq ^{131}I (Fig. 2I). While the maximum radioiodide uptake obtained in this experiment was approximately the same as that seen in the first experimental setting, radioiodide efflux was slightly more rapid and biological half-life was shorter, however the overall tumor absorbed

dose of ^{131}I was only mildly reduced.

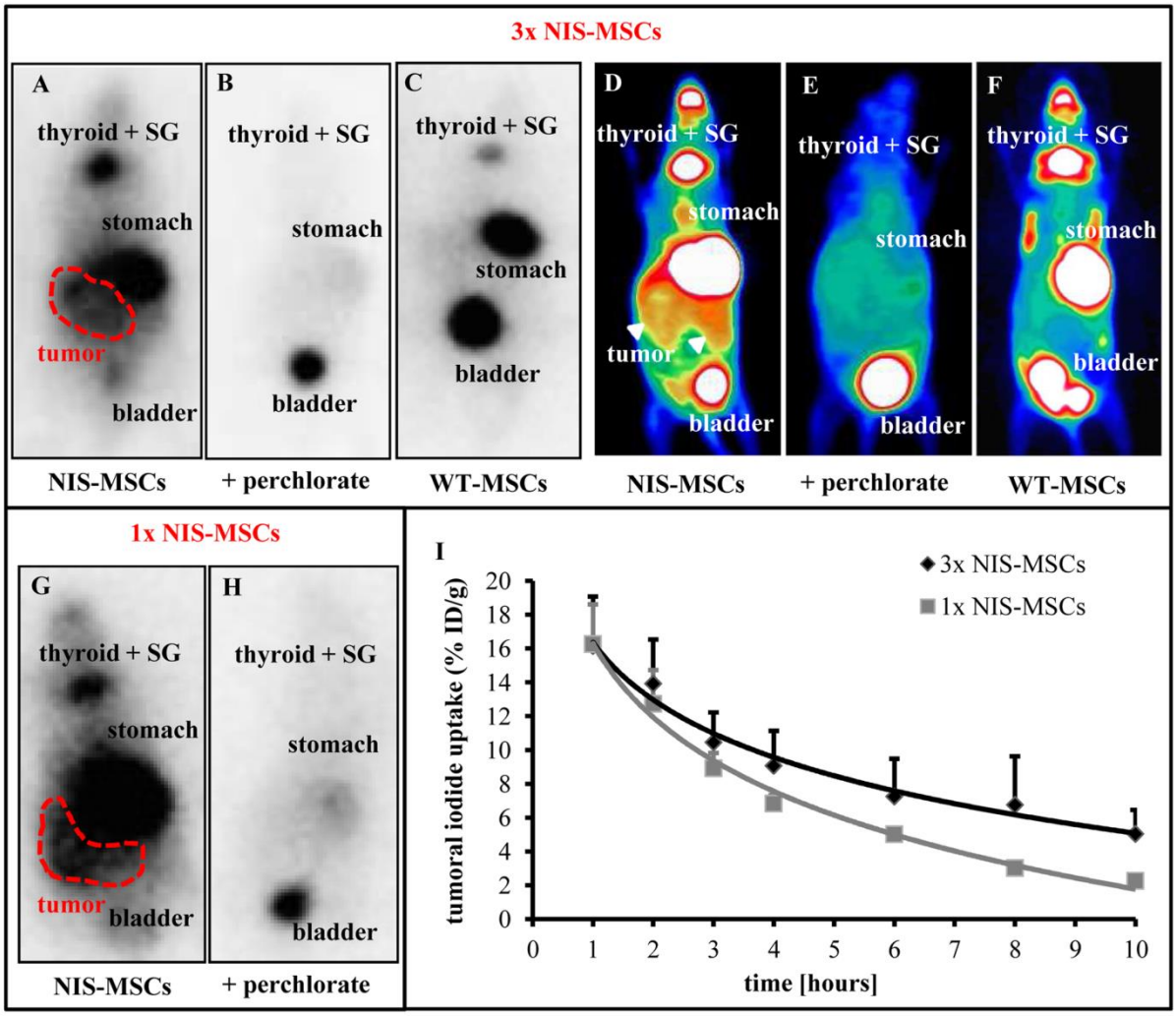

Fig. 2: *^{123}I-scintigraphy and ^{124}I-PET imaging revealed high pancreatic tumoral radioiodide uptake. One **(A)** or three **(G)** systemic injections of NIS-MSCs in mice harboring PDAC resulted in a maximum of approximately 16.2 % to 16.3 % of injected dose per gram (ID/g) tumor (n=5) **(I)**. Tumor radioiodide uptake was NIS-specific as shown by perchlorate-sensitivity (n=2) **(B, H)**. Treatment with WT-MSCs showed no NIS-specific tumoral radioiodide uptake (n=2) **(C)**. Further, application of three i.v. injections of NIS-MSCs on every second day confirmed high perchlorate-sensitive NIS-specific tumoral iodide uptake using ^{124}I-PET (n=1-5) **(D, E)**. Also, no tumoral radioiodide accumulation was observed after applications of WT-MSCs (n=2) **(F)**. One representative image is shown each. Data are represented as mean values ± SEM.*

^{124}I-PET imaging allowed a detailed 3D-analysis of tumoral iodide uptake. 3 h after injection of 10 MBq ^{124}I in a subset of mice that had received three NIS-MSCs applications every second day (Fig. 2D-F). PET-imaging confirmed a significant tumor-selective iodide accumulation, which was blocked upon perchlorate treatment (Fig. 2D, E). No iodide uptake in tumors above background levels was observed when mice were injected with WT-MSCs (Fig. 2F).

NIS protein expression in PDAC

In order to correlate the *in vivo* imaging data with NIS protein expression within the tumors and control organs (liver, spleen, lung), tissues were dissected and immunohistochemically stained. NIS-specific immunoreactivity was detected in tumors of mice that received NIS-MSCs applications demonstrating efficient MSC-mediated NIS transgene expression in PDAC after systemic application (Fig. 3A, F). MSCs genetically engineered to express NIS were localized within the tumor stroma based on detection of NIS-specific immunostaining (Fig. 3A, F, arrows). NIS-specific immunoreactivity was detected at the membrane and in the cytoplasm of MSCs in tumors of mice that received NIS-MSCs applications demonstrating efficient MSC-mediated *NIS* transgene expression in PDAC after systemic application (Fig. 3A, F). The cytoplasmic staining results from NIS protein that is not properly targeted to the membrane after *NIS* transduction of MSCs. While there was no clear visual difference detectable in NIS expression of tumors in mice receiving just a single (Fig. 3F) or three NIS-MSCs applications (Fig. 3A), a pathologist-based quantification of the amount of NIS-positive MSCs within PDAC showed following results: the analysis of hot spots (1 mm^2) revealed an average of 4.3 hot spots with a total of 18.3 NIS-positive MSCs within tumors of mice receiving a total of three MSC applications and an average of 10.3 hot spots with a total of 32 NIS-positive MSCs within the group receiving only MSCs once. Lung, liver and spleen showed no detectable NIS protein expression (Fig. 3B-I). Mice, which received three applications with WT-MSCs showed no NIS protein expression in tumors (Fig. 3E).

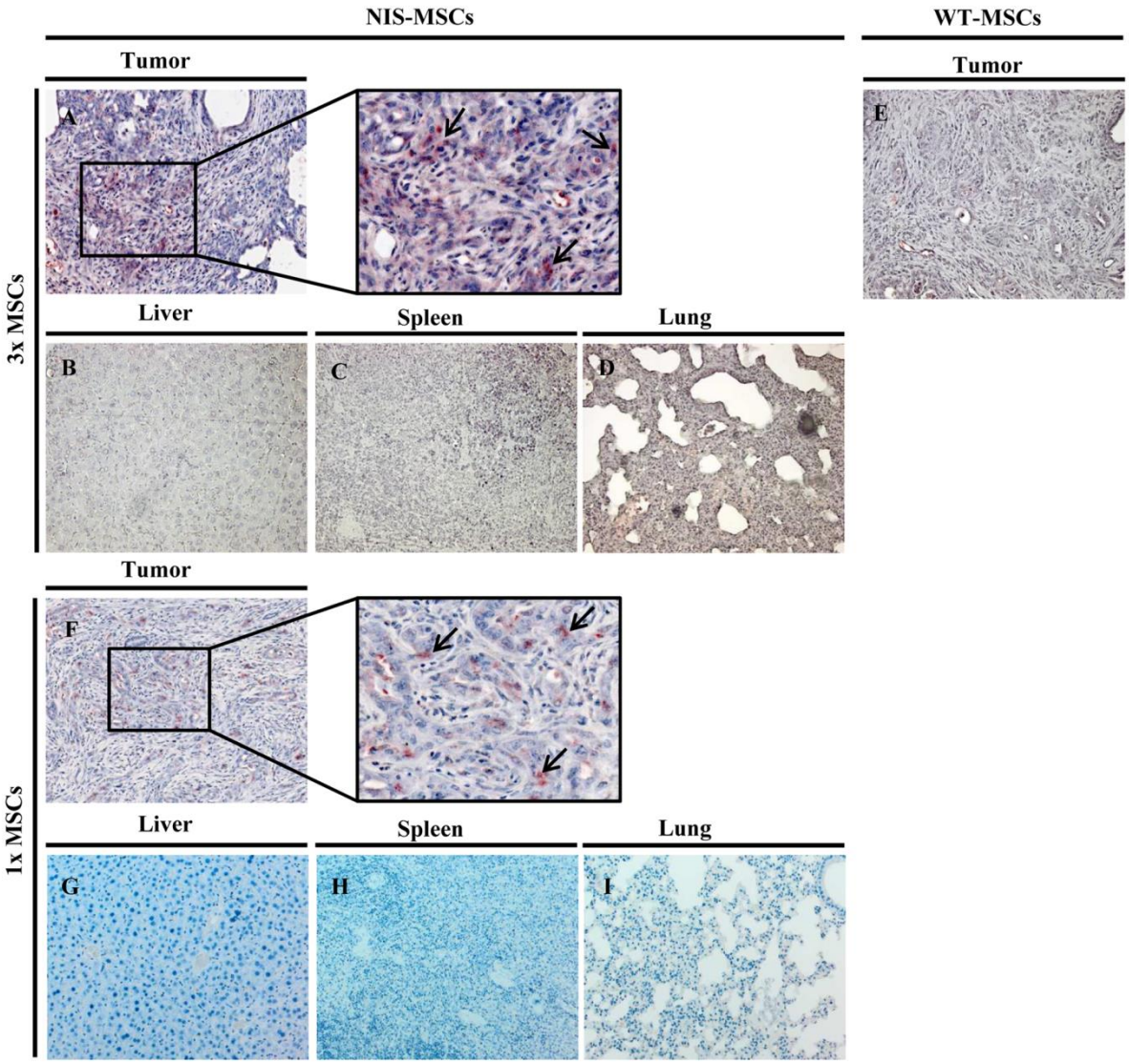

Fig. 3: *High NIS protein expression in PDAC tumors. NIS-specific immunoreactivity (red) was detected in PDAC after systemic application of NIS-MSCs (black arrows)* ***(A, F)****. No NIS protein expression was* seen in *nontarget organs* ***(B-D, G-I)*** *or tumors of mice, which received WT- MSCs* ***(E)****. One representative image is shown each using 20x magnification or also 40x magnification for tumors showing NIS specific immunoreactivity.*

Therapeutic application of radioiodine ^{131}I

A relatively short therapy cycle after imaging-guided standardized detection of advanced local tumor growth was chosen given the aggressive nature of tumor growth in this model. Based on the NIS imaging results after only one NIS-MSC application (Fig. 2G-I), the therapy study was performed with three cycles of one NIS-MSC application, followed by ^{131}I injection 48 h later (Fig. 4). Mice were then monitored on a 7T dedicated animal MR scanner as soon as they fulfilled the inclusion criteria. Treatment with NIS-MSCs started on the day of the inclusion scan.

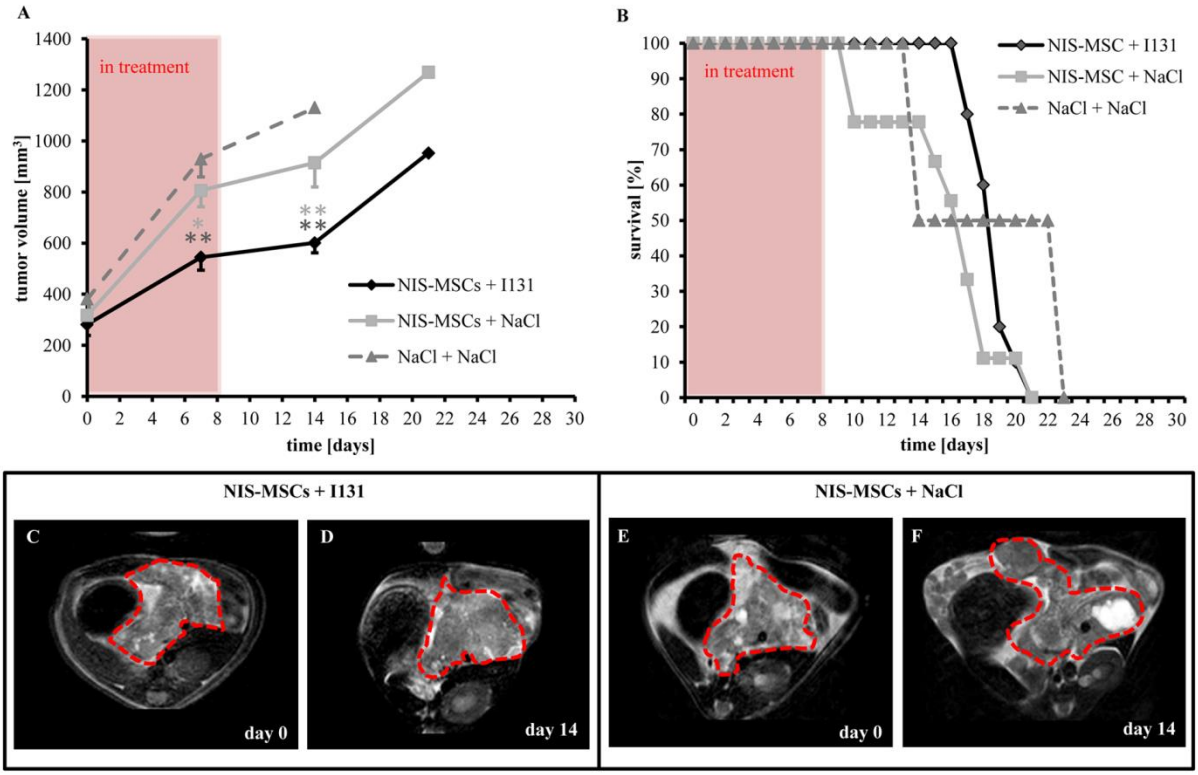

Fig. 4: *^{131}I therapy study led to a delay in tumor growth. For in vivo radionuclide therapy studies, therapy mice received a single NIS-MSC application followed by 55.5 MBq ^{131}I 48 h later and this cycle was repeated to a total of three (n=10). Therapy mice harboring PDAC resulted in a significant delay in tumor burden* ***(A, C, D)*** *as compared to controls receiving NIS-MSCs and NaCl instead (n=9)* ***(A, E, F)*** *or NaCl only* ***(A)****. However, no significantly improved survival was observed* ***(B)****.*

The MR imaging was done on a weekly basis to closely monitor PDAC growth kinetics (Fig. 4A). Tumor analysis of the different groups revealed a significant delay and reduction of tumor burden of the animals in the therapy group (NIS-MSCs + ^{131}I) (Fig. 4A, C, D) as compared to control groups (NIS-MSCs + NaCl (Fig. 4A, E, F) and NaCl + NaCl (Fig. 4A)) [39]. After an initial exponential growth in all groups, which was significantly decreased in therapy mice, a plateau occurred in the therapy group with almost complete stop of tumor growth (Fig. 4A). However, no significant difference in survival was detected (Fig. 4B).

Histological and immunohistochemical analysis

Morphologically, there were only slight differences between the pancreatic neoplasia of all groups. All tumors were moderately to poorly differentiated and showed predominantly ductal growth patterns. No tumor cell necrosis or apoptosis as signs of tumor regression were observed after treatment. Interestingly, in animals receiving

NIS-MSCs, stroma content (consisting of cancer-associated fibroblasts and extracellular matrix (glyco-) proteins) was more pronounced.

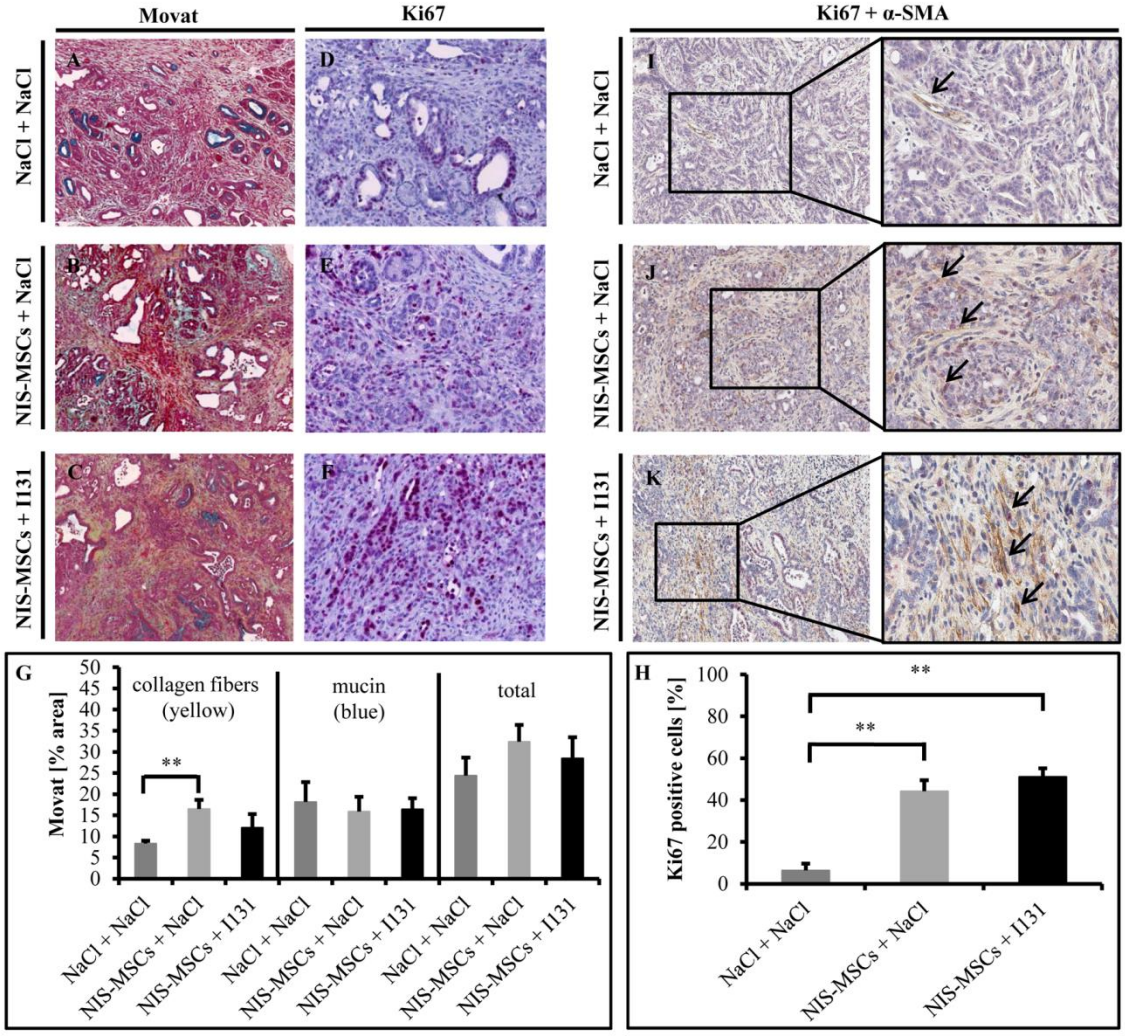

Fig. 5: *Immunohistochemical analysis. In tumors of mice receiving NIS-MSCs and saline, movat staining demonstrated a significant increase of collagen fibers as compared to mice receiving saline only* ***(A-C, G)****. Also, in tumors of mice receiving NIS-MSCs + ^{131}I a more modest increase (not reaching statistical significance) of collagen fibers was observed. No difference in extracellular interstitial or intracellular mucin was observed* ***(A-C, G)****. Ki67 staining detected more proliferating cells within the tumor and stroma of mice receiving NIS-MSCs as compared to mice receiving saline only* ***(D-F, H)****. A double stain for Ki67 and the activated fibroblast marker α-SMA* ***(I-K)*** *revealed α-SMA-positive fibroblasts within the neoplasia of all mice, regardless of the treatment, but differed in the arrangement within the tumor and stroma (black arrows)* ***(I-K)****. In the control group, which received saline only, no Ki67-positive fibroblasts were detected* ***(I)****. Single α-SMA-positive proliferating fibroblasts were visible within the tumor stroma of mice receiving NIS-MSCs* ***(J, K)****. One representative image is shown each using 5x (Movat staining), 10x (Ki67 staining) or 20x as well as 40x (Ki67 and α-SMA double staining) magnification. Data are represented as mean values ± SEM (*P<0.05; **P<0.01, ***P<0.001).*

To further analyze the changes within the tumor microenvironment due to the presence of MSCs, further immunohistochemical analysis of tumors was performed. Movat staining revealed a significant increase of collagen fibers within tumors of mice receiving NIS MSCs + NaCl, as well as a more modest increase (not reaching statistical significance) in therapy mice (NIS-MSCs + ^{131}I) as compared to tumors of control mice that received no MSCs (NaCl + NaCl) (Fig. 5A-C, G). No change in extracellular interstitial or intracellular mucin was seen between the different groups (Fig. 5A-C, G). Quantification of proliferating cells (Ki67) within the tumor and stroma cells showed a higher number of Ki67 positive cells within the tumor stroma of mice receiving NIS-MSCs as compared to mice receiving saline only (NaCl + NaCl) (Fig. 5D-F, H), a double stain for Ki67 and the activated fibroblast marker α-SMA was performed to determine if fibroblasts are proliferating within the tumor stroma (Fig. 5I-K). As expected, α-SMA positive fibroblasts were detected within the neoplasia of all mice, regardless of the treatment. In animals that received saline only, the fibroblasts were loosely arranged between tumor cell nests and ducts, and no proliferating fibroblasts were detected (Fig. 5I). In contrast to those findings, in tumors of mice receiving NIS-MSCs + NaCl or NIS-MSCs + ^{131}I an increased number of α-SMA positive fibroblasts surrounding the tumor cell nests and ducts were detected, often building one to two layers completely surrounding the neoplastic cells (Fig. 5J, K). Single fibroblasts displayed double positivity for α-SMA and Ki67 (Fig. 5J, K). Stainings for CD45, CD11b, F4/80, CD206 and cleaved Caspase-3 revealed no differences in intratumoral cell numbers between the groups.

3.5 Discussion

Due to the increasing incidence and lack of effective therapeutic options, pancreatic cancer may become the second leading cause of cancer deaths by 2030, illustrating the urgent need for new therapeutic strategies [85]. Various combinations of chemotherapies have shown some degree of therapeutic efficacy and slightly increased overall survival, but are accompanied by high toxicity [71, 86, 87]. Our increasing understanding of the central molecular targets and the pivotal role of the microenvironment and its regulation in PDAC, has suggested new directions for the development of novel therapeutic strategies. GEMMs provide a far better platform for the evaluation of these novel therapy strategies, and for the prediction of a therapy response, with a better perspective for subsequent translation to the clinic. We evaluated the effects of a MSC-mediated NIS-based radionuclide therapy approach in a GEMM showing a complex and prominent desmoplastic component. Our previous studies of *NIS*-based gene transfer using MSCs as delivery vehicles have shown excellent tumor homing and expression of the *NIS* transgene in MSCs, as well as significant therapeutic effects after ^{131}I treatment in subcutaneous and orthotopic xenograft models of human hepatocellular carcinoma and colon metastases. In the present study, we have built on these studies to further evaluate the MSC-mediated *NIS* gene therapy approach in a more challenging and clinically highly relevant PDAC mouse model [57-60]. An important advantage of the *NIS* therapy gene is its additional role as a reporter gene, allowing noninvasive monitoring by ^{123}I-scintigraphy and/or ^{124}I-PET-imaging. ^{123}I-scintigraphy of previous studies revealed a radioiodide uptake of 7-9 % ID/g tumor using the same CMV-NIS construct introduced into human MSCs, which were adoptively applied in nude mice harboring subcutaneous tumors from a human hepatocellular carcinoma cell line (HuH7) [57]. In comparison, the ^{123}I-scintigraphy data shown here demonstrate with both MSC application schemes an impressive level of tumor-selective MSC recruitment and NIS transgene expression in endogenous PDAC with an almost 100% increase in radioiodide uptake activity per gram tumor. However, the iodide efflux was slightly faster in the group with only one MSC application as compared to the group receiving a total of three MSC applications. As the tumoral iodide uptake and calculated tumor absorbed dose of 100.7 mGy/MBq for ^{131}I was expected to be high enough for a therapy effect, based on past experience, we conducted the therapy study using the

single NIS-MSC application regimen. We observed a significant delay in tumor growth in the therapy group that received NIS-MSCs followed by ^{131}I in addition to a plateau in tumor growth between the first and second week as compared to control groups, which showed continued growth over the entire observation period [39]. Interestingly, a slight plateau in tumor growth between week one and two was also seen in the control group receiving NIS-MSCs and NaCl.

The results shown here are in line with some studies demonstrating a general inhibitory effect of MSCs on tumor growth [88-91]. Kidd *et al.* detected significant tumor suppression by MSCs using an orthotopic pancreatic carcinoma xenograft mouse model [90]. Similarly, Nakamura *et al.* demonstrated reduced tumor growth in a rat glioma model induced by MSCs [90, 91]. Further, MSCs were shown to down-regulate the protein kinase Akt in Kaposi's sarcoma tumor cells *in vitro*, resulting in tumor growth inhibition [89]. Another study using human stromal cells derived from adipose tissue, which share many characteristics of MSCs, demonstrated a dose-dependent inhibitory effect on proliferation of PDAC-derived Capan-1 cells *in vitro* as well as *in vivo,* where reduced tumor growth was seen in Capan-1 xenograft tumors [88]. Further, less proliferation and even an induction of tumor cell death was observed *in vitro* using conditioned medium from stromal cells derived from adipose tissue and MSCs. This effect was driven by inhibition of the cell cycle G1-phase [88]. Taken together, these studies suggest that MSCs are able to modulate and influence cancer cells in their proliferative and apoptotic behavior and this might explain the phenomenon seen in our therapy trial. Another aspect worth looking at is the tumor stroma. Previous studies point out the tumor-suppressive, rather than supportive, role of the tumor stroma and its compartments in PDAC [92, 93]. Rhim *et al.* suggest that specific components of the tumor stroma, such as myofibroblasts among others, play a tumor-suppressive role [93]. Furthermore, fibrosis associated with myofibroblasts and type-1 collagen seems to have rather a protective role for the host than a supportive role for pancreatic cancer [92]. In the present study we were able to demonstrate a change in the content of collagen fibers in tumors of mice that were injected with NIS-MSCs, as compared to tumors without MSCs (NaCl-NaCl group). These findings go along with the observation that some types of collagens are more likely to be tumor-suppressive [92]. Further, a major difference in the number of proliferating cells was observed in tumors containing NIS-MSCs as compared to tumors without. In contrast to those findings, former studies of our group, using

subcutaneous or orthotopic liver carcinoma as well as colon cancer liver metastasis mouse models, demonstrated a significant decrease of proliferating tumor cells of therapy tumors as compared to control groups [57, 58, 60]. Completely unexpected in the current study, we observed a significant increase of Ki67 in tumors containing NIS-MSCs (therapy and control group) as compared to tumors without MSCs (saline only). As it seemed that in both groups receiving NIS-MSCs proliferating cells were rather cells of the stromal compartment than tumor cells, we performed a Ki67 and α-SMA double staining to examine the content and proliferating potential of fibroblasts within these groups. Results demonstrated a higher content of activated fibroblasts within the tumor stroma of tumors containing NIS-MSCs as compared to the saline only control group. Further, it was observed that fibroblasts were located immediately around tumor cell nests and infiltrative ducts, which was not seen in the absence of NIS-MSCs. These findings resemble observations in human pancreatic tumors, where cancer-associated fibroblast (CAFs) are also densely arranged around the tumorous structures [94]. How these CAFs affect tumor development and growth is not fully understood yet. Some studies suggest that they promote tumor growth and that an increased number of α-SMA-positive myofibroblasts is associated with a poor prognosis, whereas other studies, as already discussed and which corroborate our findings, allot fibroblasts a rather protective role for the host [95]. Altogether the data presented here suggest that the systemically applied NIS-MSCs are actively recruited to the growing pancreatic carcinoma stroma, where they seem to influence the proliferation of various tumor associated cells through their secretion of growth factors resulting in increased Ki67 stain and altered arrangement of α-SMA-positive cells. As NIS-MSCs should be destroyed in the context of ^{131}I treatment, the described processes would already take place before radioiodine treatment. Further investigations of changes in CD45, CD11b, F4/80, CD206 and cleaved Caspase-3 did not reveal differences between therapy and control groups and showed rather a heterogeneous staining within the same group. However, a focus on secondary effects of MSC delivery on intratumoral immune cell regulation is a key aim in future studies albeit beyond the scope of this current work. Although our findings demonstrated changes in the composition of the tumor stroma and the tumor micromilieu, the exact mechanisms underlying the reduced tumor growth in this mouse model under our experimental conditions have to be further investigated. A more intensive investigation, taking the tissue complexity of PDAC into consideration

as well as the ability of MSCs themselves to modulate the tumor microenvironment, might provide the possibility to use MSCs not only for targeted therapy but also in combination with chemotherapy or immune approaches.

Although tumor growth was significantly reduced in the present study, no prolonged survival was observed in mice receiving treatment likely due to the overall highly aggressive course of disease in this model. Mice in the control group receiving NIS-MSCs and NaCl had to be sacrificed as early as 9 days after treatment start, whereas the first mice in the therapy group had to be sacrificed at day 16. Around that time, therapy mice showed rapid health deterioration and had all to be sacrificed within a few days. Despite smaller tumors, these mice showed adverse symptoms such as ascites or icterus, which also occurred in the control group and were reasons for sacrifice.

Recently our group had also reported the application of the *NIS* gene therapy approach in the same PDAC GEMM using EGFR-targeted polyplexes for *NIS* transgene delivery, which resulted in tumor reduction and prolongation of survival [39]. Polyplexes based on linear polyethylenimine (LPEI) are accompanied by endogenous cytotoxic effects. While these effects were not seen in former studies using subcutaneous xenograft mouse models, toxicity to the LPEI-based polyplexes was observed in *Kras;p53* mice. In contrast to those findings, MSCs did not show toxic side effects in animals of former studies as well as of the current study using the same PDAC mouse model. For this mouse model, MSCs thus might be a better choice for NIS-mediated radioiodine therapy. Our results demonstrate the potential of genetically modified MSCs in PDAC to reduce tumor growth. We are aiming at further optimization of MSC-mediated *NIS* gene therapy approach to enhance therapeutic efficacy. For proof-of-principle of MSC-mediated *NIS* gene delivery in this PDAC model, the unspecific CMV-promoter was used to control NIS expression. More specific promoters with enhanced tumor-specificity specifically designed for the respective tumor environments are currently under evaluation. Recent studies using a tumor stroma-specific RANTES/CCL5 promoter in an orthotopic liver metastases mouse model led to reduced metastases growth and improved survival of animals [59]. Further, as hypoxia is a common feature in tumors driving angiogenesis and resistance to conventional therapies, a synthetic hypoxia inducible factor (HIF)-responsive promoter was designed to target NIS expression into hypoxic tumor cells in an orthotopic HCC xenograft mouse model by our group, resulting in reduced

tumor growth and prolonged survival [60]. Using a tumor-specific promoter designed for the tumor stroma of PDAC might enable increased *NIS* transgene expression and improved therapeutic efficacy of radionuclide therapy. Additionally, application of the alternative radionuclide ^{188}Re instead of ^{131}I will be considered for therapy. ^{188}Re is also transported by NIS and offers different advantages compared to ^{131}I: it provides the possibility to enhance tumor absorbed doses due to higher energy and shorter half-life, and is associated with an increased crossfire effect due to a longer path length (up to 10.4 mm as compared to ^{131}I with 2.4 mm) [58]. A further option for improvement would be the combination with radiosensitizing agents, such as gemcitabine – a commonly used chemotherapeutic drug in pancreatic cancer, to increase radiosensitivity of tumors, which in turn might lead to enhanced therapeutic effectiveness of MSC-based NIS-mediated radioiodine therapy.

Taken together, our results show great potential of MSC-mediated *NIS* gene delivery in PDAC. Adoptively applied NIS-MSCs were actively recruited to PDAC in a highly efficient manner resulting in high tumor-specific radioiodide uptake as confirmed by ^{123}I-scintigraphy and ^{124}I-PET imaging. The translation of these results into a therapy study showed significantly delayed and reduced tumor growth. Our data also demonstrate the high potential of the application of NIS reporter gene imaging for monitoring and planning of a *NIS* gene therapy approach in PDAC in a clinical setting.

3.6 Acknowledgments

We are grateful to Prof. Dr. K. Scheidhauer and Jakob Allmann, Department of Nuclear Medicine, Klinikum rechts der Isar der Technischen Universität München, Munich, Germany, for their assistance with the imaging studies. We thank Doris Mayr (Department of Pathology, Ludwig-Maximilians-University, Munich, Germany) for preparation of paraffin-embedded slides and Marion Mielke (Department of Pathology and Comparative Experimental Pathology, TU Munich) for performing the immunohistochemistry. This work was supported by grants from the Deutsche Forschungsgemeinschaft within the Collaborative Research Center SFB 824 to C Spitzweg (project C8), to J Siveke (project C4) and to K Steiger (project Z2), within the Priority Program SPP1629 to C Spitzweg and PJ Nelson (SP 581/6-1, SP 581/6-2, NE 648/5-2), within the European Community's Seventh Framework Program (FP7/CAM-PaC) under grant agreement no. 602783, by the German Cancer Consortium (DKTK) to J Siveke as well as within a grant from the Wilhelm-Sander-Stiftung to C Spitzweg (2014.129.1). The authors declare no conflict of interest. This work was performed as partial fulfillment in the doctoral thesis of Christina Schug within the LMU Medical Faculty and Aayush Gupta within the TUM Medical Faculty.

4. Chapter 2: TGFB1-driven mesenchymal stem cell-mediated *NIS* gene transfer

This chapter has been adapted from:

Schug C[1], Urnauer S[1], Jaeckel C[2], Schmohl KA[1], Tutter M[1], Steiger K[3], Schwenk N[1], Schwaiger M[4], Wagner E[5], Nelson PJ[2] and Spitzweg C[1], TGFB1-driven mesenchymal stem cell-mediated *NIS* gene transfer. Endocrine-Related Cancer. 2018 August. [Epub ahead of print]

[1]Medizinische Klinik und Poliklinik IV - Campus Grosshadern, University Hospital of Munich, LMU Munich, Munich, Germany, [2]Clinical Biochemistry Group, Medizinische Klinik und Poliklinik IV, University Hospital of Munich, LMU Munich, Munich, Germany, [3]Institute of Pathology, Klinikum rechts der Isar der Technischen Universität München, Munich, Germany, [4]Department of Nuclear Medicine, Klinikum rechts der Isar der Technischen Universitaet Muenchen, Munich, Germany, [5]Department of Pharmacy, Center of Drug Research, Pharmaceutical Biotechnology, LMU Munich, Munich, Germany

4.1 Abstract

Based on their excellent tumor-homing capacity, genetically engineered mesenchymal stem cells (MSCs) are under investigation as tumor-selective gene delivery vehicles. Transgenic expression of the sodium iodide symporter (*NIS*) in genetically engineered MSCs allows noninvasive tracking of MSC homing by imaging of functional NIS expression as well as therapeutic application of ^{131}I. The use of tumor-stroma activated promoters can improve tumor-specific MSC-mediated transgene delivery. The essential role of transforming growth factor B1 (TGFB1) and the SMAD downstream target in the signaling between tumor and the surrounding stroma makes the biology of this pathway a potential option to better control *NIS* expression within the tumor milieu. Bone marrow-derived MSCs were stably transfected with a *NIS*-expressing plasmid driven by a synthetic SMAD-responsive promoter (SMAD-NIS-MSCs). Radioiodide uptake assays revealed a 4.9-fold increase in NIS-mediated perchlorate-sensitive iodide uptake in SMAD-NIS MSCs after TGFB1 stimulation compared to unstimulated cells demonstrating the successful establishment of MSCs which induce NIS expression in response to activation of TGFB1 signaling using a SMAD-responsive promoter. ^{123}I-scintigraphy revealed significant tumor-specific radioiodide accumulation and thus NIS expression after systemic application of SMAD-NIS-MSCs into mice harboring subcutaneous tumors derived from the human hepatocellular carcinoma (HCC) cell line HuH7, which express TGFB1. ^{131}I therapy in SMAD-NIS-MSCs-treated mice demonstrated a significant delay in tumor growth and prolonged survival. Making use of the tumoral TGFB1 signaling network in the context of MSC-mediated NIS gene delivery is a promising approach to foster tumor stroma-selectivity of NIS transgene expression and tailor NIS-based gene therapy to TGFB1-rich tumor environments.

4.2 Introduction

Therapeutic options for hepatocellular carcinoma (HCC) are limited and novel targets and therapeutic strategies are urgently needed considering the increasing incidence of HCC worldwide [2, 72]. Solid tumors are thought to be seen by the body as “wounds that never heal” driving tissue repair and remodeling with active recruitment of mesenchymal stem cells (MSCs). This biology has been used to generate engineered versions of adoptively applied MSCs as a tool to deliver therapeutic genes, such as the sodium iodide symporter (*NIS*), deep into tumor microenvironments [45, 46]. NIS is an intrinsic transmembrane glycoprotein with 13 putative transmembrane domains that mediates the active transport of iodide into the thyroid. When used in the context of a reporter gene, *NIS* can be used for noninvasive imaging of *NIS* transgene biodistribution by well-established multimodal nuclear medicine techniques, such as ^{123}I-scintigraphy and ^{124}I-PET imaging. At the same time, it can be used as an effective therapy gene after application of radioiodine ^{131}I [20-23]. A diverse series of studies have demonstrated the efficacy of NIS-mediated radioiodide accumulation in a variety of non-thyroidal tumors using different gene delivery vehicles for *NIS* transgene expression [28, 30, 33, 34, 36-38, 41, 56-60, 96-101]. The use of genetically engineered MSCs to deliver *NIS* into various types of tumors has been demonstrated in many studies [56-60]. Although these results have shown comparably high levels of *NIS* transgene expression in the tumor microenvironment followed by a therapeutic effect of ^{131}I, with a delay in tumor growth and prolonged survival of treated animals, the use of specific gene promoters for *NIS* expression that are activated by tumor micromileu-derived signals has been shown to enhance selectivity and effectiveness and limit potential off-target effects following MSC recruitment to tissues as part of normal tissue homeostasis [28, 30, 33, 34, 36-38, 41, 57-60, 81]. We have studied various gene promoters for the delivery of MSC-transgene expression in tumor stroma. These include a RANTES (Regulated on Activation, normal T-cell Expressed and presumably Secreted)/CCL5 promoter activated by proinflammatory signals in tumor settings and a synthetic hypoxia-inducible factor (HIF)1-responsive promoter that selectively activates *NIS* transgene expression in tumors by targeting hypoxia, a central feature of solid tumors [58-60]. The use of gene promoters activated by micromilieu-derived signals also offers the possibility of tailoring the NIS-therapy approach to the individual tumor

micromilieu. The transforming growth factor B (TGFB) signaling pathway is strongly linked to the biology of tumor cells and their microenvironment. The TGFB signaling pathway is involved in cell growth, apoptosis, invasion, angiogenesis and immune response regulation [102]. The isoforms of TGFB (TGFB1, -B2 and -B3) bind to heteromeric complexes of type I and II transmembrane Ser/Thr kinase receptors leading to transphosphorylation of the GS domain of the type I kinase through the type II receptor kinase resulting in phosphorylation of downstream target proteins such as SMADs [103-105]. Activated SMAD2 and SMAD3 form heterotrimeric complexes with the signal mediator SMAD4. The complex translocates to the nucleus to modulate transcription of target genes. Inhibitory SMADs, such as SMAD6 and SMAD7, interfere with the type I receptors, thereby blocking phosphorylation of other SMADs [106]. SMAD7 expression is also driven by TGFB signaling thus inducing a TGFB-induced negative feedback loop [106]. Depending on early or late steps of carcinogenesis, some tumors are able to shut down the tumor-suppressive part of this signaling pathway thereby restricting it to pro-tumoral effects [107]. TGFB is present in the micromileu of most tumors [108]. In addition to the tumor cells, cancer-associated fibroblasts (CAFs) and stellate cells of the surrounding tumor stroma also secrete TGFB to control inflammatory response [102, 107]. CAFs and stellate cells can promote tumor growth and metastasis among others [107]. The TGFB pathway is strongly associated with HCC as it is well known to be dysregulated in these tumors [106]. Several studies demonstrated that in almost 50% of HCCs TGFB signaling is significantly upregulated [109, 110]. TGFB plays an important role in tumor angiogenesis and its regulation in HCC [102]. From the three different isoforms of TGFB (TGFB1, -B2 and -B3), TGFB1 is most commonly upregulated isoform in cancer cells [103]. The critical role of TGFB1 in HCC tumor biology makes the TGFB signaling pathway a promising tool for targeting *NIS* transgene expression by engineered MSCs in experimental HCC, with the aim to enhance tumor stroma selectivity and improve therapeutic effectiveness.

In the current study, we used a TGFB1-inducible SMAD-responsive promoter to control *NIS* transgene expression in genetically engineered human MSCs. After adoptively applying MSCs in HCC xenografts, MSC biodistribution and biological targeting of *NIS* expression to the tumor stroma through NIS-mediated accumulation of radioiodide was examined by ^{123}I-scintigraphy. Therapeutic efficacy was determined by ^{131}I application after systemic MSC-mediated *NIS* transgene delivery.

4.3 Materials and methods

Cell culture

The human hepatocellular carcinoma cell line HuH7 was authenticated and purchased from JCRB Cell Bank (JCRB 0403, Osaka, Japan). Cells were cultured in DMEM (Sigma-Aldrich, St. Louis, Missouri, USA) supplemented with 10% FBS (FBS Superior, Biochrom/Merck Millipore, Berlin, Germany) and 100 U/ml penicillin/100 µg/ml streptomycin (Sigma-Aldrich). The human breast adenocarcinoma cell line MDA-MB 231 was cultured in RPMI (Sigma-Aldrich), supplemented with 10% FBS and 100 U/ml penicillin/100 µg/ml streptomycin. The human bone marrow-derived, SV40 large T antigen immortalized MSC cell line used here was established as described previously [111] and cultured in RPMI (Sigma-Aldrich), supplemented with 10% FBS and 100 U/ml penicillin/100 µg/ml streptomycin. The easily engineered and expandable cells were previously shown to demonstrate similar homing and activation characteristics as seen in primary human MSCs (Von Luttichau, et al. 2005). All cells were maintained in an incubator at 37°C and 5% CO_2.

Plasmid constructs

The expression vector pcDNA6-2ITRNEO-SMAD-NIS was established using the Multiside Gateway Pro Plus Kit (Invitrogen Thermo Scientific, Waltham, Massachusetts, USA) following the manufacturer's instructions. The promoterless Gateway destination vector (pcDNA6) contains a Sleeping Beauty transposon system as described previously [112]. The used SMAD-responsive promoter consists of a 5× multimer of the *SMAD* binding site AGCCAGACAGT. The vector pSBTR.TGF/SMAD2 containing the promoter was established as described previously [112]. Full length *NIS* cDNA was removed from the pcDNA3 expression vector and was cloned into the vectors provided in the Multiside Gateway Pro Plus Kit. After a 2-fragment recombination the pcDNA6-2ITRNEO-SMAD-NIS plasmid was obtained. The resulting plasmid contains the *NIS* gene driven by a SMAD-responsive promoter, two sleeping beauty transposition sites and a geneticin resistance gene. The vectors pSB.H.CMV/TO.SMAD3 (expressing SMAD3) and pSB.H.CMV/TO.SMAD4 (expressing SMAD4) were constructed as described previously [112].

Stable transfection of MSCs

Wild type MSCs (WT-MSC) were stably transfected with the pcDNA6-2ITRNEO-SMAD-NIS expression vector in combination with the pCMV(CAT)T7-SB100X plasmid (provided from Z Ivics, Max Delbrück Center for Molecular Medicine, Berlin, Germany). The pCMV(CAT)T7-SB100X vector contains a Sleeping Beauty transposase system for transgene insertion into the host cell genome. 0.5×10^6 MSCs and a total amount of 3 µg plasmid were electroporated at 1300 V, 30 ms width and 1 pulse using the Neon® transfection system (Invitrogen, Karlsbad, California, USA). Selection medium was given 24 h after electroporation and contained 0.5 mg/ml geneticin (Invitrogen) in RPMI medium supplemented with 10% fetal bovine serum and 100 U/ml penicillin/100 µg/ml streptomycin. The resulting clones were isolated and analyzed for NIS-mediated radioiodide uptake activity using an iodide uptake assay (see below). Among ~40 screened colonies, the stably transfected cell clone with the highest levels of iodide accumulation was termed SMAD-NIS-MSC and used for further experiments.

For a more precise investigation of the SMAD-responsive promoter, SMAD-NIS-MSCs were further stably transfected with pSB.H.CMV/TO.SMAD3 (SMAD-NIS-MSCs+SMAD3), pSB.H.CMV/TO.SMAD4 (SMAD-NIS-MSCs+SMAD4), pSB.H.CMV/TO.SMAD3 and pSB.H.CMV/TO.SMAD4 (SMAD-NIS-MSCs+SMAD3+SMAD4) vector. For cells transfected with expression vectors for SMAD3 and/or SMAD4, 0.2 mg/ml Hygromycin was added to the cell culture medium described above. This stably transfected cell lines were maintained and tested as bulk cultures.

Tumor cell conditioned medium

1×10^6 HuH7 or MDA-MB 231 cells were seeded on 100 mm^3 surface cell culture plates and starved for 12 h. Supernatant from the tumor cells (HuH7 conditioned medium (HuH7-CM) or MDA-MB 231-CM) was removed after 48 h, centrifuged and stored at -80°C.

^{125}I uptake assay

Inducibility of the promoter was determined by starving cells overnight (medium without FBS) followed by stimulation of SMAD-NIS-MSCs and variants of those (see above) with 0-25 ng/ml recombinant TGFB1 for 24h in normal medium as described

above. NIS-mediated radioiodide uptake was determined at steady-state conditions as described previously by Spitzweg *et al*. [66]. Results were normalized to cell viability.

Cell viability assay

Cell viability was measured using the commercially available MTT assay (Sigma-Aldrich, ratio 1:100) according to the manufacturer's recommendations. For the measurement of the absorbance of the formazan product at a wavelength of 620 nm, a Sunrise Microplate Absorbance Reader (Tecan, Männedorf, Switzerland) was used.

Animals

Female 5-week-old CD1 nu/nu mice from Charles River (Sulzfeld, Germany) were housed under specific pathogen-free conditions. Mice had access to mouse chow and water *ad libitum*. Experiments were approved by the regional governmental commission for animals (Regierung von Oberbayern).

HuH7 xenograft tumors

For HuH7 xenograft tumor establishment, 5×10^6 HuH7 cells in 100 µl PBS were injected subcutaneously into the right flank region as described previously [57]. Tumor volumes were regularly measured and estimated using the equation: length × width × height × 0.52. Mice were sacrificed when tumors exceeded a size of 1500 mm^3.

^{123}I-scintigraphy

To suppress thyroidal iodide uptake the drinking water of the mice was supplemented with 5 mg/ml L-T4 (Sigma-Aldrich). SMAD-NIS-MSCs were applied three times every second day *via* the tail vein at a concentration of 5×10^5 cells in 500µl PBS. 72 h after the last MSC application mice were injected intraperitoneally with 18.5 MBq (0.5 mCi) ^{123}I. The gamma camera was equipped with a low-energy high resolution collimator (e.cam, Siemens, Munich, Germany) and was used to measure radioiodide biodistribution. For the analysis of regions of interests (ROIs) HERMES GOLD (Hermes Medical Solutions, Stockholm, Sweden) software was used. Results are expressed as % ID/g. The radionuclide retention time was determined by serial scanning within the tumors. Dosimetric calculations were performed according to the

concept of medical internal radiation dose using the dosis factor of RADARgroup (www.dosisinfo-radar.com).

Immunohistochemical staining

After systemic SMAD-NIS-MSC administration and imaging studies, HCC xenografts or other organs (liver, lung and spleen) were dissected from all mice of the ^{123}I-scintigraphy study and tissues embedded in paraffin. Immunohistochemical NIS staining of paraffin-embedded tissue sections was performed as described previously [84]. Immunohistochemical staining of TGFB1 was performed on HuH7 tumors on a BenchMark XT automated stainer (Ventana, Tucson, AZ) with an antibody against TGFB (ab92486, abcam, Cambridge, UK) using the ultraVIEW DAB Detection Kit (all reagents from Ventana, Tucson, AZ). The tumor sections were deparaffinized with EZ Prep at 75°C and 76°C, heat pretreated in Cell Conditioning 1 (CC1) for antigen retrieval at 76°C – 100°C and then incubated with the primary antibody diluted in antibody diluent 1:150 for 32 min at 37°C after inactivation of the endogenous peroxidase using UV-inhibitor for 4 min at 37°C. The slides were incubated with a HRP Universal Multimer for 8 min. Antibody binding was detected using DAB as chromogen and counterstained with hematoxylin for 10 min with subsequent bluing in bluing reagent for 10 min. Afterwards, slides were manually dehydrated by washing with alcohol of increasing concentration (70%, 96%, 100%) and xylene, and coverslipped using Pertex® mounting medium (Histolab, Goeteborg, Sweden, 00801).

Radioiodine therapy study

Mice were treated 10-days before therapeutic application of radioiodide with 5 mg/ml L-T4 in their drinking water as described above. The therapy group received three SMAD-NIS-MSC injections on every second day (each 5 × 10^5 cells/500 µl PBS) followed by 55.5 MBq ^{131}I 48 hours after the last SMAD-NIS-MSC injection (n=6; SMAD-NIS-MSCs + ^{131}I). As a control, a subset of mice received saline (NaCl) instead of radioiodine (n=6; SMAD-NIS-MSCs + NaCl). 24 h after the ^{131}I or NaCl application the treatment cycle was repeated. One additional MSC application followed by a third ^{131}I (55.5 MBq) or NaCl injection 48 hours later was done for therapy completion. A further control group was injected with NaCl only (n=5; NaCl + NaCl). Tumor volume was measured regularly and estimated as described above. Mice were euthanized when the tumor volume exceeded 1500 mm^3.

Indirect immunofluorescence assay

Frozen tissue sections of tumors from the radioiodine therapy study were used for indirect immunofluorescence analysis of Ki67 (cellular proliferation) and CD31 (blood vessel density) as described previously [60]. Identical conditions as for illumination, exposure time and system settings for digital image processing were used for capturing regions of the slides. The percentage of positive cells for Ki67 and areas for CD31 in the tumors was quantified by evaluation of 6 high-power fields per tumor using ImageJ software (NIH, Bethesda, MD). Results are presented as means ± SEM.

Statistical methods

Results are expressed as mean ± SEM, mean-fold change ± SEM or percentage. Statistical significance for *in vitro* experiments was tested by two-tailed Student´s *t*-test. Statistical significance for *in vivo* experiments was perfomed by one-way ANOVA for tumor volumes and log-rank test for survival plots. *P* values of < 0.05 were considered significant (*$p < 0.05$; **$p < 0.01$; ***$p < 0.001$).

4.4 Results

SMAD-NIS-MSCs show enhanced NIS-mediated radioiodide accumulation following TGFB1 stimulation

Radioiodide uptake assays revealed a 3.4 to 4.9 fold increase in NIS-mediated radioiodide uptake activity in MSCs stably transfected with the *NIS* gene under control of a SMAD-responsive promoter (SMAD-NIS-MSCs) after stimulation with TGFB1 (5-25 ng/ml) (Fig. 1A). Stimulation with 5-15 ng/ml TGFB1 resulted in a dose dependent increase of radioiodide accumulation, which reached a plateau at higher doses of TGFB1 (20 or 25 ng/ml). NIS-specificity was confirmed using the NIS-specific inhibitor perchlorate, which blocked radioiodide uptake in all experiments (Fig. 1A).

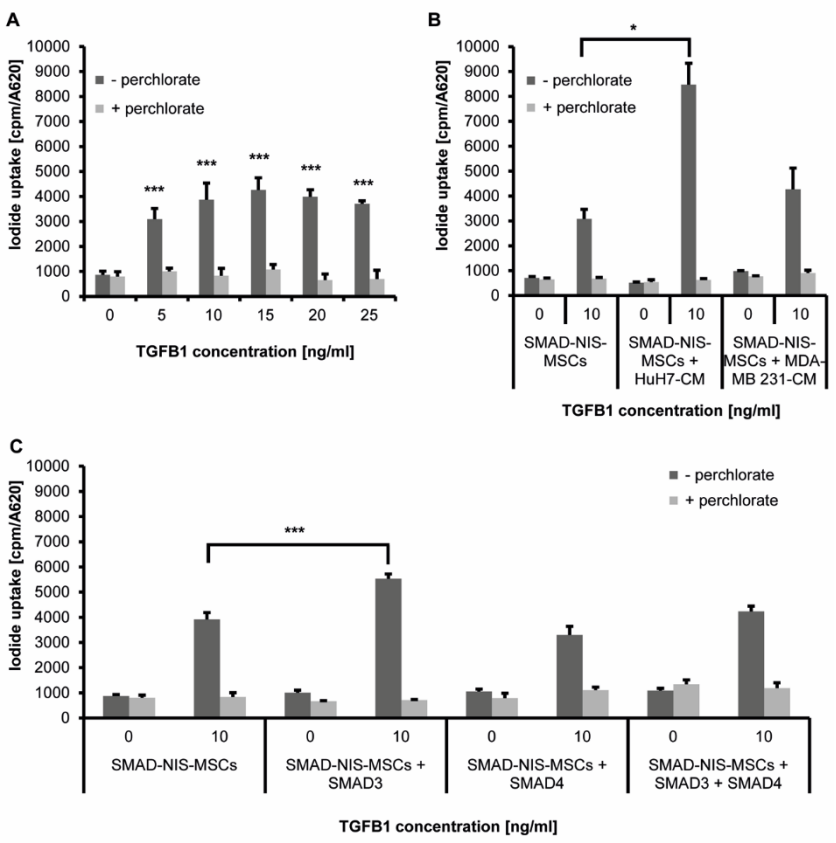

Fig. 1: *Establishment of mesenchymal stem cells (MSCs) stably expressing NIS under control of a SMAD-responsive promoter. Iodide uptake studies revealed a 3.4 up to 4.9-fold high NIS-specific and perchlorate-sensitive ^{125}I uptake in SMAD-NIS-MSCs stimulated with TGFB1 (5-25 ng/ml) as compared to unstimulated cells, where no radioiodide uptake above background levels was observed*

***(A)**. Combined treatment of SMAD-NIS-MSCs with TGFB1 (10 ng/ml) and HuH7-CM led to further increased radioiodide uptake as compared to stimulated cells without HuH7-CM **(B)**. In contrast to that, a stimulation with MDA-MB 231-CM and TGFB1 did not result in a significant increase in radioiodide uptake activity of SMAD-NIS-MSCs **(B)**. SMAD-NIS-MSCs were additionally transfected with constructs expressing SMAD3 (SMAD-NIS-MSCs + SMAD3), SMAD4 (SMAD-NIS-MSCs + SMAD4) or transfected with both expression constructs (SMAD-NIS-MSCs + SMAD3 + SMAD4) **(C)**. Higher radioiodide uptake activity after TGFB1 (10 ng/ml) treatment was revealed in the presence of SMAD3, whereas it did not increase with higher expression levels of SMAD4. SMAD-NIS-MSCs expressing SMAD3 and SMAD4 showed a radioiodide uptake higher than SMAD-NIS-MSCs and SMAD-NIS-MSCs + SMAD4, but was lower than SMAD-NIS-MSCs + SMAD3 after TGFB1 treatment **(C)**. Data are represented as means of three independent experiments ± SEM (n=3; two-tailed Student's t-test: *p<0.05; ** p <0.01, *** p <0.001).*

SMAD-NIS-MSCs were additionally stimulated by adding HCC (HuH7)-conditioned medium (CM) (Fig. 1B). Stimulation of SMAD-NIS-MSCs with both TGFB1 (10 ng/ml) and HuH7-CM resulted in a robust increase in radioiodide accumulation as compared to stimulation with TGFB1 alone. No radioiodide uptake activity was observed when SMAD-NIS-MSCs were exposed to HuH7-CM only (Fig. 1B). TGFB1 protein levels in HuH7-CM were analyzed by enzyme-linked immunosorbent assay (ELISA), which confirmed TGFB1 protein expression in HuH7 cells, but showed that HuH7-CM contains only inactive TGFB1 (data not shown). These findings correlate with the results shown above, where no radioiodide uptake is seen in SMAD-NIS-MSCs stimulated with HuH7-CM only. Additionally, to determine this effect is also seen with other tumor cells, SMAD-NIS-MSCs were treated with CM from MDA-MB 231 cells (human breast carcinoma cells) (Fig. 1B). Again, stimulation of SMAD-NIS-MSCs with MDA-MB 231-CM alone resulted in no radioiodide uptake activity. Further, only a slight increase of radioiodide uptake was observed after combined treatment with MDA-MB 231-CM and TGFB1 which was not statistically significant.

To further investigate activation of the promoter through TGFB1 (SMAD) signaling, variants of SMAD-NIS-MSCs where established by stably transfecting SMAD-NIS-MSCs with SMAD3 or SMAD4 expression constructs (Fig. 1C). In SMAD-NIS-MSCs transfected with the SMAD3 expression vector (SMAD-NIS-MSCs + SMAD3) TGFB1 stimulation (10 ng/ml) led to significantly increased NIS-mediated perchlorate-sensitive radioiodide uptake as compared to stimulated SMAD-NIS-MSCs. Transfection of SMAD-NIS-MSCs with a SMAD4 expression vector (SMAD-NIS-MSCs + SMAD4) resulted in no increase of radioiodide uptake activity upon TGFB1

stimulation as compared to stimulated SMAD-NIS-MSCs. Combination of SMAD3 and SMAD4 expression in SMAD-NIS-MSCs (SMAD-NIS-MSCs + SMAD3 + SMAD4) revealed an increase of radioiodide uptake after TGFB1 stimulation as compared to stimulated SMAD-NIS-MSCs and as compared to SMAD-NIS-MSCs + SMAD4, but a decrease as compared to TGFB1 stimulated SMAD-NIS-MSCs + SMAD3 (Fig. 1C). No radioiodide uptake activity above background levels was observed without TGFB1 stimulation or upon treatment with perchlorate (Fig. 1C).

Radioiodide biodistribution in vivo

SMAD-NIS-MSCs (0.5×10^6) where injected intravenously via the tail vein into nude mice harboring subcutaneous HCC xenograft tumors, three times in 48 h intervals. 72 h after the last MSC application, 18.5 MBq ^{123}I were administered intraperitoneally. Radioiodide biodistribution monitored by ^{123}I-scintigraphy (Fig. 2) revealed approximately 6.8 ± 0.8 % of the injected dose per gram (ID/g) radioiodide accumulation in tumors after SMAD-NIS-MSC application (Fig. 2A, C). A biological half-life of 2.2 h and a tumor absorbed dose of 28.2 mGy/MBq was calculated for ^{131}I. Endogenous NIS-mediated radioiodide uptake was observed in the stomach, salivary glands and thyroid gland. Radioiodide uptake in the urinary bladder is due to renal excretion of ^{123}I (Fig. 2A). Injection of perchlorate 30 min prior to ^{123}I administration resulted in blockage of radioiodide accumulation in tumors, stomach, salivary glands and thyroid gland (Fig. 2B).

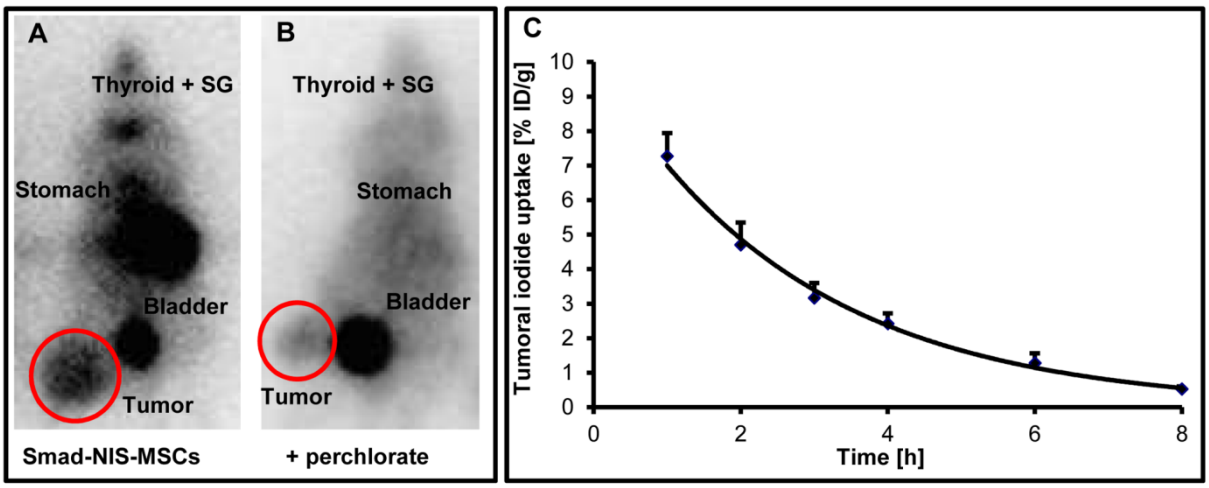

Fig. 2: *^{123}I-scintigraphy showed high NIS-specific tumoral radioiodide uptake. Three systemic injections of SMAD-NIS-MSCs on every second day in mice harboring subcutaneous HuH7 tumors resulted in a maximum of approximately 6.8 % ID/g tumor (n=5)* ***(A, C)****. Tumoral radioiodide uptake*

was blocked upon treatment with the NIS-specific inhibitor perchlorate (n=1) ***(B)****. Data are represented as mean values ± SEM.*

NIS and TGFB1 protein expression in HuH7 tumors ex vivo

To evaluate biodistribution of SMAD-NIS-MSCs *ex vivo*, NIS protein expression in resected tumors and non-target organs (liver, lung, spleen) was investigated by NIS-immunohistochemistry (Fig. 3).

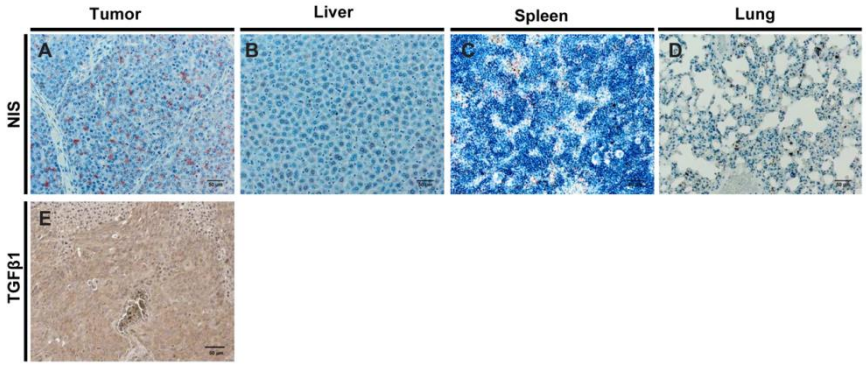

Fig. 3: *Tumor-specific NIS and TGFB1 protein expression. NIS-specific immunoreactivity was detected in all tumors of mice that received systemically applied* SMAD-NIS-MSC*s* **(A)** as c*ompared to non-target organs, where no NIS protein expression was detected* ***(B-D)****. Further,* TGFB1 protein expression was confirmed within subcutaneous HuH7 tumors and the tumor stroma **(E)**. One representative image at 20× magnification is shown each.

Throughout the tumor stroma, NIS-specific immunoreactivity was detected in mice that were injected with SMAD-NIS-MSCs (Fig. 3A), whereas no NIS protein expression was observed in non-target organs (Fig. 3B-D). These data show efficient MSC recruitment into the tumor stroma after systemic application and activation of the SMAD-responsive promoter resulting in NIS protein expression.
To confirm TGFB1 expression in subcutaneous HuH7 tumors, tumors were stained for TGFB1 protein expression, showing TGFB1 expression within tumor and its stroma (Fig. 3E).

In vivo radioiodine therapy studies

Therapeutic efficacy of ^{131}I was evaluated using SMAD-NIS-MSCs in HuH7 tumors (Fig. 4). Animals of the therapy group received two cycles of three SMAD-NIS-MSC applications in 48 h intervals followed by a single ^{131}I injection (55.5 MBq each) after the third MSC application.

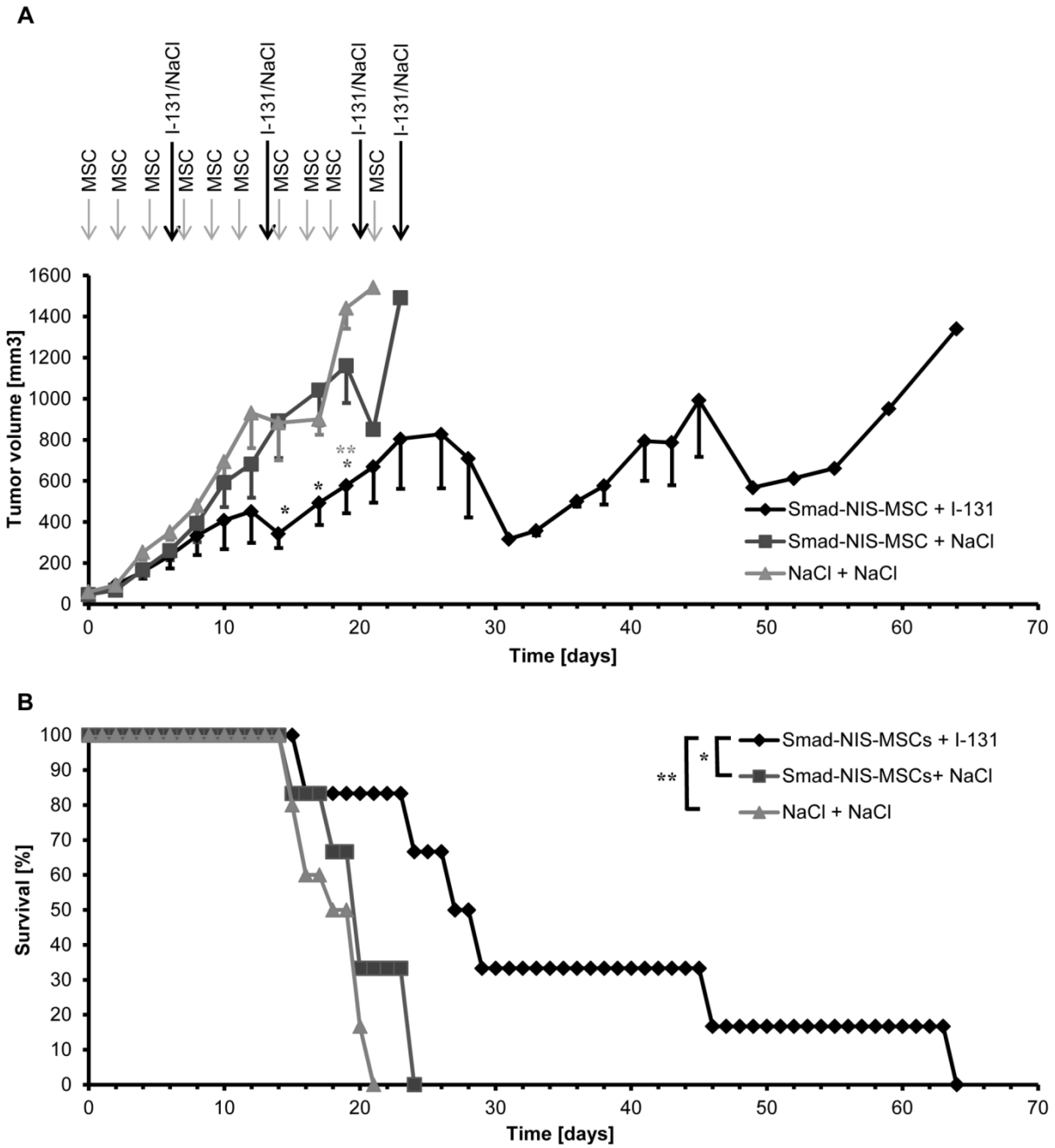

Fig. 4: *^{131}I therapy of subcutaneous HuH7 tumors led to a delay in tumor growth and improved survival. For an in vivo radionuclide therapy study, mice received three SMAD-NIS-MSC applications on every second day followed by 55.5 MBq ^{131}I 48 h after the last MSC injection. For therapy end, a final cycle was done consisting of a single SMAD-NIS-MSC application and ^{131}I injection 48 h afterwards (n=6; SMAD-NIS-MSC + ^{131}I)* ***(A)****. Therapy of mice harboring HuH7 tumors resulted in a significant delay in tumor growth as compared to controls receiving SMAD-NIS-MSCs and NaCl (n=6; SMAD-NIS-MSC + NaCl) or NaCl only (n=5; NaCl + NaCl)* ***(A)****. Further, therapy led to an improved overall survival in therapy animals* ***(B)****.*

For a third and last therapy round, a single SMAD-NIS-MSC application was given followed by a therapeutic dose of ^{131}I. A significant delay in tumor growth was seen in

therapy mice treated with SMAD-NIS-MSCs followed by ^{131}I application (SMAD-NIS-MSCs + ^{131}I) as compared to controls, which received either SMAD-NIS-MSCs followed by application of saline (NaCl) instead of ^{131}I (SMAD-NIS-MSCs + NaCl) or NaCl only (NaCl + NaCl) (Fig. 4A). Both controls showed continuous exponential tumor growth (Fig. 4A). Analysis of survival revealed a maximum of 21-24 days for mice in control groups, whereas mice in therapy showed prolonged survival of up to 63 days (Fig. 4B).

For a more detailed analysis, dissected tumors were stained for Ki67 (green; proliferation marker) and CD31 (red; marker for blood vessels) immunofluorescence (Fig. 5). Striking differences were seen between mice in therapy (SMAD-NIS-MSCs + ^{131}I) and mice in control groups (SMAD-NIS-MSCs + NaCl; NaCl + NaCl) (Fig. 5A). Tumors after ^{131}I-therapy revealed a lower Ki67-index of 35.3 ± 5% and a mean blood vessel density of 1.4 ± 0.4%, whereas tumors of control groups showed a higher proliferation index of 52.9 ± 2.8% (SMAD-NIS-MSCs + NaCl) and 64.4 ± 4.2% (NaCl + NaCl) and blood vessel density of 2.7 ± 0.5% (SMAD-NIS-MSCs + NaCl) and 2.2 ± 0.2% (NaCl + NaCl) (Fig. 5B, C).

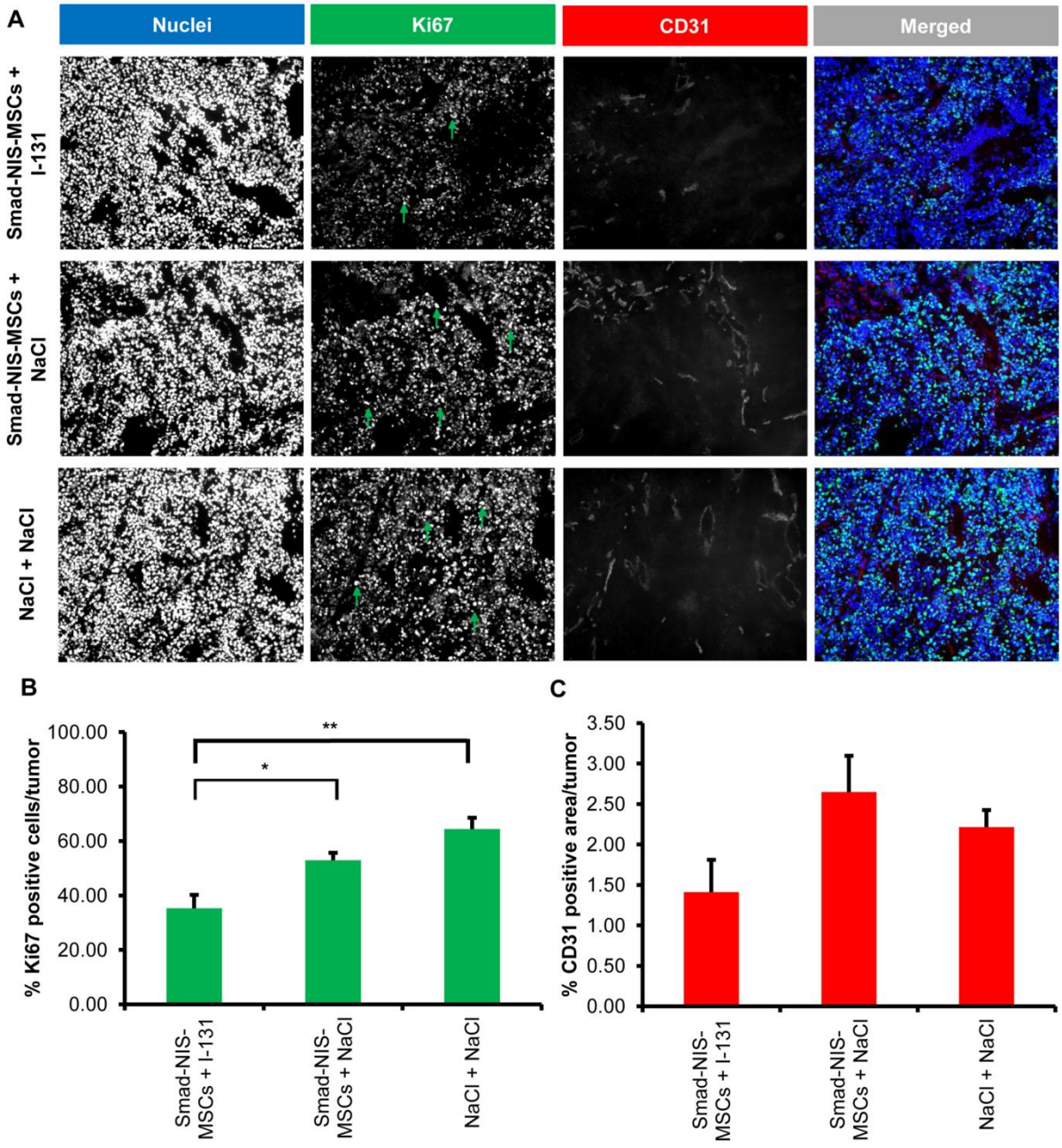

Fig. 5: *Ki67 and CD31 immunofluorescence staining. Immunofluorescence analysis for Ki67 (green) and CD31 (red, labeling blood vessels)* ***(A)*** *showed significantly decreased proliferation (Ki67, 35.3 ± 5 %) as well as reduced blood vessel density (CD31, 1.4 ± 0.4%) in resected tumors of mice treated with SMAD-NIS-MSC followed by ^{131}I treatment as compared to tumors of mice injected with SMAD-NIS-MSCs and NaCl (Ki67, 52.9 ± 2.8%; CD31, 2.7 ± 0.5%) or NaCl only (Ki67, 64.4 ± 4.2%; CD31, 2 ± 0.2%). Slides of tumors were counterstained with Hoechst nuclear stain. One representative image at 20× magnification is shown each.*

4.5 Discussion

The theranostic *NIS* gene allows noninvasive imaging of functional NIS expression by ^{123}I-scintigraphy, thereby enabling tracking of gene delivery vehicles by radioiodide imaging, as well as application of ^{131}I for a therapeutic purpose. Our laboratory and others have extensively investigated the capacity and efficacy of *NIS* gene transfer to induce radioiodide accumulation in non-thyroidal tumors using MSCs as *NIS* transgene delivery vehicles [56-60]. Earlier studies of active MSC engraftment in a HCC xenograft model using the constitutively active cytomegalovirus (CMV) promoter to express *NIS* in MSCs showed the proof-of-principle of active NIS-MSC tumor homing, followed by effective *NIS* expression in the tumor stroma and a significant delay in tumor growth after application of ^{131}I [57]. Although these results were highly promising for a MSC-based NIS-mediated radionuclide therapy approach in non-thyroidal tumors, using the non-selectively activated CMV-promoter involves the risk of potential side effects due to MSC recruitment to normal tissues in the process of normal tissue homeostasis. To reduce toxicity by undesired effects in non-target organs, further studies focused on restricting *NIS* expression to the tumor environment. Growing HCC tumors require an active tumor stroma consisting of various tumor stroma-specific cells such as cancer-associated fibroblasts (CAFs) and inflammatory cells, but are also marked by high angiogenesis. The inflammatory response within the tumor leads to increased levels of various cytokines and chemokines [51, 58, 59, 113]. In previous studies from our group a RANTES/CCL5 promoter was used to drive *NIS* expression in MSCs thus enhancing tumor stroma-specificity in subcutaneous HCC xenografts as well as colon cancer liver metastases mouse models [58, 59]. The NIS-mediated therapy approach resulted in an improved therapeutic response in animals harboring subcutaneous HCC tumors, namely a significant delay in tumor growth and prolonged animal survival, as compared to the former study using a CMV-promoter for *NIS* transgene expression [57, 58]. The clinically more relevant question whether this therapy approach could also be used in metastatic disease was examined using a colon cancer liver metastases model, where similarly high therapeutic efficacy and improved survival was observed [59]. Further studies to limit activation of *NIS* transgene expression to the tumor environment of subcutaneous and orthotopic HCC xenografts have included targeting the tumor hypoxia response [60]. A synthetic HIF1α-responsive promoter was

designed to activate *NIS* transgene expression as soon as MSCs encounter hypoxic regions of solid tumors. Interestingly, systemic application of these HIF-NIS-MSCs followed by ^{131}I injection resulted in a significant delay in tumor growth and prolonged animal survival only an orthotopic HCC model [60]. Although these approaches revealed promising therapeutic responses, our aim in the present study was to expand the individualized design of genetically engineered MSCs for *NIS* expression under control of promoters activated by micromileu-derived signals to enhance selectivity, effectiveness and flexibility of MSC-based *NIS* gene delivery, and in parallel, potentially addressing issues related to tumor heterogeneity. As interindividual and intraindividual tumor heterogeneity is an enormous challenge for successful cancer therapy, the search for tools for individualization of cancer treatment is critical for future personalized care of cancer patients. In this context, the growing knowledge of tumor stroma biology offers interesting strategies to tailor tumor stroma targeted therapy approaches. TGFB1 is known to be a central player in tumor biology, in particular tumor micromilieu-associated signaling, and has also been characterized to be significantly upregulated in HCC to promote tumorigenesis and exert immunosuppressive effects [114]. While at first TGFB1 is expressed in the microenvironment of pre-malignant tumors to control tumor progression, its local expression is later required to promote tumor growth as well as metastasis [115]. Source of this cytokine is not only its expression in tumor cells but also in endothelial cells, fibroblasts, leucocytes, mesenchymal and myeloid precursor cells, among others, where it can act in a paracrine or autocrine manner [115].

TGFB plays an important role for HCC treatment as higher levels of TGFB lead to resistance to anticancer treatments. As radiotherapy and chemotherapy can increase TGFB expression and activity, a combination with TGFB inhibitors is thought to enhance tumor sensitivity to those treatment strategies [102]. Further, TGFB is linked to hypoxia in terms of epithelial-mesenchymal transition (EMT) induction and VEGF signaling and a combination of TGFB inhibitors with anti-angiogenic or hypoxia-induced treatment strategies might be an option as well [102]. Other than that, the high expression levels of TGFB1 in tumor cells and the tumor microenvironment makes TGFB1 signaling an interesting candidate to create novel promoters for tumor stroma targeted *NIS* expression in the context of *NIS* gene therapy. In the present study a TGFB1-inducible SMAD-responsive promoter, consisting of a 5× multimer of the *SMAD* binding site AGCCAGACAGT, was designed to drive transgene MSCs

(referred to as SMAD-NIS-MSCs). *In vitro* analysis of SMAD-NIS-MSCs showed a robust dose-dependent NIS-mediated accumulation of radioiodide upon TGFB1 stimulation. Accumulation of radioiodide in SMAD-NIS-MSCs was further enhanced through combined stimulation with TGFB1 and HuH7-CM. This additive increase in radioiodide uptake activity appears to be dependent on the tumor line used, as treatment of SMAD-NIS-MSCs with CM from MDA-MB 231 cells did not result in a significant increase in promoter activity. An explanation might be the presence of co-factors in CM, which trigger SMAD expression in MSCs and thus altering sensitivity for TGFB1. As HuH7-CM only contained inactive TGFB1 protein, the exact mechanisms of the increased activity are not known yet and have to be further investigated in future studies.

The canonical TGFB signaling pathway (SMAD dependent) is regulated by different SMAD proteins. After binding of active TGFB1 to the respective receptor, SMAD1, 2, 3, 5 and 8 are phosphorylated and form complexes with the common mediator SMAD4 [115]. Translocation of the SMAD complex into the cell nucleus leads to gene expression regulation. To understand the exact mechanisms of promoter activation of SMAD-NIS-MSCs in our study, SMAD-NIS-MSCs were additionally transfected with vectors expressing SMAD3 or SMAD4. These vectors are driven by the CMV-promoter and are thus permanently expressing SMAD3 or SMAD4. To investigate regulation of NIS expression, the additionally transfected SMAD-NIS-MSCs were tested by iodide uptake assay with or without TGFB1 stimulation. As TGFB signaling requires phosphorylated SMADs to become active, no radioiodide activity was observed in SMAD-NIS-MSCs, containing expression vectors for SMAD3 or SMAD4, in the absence of TGFB1 stimulation. Upon TGFB1 stimulation an enhanced NIS-mediated radioiodide uptake activity in the presence of SMAD3 was observed, whereas this effect was not observed by SMAD4, showing the influence of different SMADs on the SMAD-responsive promoter used to control NIS expression. The subsequent *in vivo* ^{123}I-scintigraphy studies showed the recruitment of SMAD-NIS-MSCs into the tumor environment of experimental HuH7 tumors and led to a robust tumor-selective TGFB1-driven induction of the *NIS* transgene as shown by tumor-specific radioiodide accumulation.

NIS expression within the tumors was further confirmed by NIS immunoreactivity, which demonstrated high NIS protein expression within tumors but not in non-target organs such as liver, lung or spleen. Further, TGFB1 immunohistochemistry

confirmed expression of TGFB1 within the experimental HuH7 tumors. SMAD-NIS-MSCs were then applied followed by therapeutic application of ^{131}I which resulted in a significant reduction in tumor growth and prolonged survival. Although the calculated biological half-life of 2.2 h and tumor-absorbed dose of 28.2 mGy/MBq/g tumor was lower than those observed in previous studies, the therapy study revealed as strong a therapeutic effect comparable to our previous studies using the specific RANTES/CCL5 promoter [58].

The use of traditional anticancer therapies, such as radiation treatment or chemotherapy, demonstrated an induction of TGFB1 expression. Biswas *et al.* illustrated enhanced levels of circulating TGFB1 in plasma after thoracic irradiation or chemotherapy (doxorubicin) in mice with mammary carcinoma [116]. Further, as shown by our group (unpublished data) and others, external beam radiation therapy of tumors is able to induce an enhanced inflammatory response resulting in increased secretion of diverse growth factors and chemokines, including TGFB1, which in turn also led to an enhanced recruitment of MSCs [64, 65, 117]. Therefore, the approach outlined in the present study based on *NIS* gene expression driven by a TGFB1-inducible SMAD-responsive promoter opens the prospect of combination with conventional therapies, such as external beam radiation or chemotherapy, to take advantage of synergistic effects thereby fostering TGFB1-induced tumoral *NIS* expression and improving therapeutic efficacy of MSC-based NIS-induced radioiodide therapy. The results presented here build on previous studies, including the initial clinical trials of engineered MSCs for tumor therapy, by providing new targeting approaches that could expand targeting options in the next generation of engineered anti-tumor MSCs.

Taken together, our study demonstrates high tumor stromal recruitment of SMAD-NIS-MSCs and a robust, biologically targeted *NIS* transgene expression in subcutaneous HuH7 tumors through TGFB1-induced SMAD promoter activity. After systemic application of SMAD-NIS-MSCs followed by ^{131}I injection, a significant therapeutic effect was observed, resulting in reduction of tumor growth and improved survival. The proof-of-principle in this study opens the exciting prospect for future studies, where we will build on the presented results to investigate the enormous potential of TGFB1-induced promoters for *NIS* transgene expression for an improved and novel theranostic *NIS* gene approach. As native gene promoters are generally more efficient than the synthetic promoters used in this study as a proof of concept,

in future studies it will be important to identify efficient TGFB1-regulated native promoters that may allow a more robust level of transgene induction in the context of the tumor environment.

4.6 Acknowledgements

We are grateful to Dr. S.M. Jhiang, Ohio State University, Columbus, OH, USA for supplying the full-length human NIS cDNA. We also thank Prof. Dr. K. Scheidhauer and Jakob Allmann, Department of Nuclear Medicine, Klinikum rechts der Isar der Technischen Universität München, Munich, Germany, for their assistance with the imaging studies. We thank Doris Mayr (Department of Pathology, LMU Munich, Munich, Germany) for preparation of paraffin-embedded slides and Marion Mielke (Department of Pathology and Comparative Experimental Pathology, Klinikum rechts der Isar der Technischen Universitaet Muenchen) for performing the immunohistochemistry. This work was supported by grants from the Deutsche Forschungsgemeinschaft within the Collaborative Research Center SFB 824 to C Spitzweg (project C8) and within the Priority Program SPP1629 to C Spitzweg and PJ Nelson (SP 581/6-1, SP 581/6-2, NE 648/5-2) as well as within a grant from the Wilhelm-Sander-Stiftung to C Spitzweg (2014.129.1).

5. Chapter 3: External beam radiation therapy enhances mesenchymal stem cell-mediated sodium iodide symporter gene delivery

This chapter has been adapted from:

Schug C[1], Sievert W[2], Urnauer S[1], Müller AM[1], Schmohl KA[1], Wechselberger A[3], Schwenk N[1], Lauber K[4], Schwaiger M[5], Multhoff G[2], Wagner E[6], Nelson PJ[3] and Spitzweg C[1], External beam radiation therapy enhances mesenchymal stem cell-mediated sodium iodide symporter gene delivery. Human Gene Therapy. 2018 May. [Epub ahead of print]

[1]Department of Internal Medicine IV, University Hospital of Munich, LMU Munich, Munich, Germany, [2]Department of Radiation Oncology, Klinikum rechts der Isar, Technische Universitaet Muenchen, Munich, Germany, [3]Clinical Biochemistry Group, Department of Internal Medicine IV, University Hospital of Munich, LMU Munich, Munich, Germany, [4]Department of Radiation Oncology, University Hospital of Munich, LMU Munich, Munich, Germany, [5]Department of Nuclear Medicine, Klinikum rechts der Isar, Technische Universitaet Muenchen, Munich, Germany, [6]Department of Pharmacy, Center of Drug Research, Pharmaceutical Biotechnology, LMU Munich, Munich, Germany

5.1 Abstract

The tumor-homing properties of mesenchymal stem cells (MSC) have led to their development as delivery vehicles for the targeted delivery of therapeutic genes such as the sodium iodide symporter (NIS) to solid tumors. External beam radiation therapy (EBRT) may represent an ideal setting for the application of engineered MSC-based gene therapy as tumor irradiation may enhance MSC recruitment into irradiated tumors through the increased production of select factors linked to MSC migration. In the present study, the irradiation of human liver cancer cells (HuH7) (1-10 Gy) showed a strong dose-dependent increase in steady state mRNA levels of CXCL8, CXCL12/SDF-1, FGF2, PDGFβ, TGFB1, TSP-1 and VEGF (0-48 h), which was verified for most factors at the protein level (after 48 h). Radiation effects on directed MSC migration was tested *in vitro* using a live cell tracking migration assay and supernatants from control and irradiated HuH7 cells. A robust increase in mean forward migration index (yFMI), mean center of mass (yCoM) and mean directionality of MSCs towards supernatants was seen from irradiated as compared to nonirradiated tumor cells. Transferability of this effect to other tumor sources was demonstrated using the human breast adenocarcinoma cell line (MDA-MB-231), which showed a similar behavior to radiation as seen with HuH7 cells in qPCR and migration assay. To evaluate this in a more physiologic *in vivo* setting, subcutaneously growing HuH7 xenograft tumors were irradiated with 0, 2 or 5 Gy followed by CMV-NIS-MSC application 24 h later. Tumoral iodide uptake was monitored using ^{123}I-scintigraphy. The results showed increased tumor-specific dose-dependent accumulation of radioiodide in irradiated tumors. Our results demonstrate that EBRT enhances the migratory capacity of MSCs and may thus increase the therapeutic efficacy of MSC-mediated NIS radionuclide therapy.

5.2 Introduction

The sodium iodide symporter (NIS) is an intrinsic transmembrane glycoprotein with 13 putative transmembrane domains. NIS mediates the active uptake of iodide into the thyroid gland and as such, has formed the basis for the diagnostic and therapeutic application of radioiodine in benign and especially malignant thyroid diseases for almost 70 years [20]. Its properties as a reporter and therapy gene allows noninvasive imaging of functional NIS expression by ^{123}I-scintigraphy and ^{124}I-PET imaging and robust therapeutic effects by the application of ^{131}I and related radionuclides [20-23]. The extensive clinical experience derived from work with NIS-biology and NIS-mediated radioiodine accumulation in diagnosis and imaging of differentiated thyroid cancer has allowed expansion of this effective theranostic strategy to non-thyroidal tumor settings through the use of various delivery vehicles for tumor-targeted NIS gene expression. The approaches under evaluation include viral and non-viral vectors such as genetically engineered mesenchymal stem cells (MSC). The results to date have demonstrated tumor-selective NIS-mediated radioiodine accumulation leading to decreased tumor growth and prolonged survival of treated animals [28, 30, 33, 34, 36-38, 41, 56-60, 96-99, 101]. MSCs are very promising potential vehicles for the delivery of therapeutic genes to tumors, as solid tumors are thought to have many of the characteristics of chronic wounds due to ongoing and extensive hypoxia, necrosis and angiogenesis, which drive MSC recruitment [45, 46]. The enhanced production of inflammatory cytokines, growth factors and chemokines by the tumor cells is thought to underlie the directed migration of MSCs to solid tumors. Previous reports have suggested that platelet-derived growth factor (PDGF), epidermal growth factor (EGF), vascular endothelial growth factor (VEGF), interleukin-6 (IL-6) and the chemokine (C-X-C motif) ligand 12/stromal cell-derived factor 1 (CXCL12/SDF-1) play important roles in the recruitment of MSCs into tumors environments.[5] Tumor external beam irradiation may represent a promising tool to enhance MSC homing to tumor microenvironments based on the localized tissue damage seen with irradiation leading to the increased secretion of inflammatory chemokines and growth factors [64, 65].

In the present study we sought to evaluate the effect of external beam radiation on tumor-homing of adoptively applied engineered MSCs to determine if this treatment would improve or enhance functional MSC-mediated NIS gene expression within the

experimental tumors. To this end, we investigated the effect of radiation on the chemokine and growth factor expression profile of the human hepatocellular carcinoma (HCC) cell line HuH7, as well as of the human breast adenocarcinoma cell line MDA-MB-231, and the overall effect on the directed migration of MSC. The *in vitro* results where then validated in a HCC xenograft mouse model taking advantage of the reporter gene function of NIS.

5.3 Materials and methods

Cell culture

The human hepatocellular carcinoma cell line HuH7 was purchased from JCRB Cell Bank (JCRB 0403, Osaka, Japan) and cultured in DMEM (Sigma-Aldrich, St. Louis, Missouri, USA) supplemented with 10% FBS (Biochrom/Merck Millipore, Berlin, Germany) and 100 U/ml penicillin/100 µg/ml streptomycin (Sigma-Aldrich). The human breast adenocarcinoma cell line MDA-MB-231 was cultured in RPMI (Sigma_Aldrich), supplemented with 10% FBS and 100 U/ml penicillin/100 µg/ml streptomycin. A previously established, SV40 large T antigen immortalized MSC cell line derived from human bone marrow [111], was cultured in RPMI supplemented with 10% FBS and 100 U/ml penicillin/100 µg/ml streptomycin. Primary human bone marrow-derived CD-34-negative MSCs were cultured as described previously [112]. Cells were maintained at 37°C and 5% CO_2 in an incubator.

Stable transfection and establishment of MSCs

The establishment of wild type MSCs (WT-MSC) transfected with the expression vector CMV-NIS-pcDNA3 (full length NIS cDNA coupled to the cytomegalovirus (CMV) promoter) and the resulting stably transfected cell line (CMV-NIS-MSC) was described previously [57].

^{125}I uptake assay

Radioiodide uptake of CMV-NIS-MSC was determined at steady-state conditions before in vivo application as described previously by Spitzweg *et al*. [66]. Results were normalized to cell survival measured by cell viability assay (see below).

Cell viability assay

Cell viability was determined as described previously [60].

Irradiation of HuH7 and MDA-MB-231 cells

1×10^6 HuH7 or MDA-MB-231 cells, respectively, were seeded on 100 mm^3 surface cell culture plates. 12 h before radiation, cells were switched to serum-free medium. Tumor cells were irradiated with doses from 0 to 10 Gray (Gy) using an Xstrahl

cabinet Irradiator RS225 (200 kV, 10 mA, Thoraeus filter, 1 Gy in 1 min 3s; Xstrahl LTD, Camberley, Surray, England).

Quantitative real-time PCR (qRT-PCR)

Total RNA from HuH7 cells was extracted after 4, 8, 12, 24 and 48 h post radiation (0-10 Gy respectively) using the RNeasy Mini Kit with QIAshredder (Qiagen, Hilden, Germany). The same procedure was performed for MDA-MB-231 cells after 8, 24 and 48 h post radiation. Reverse transcription and quantitative real-time PCR were conducted as previously described using a Mastercycler ep gradientS PCR cycler (Eppendorf, Hamburg, Germany) [58]. The following primers were used: *ACTB* (β-actin): Forward primer (5′-AGAAAATCTGGCACCACACC-3′) and reverse primer (5′-TAGCACAGCCTGGATAGCAA-3′), *CXCL8*: Forward primer (5′-TCTGCAGCTCTGTGTGAAGG-3′) and reverse primer (5′-TTCTCCACAACCCTCTGCAC-3′), *CXCL12/SDF-1*: Forward primer (5′-AGAGCCAACGTCAAGCATCT-3′) and reverse primer (5′-TAGCACAGCCTGGATAGCAA-3′), *FGF2*: Forward primer (5′-GGAGAAGAGCGACCCTCAC-3′) and reverse primer (5′-AGCCAGGTAACGGTTAGCAC-3′), *PDGFB*: Forward primer (5′-TTGGCTCGTGGAAGAAGG-3′) and reverse primer (5′-CGTTGGTGCGGTCTATGA-3′), *TGFB1*: Forward primer (5′-CAGCACGTGGAGCTGTACC-3′) and reverse primer (5′-AAGATAACCACTCTGGCGAGTC-3′), *THBS1* (TSP1): Forward primer (5′-TTGTCTTTGGAACCACACCA-3′) and reverse primer (5′-CTGGACAGCTCATCACAGGA-3′), *VEGF*: Forward primer (5′-CTACCTCCACCATGCCAAGT-3′) and reverse primer (5′-ATGATTCTGCCCTCCTCCTT-3′). Relative expression levels were calculated from ΔΔCt values normalized to internal β-actin. Results are expressed as fold change relative to controls.

Enzyme-linked Immunosorbent Assay (ELISA)

Supernatant from untreated and irradiated HuH7 cells was removed after 4, 8, 12, 24 or 48 h, centrifuged and stored at -80°C. ELISA assays for CXCL8, CXCL12/SDF-1, FGF2, PDGF beta homodimer (PDGF BB), TGF-β1, TSP1 and VEGF were performed using the respective DuoSet ELISA kit (R&D Systems, Abington, UK)

following the manufacturer's instructions. Results are expressed as fold change relative to controls.

Cell Migration Assay

Chemotaxis of MSCs in relation to a gradient between irradiated and non-irradiated supernatants of HuH7 or MDA-MB-231 cells (48 h post radiation respectively) was tested using a live cell tracking migration assay (IBIDI µ-slide Chemotaxis; Martinsried, Germany) used according to the manufacturer's directions. After seeding of 0.3×10^6 MSC/ml in collagen, MSCs were exposed to a gradient between supernatants of non- and irradiated HuH7 or MDA-MB-231 cells. Monitoring of chemotaxis and tracking of twenty randomly selected cells was done as previously described [68]. For quantification of the migratory behavior of MSCs, the forward migration index (FMI), the center-of-mass (CoM) and directness were calculated, reflecting the distance and directness of migration for all tracked cells.

Animals

Five-week-old female CD1 nu/nu mice from Charles River (Sulzfeld, Germany) were housed under specific pathogen-free conditions with access to mouse chow and water *ad libitum* and were allowed to acclimatize for 1 week before tumor cell implantation. The experimental protocol was approved by the regional governmental commission for animals (Regierung von Oberbayern) and experiments were performed in accordance with institutional guidelines of the Klinikum rechts der Isar, Technische Universität München.

HuH7 xenograft tumors

HuH7 xenograft tumors were established by subcutaneous injection of 5×10^6 HuH7 cells in 100 µl PBS into the flank region as described previously [57]. Tumor volumes, which were regularly measured, were estimated using the equation: length × width × height × 0.52 and animals were sacrificed when tumors exceeded a size of 1500 mm^3.

Irradiation of HCC xenografts

Experiments were initiated when the tumors had reached a diameter of approximately 5-10 mm. The irradiation was performed using the high precision

image-guided small animal radiation research platform (SARRP, X-Strahl, West Midlands, UK). Mice were anaesthetized by isoflurane/oxygen inhalation for the duration of each treatment. Cone-beam computed tomography (CBCT) using 60 kV and 0.8 mA photons was performed for each mouse to visualize the subcutaneous tumors. All tumors were irradiated using 220 kV and 13 mA x-ray beams using a 3×9 mm^2, 5×5 mm^2 or 10×10 mm^2 collimator. The central axis of the beams was set in the isocenter of the tumor with a mean irradiation dose of 2 or 5 Gy. The SARRP control software and Muriplan were used to precisely target tumors and irradiation doses.

MSC application and ^{123}I-scintigraphy

Mice were given 5 mg/ml L-T4 (Sigma-Aldrich) in their drinking water, to suppress thyroidal iodide uptake. CMV-NIS-MSCs were applied once *via* the tail vein at a concentration of 5×10^5 cells/500µl PBS 24 h post tumor radiation. 72 h after MSC application mice received 18.5 MBq (0.5 mCi) ^{123}I i.p. and radioiodide biodistribution was assessed using a gamma camera provided with a low-energy high resolution collimator (e.cam, Siemens, Munich, Germany). Regions of interest were analyzed using HERMES GOLD (Hermes Medical Solustions, Stockholm, Sweden), quantified and results expressed as a fraction of the total amount of applied radionuclide per gram tumor tissue (% ID/g). The radionuclide retention time was determined as described previously [60].

Immunohistochemical NIS staining

Immunohistochemical NIS staining of paraffin-embedded tissue sections derived from HCC xenografts or other organs (liver, lung and spleen) after systemic CMV-NIS-MSCs administration was performed as described previously [84].

Statistical methods

Results are expressed as mean ± SEM or mean-fold change ± SEM and statistical significance was tested by two-tailed Student´s t-test, where p values < 0.05 were considered significant (*p < 0.05; **p < 0.01; ***p < 0.001). For migration assays, results are shown by Rayleigh test, where p values < 0.05 were considered significant (*p < 0.05; **p < 0.01; ***p < 0.001).

5.4 Results

Irradiated HuH7 cells show increased expression of chemokines and growth factors implicated in MSC migration

Tumor irradiation is thought to increase the expression of diverse chemokines and growth factors, many of which have been implicated in directed migration of MSCs. To study this in detail, HuH7 cells were evaluated for their steady state mRNA expression of CXCL8, CXCL12/SDF-1, PDGFB, FGF2, TGFB1, TSP1 and VEGF using qRT-PCR. Upon irradiation, the mRNA expression for each of these factors was increased as compared to nonirradiated cells, but the time course and response to radiation levels varied among the genes tested (Fig.1). The *in vitro* irradiation (1-10 Gy) of HuH7 cells did not result in a change in cell viability as compared to nonirradiated cells during 0-48 h (data not shown). For radiation with 0, 2 and 5 Gy (as used *in vivo*), HuH7 cell viability was examined later time points, such as 5 or 7 days, and no decrease in cell viability was seen except after 5 days using 5 Gy, where a decrease of 18 % was seen (data not shown).

Changes in mRNA levels were observed as early as 4 h post radiation treatment for all factors, with some of them increasing in a radiation dose-dependent manner (CXCL8, PDGFB, TGFB1 and TSP-1) (Fig. 1A, C, E, F). A peak in mRNA levels after irradiation was observed at 12 h for CXCL8 and FGF2, which was also dose-dependent, whereas a dose-dependent peak in CXCL12/SDF-1 and TSP-1 mRNA expression was seen at 24 h (Fig. 1A, B, D, F). The maximum dose-dependent increase in PDGFB, TGFB1 and VEGF mRNA expression was seen similarly at 12 h and 24 h post irradiation (Fig. 1C, E, G). An effect of radiation on the steady state mRNA expression of CXCL12/SDF-1, PDGFB and TSP-1 was observed up to 48 h (Fig. 1B, C, F).

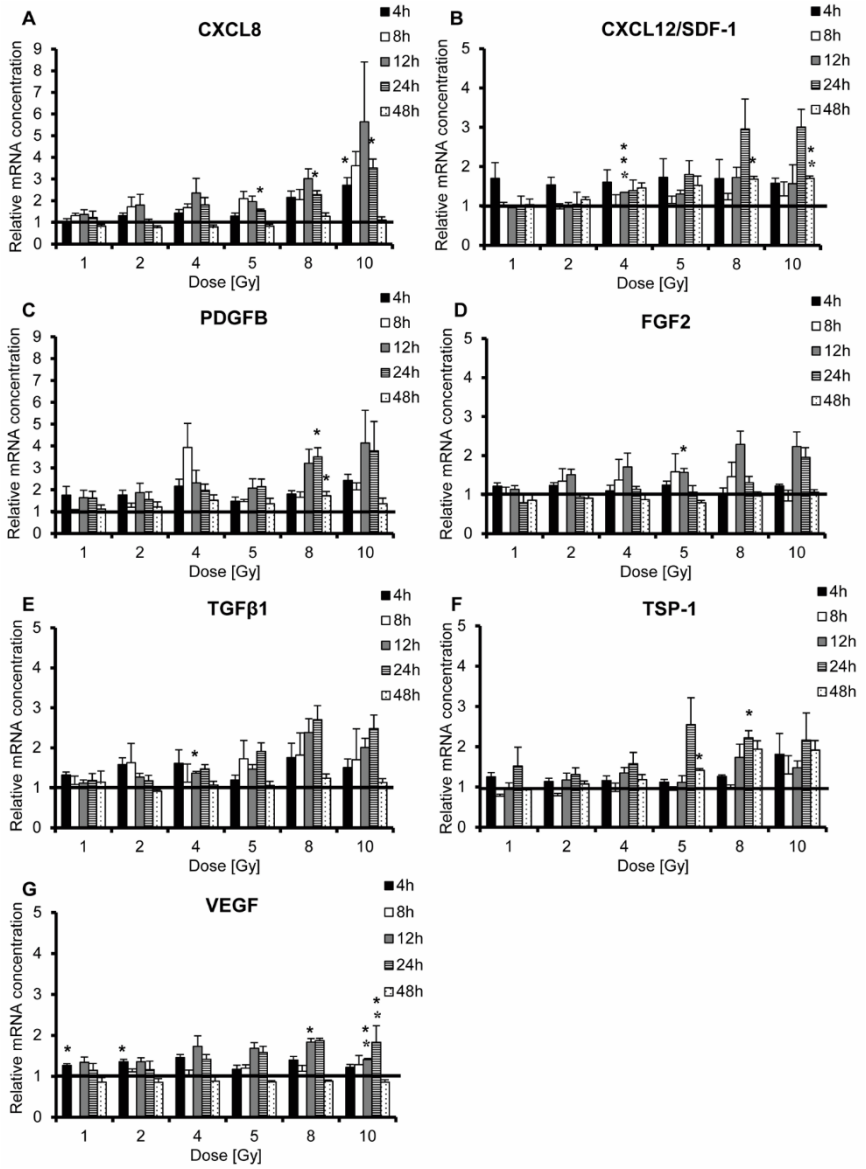

Fig. 1: *Gene expression of inflammatory cytokines and growth factors is enhanced by irradiation of HuH7 cells (1-10 Gy) during a period of 4 to 48 h* ***(A-G)****. Data are represented as mean fold change ± SEM as compared to nonirradiated control cells (n=3; two-tailed Student's t-test: *P<0.05; **P<0.01, ***P<0.001).*

Effects seen on the mRNA level were then confirmed by ELISA (CXCL8, CXCL12/SDF-1, TGFB1, TSP-1 and VEGF) (Fig. 2). Protein levels for FGF2 and PDGFB remained below the detection limit of the ELISA kits. No increase in protein secretion was detected from 4-24 h post radiation (data not shown). CXCL8, CXCL12/SDF-1 and TGFB1 secretion showed a strong increase 48h after the irradiation of HuH7 cells, that also occurred in a dose-dependent manner with peak production seen at 4-5 Gy (Fig. 2A-C), whereas only a marginal increase of TSP-1 and VEGF was observed (Fig. 2D, E). Significant secretion of CXCL8 protein was

observed after irradiation with 8 or 10 Gy and of CXCL12/SDF-1 when using 2 Gy (Fig. 2A, B). Irradiation of HuH7cells with 4 Gy showed a significant increase in TGFB1 protein secretion (Fig. 2 C).

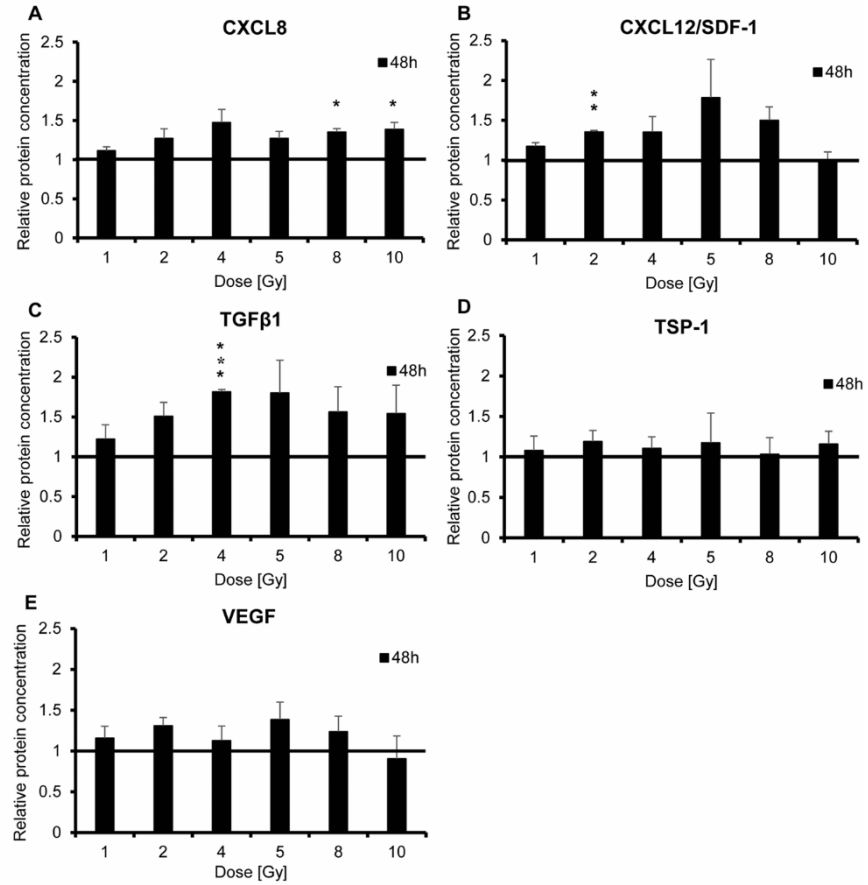

Fig. 2: *Protein secretion was assessed by ELISA and showed enhanced secretion of CXCL8, CXCL12/SDF-1, TGFB1, TSP-1 and VEGF 48 h post irradiation of HuH7 cells (1-10 Gy)* ***(A-E)****. Data are represented as mean fold change ± SEM as compared to nonirradiated control cells (n=3; two-tailed Student's t-test: *P<0.05; **P<0.01, ***P<0.001).*

MSCs exposed to irradiated HuH7 supernatant show enhanced directed migration

Based on the results detailed above, it is clear that a complex set of factors linked to MSC recruitment are induced in the tumor line in response to external beam radiation. To functionally validate the effect of HuH7 irradiation on the directed migration of MSCs, a commercial 2D migration chamber and pseudo video imaging was applied. MSCs were subjected to a gradient generated between supernatants derived from nonirradiated and irradiated HuH7 cells, and the migratory behavior of individual cells was monitored over a 24 h period (Fig. 3). MSCs showed enhanced

and directed chemotaxis towards the irradiated supernatants. The analysis revealed a robust increase of mean forward migration index (yFMI), mean center of mass (yCoM) and mean directionality of MSCs towards supernatants from irradiated as compared to nonirradiated tumor cells (Fig. 3I-K). Enhanced MSC migration towards the supernatant isolated from irradiated cells was seen at 4 Gy (yFMI: 0.115±0.015; Rayleigh values $p<0.05$, yCoM: 94.42±3.19 µm) (Fig. 3E, I-J), 5 Gy (yFMI: 0.105±0.026; Rayleigh values $p<0.05$, yCoM: 73.67±12.69 µm) (Fig. 3F, I-J) and 10 Gy (yFMI: 0.105±0.005; Rayleigh values $p<0.05$, yCoM: 103.02±4.57 µm) (Fig. 3H, I-J) as compared to controls. MSCs that were subjected to medium and supernatant from untreated HuH7 cells (yFMI: -0.01±0.025, yCoM: -9.04±15.07 µm) (Fig. 3A, I-J) or to supernatant from untreated HuH7 cells in both chambers (yFMI: 0.055±0.03, yCoM: 46.94 ±20.64 µm) (Fig. 3B, I-J) showed random chemokinesis, but no directed migration.

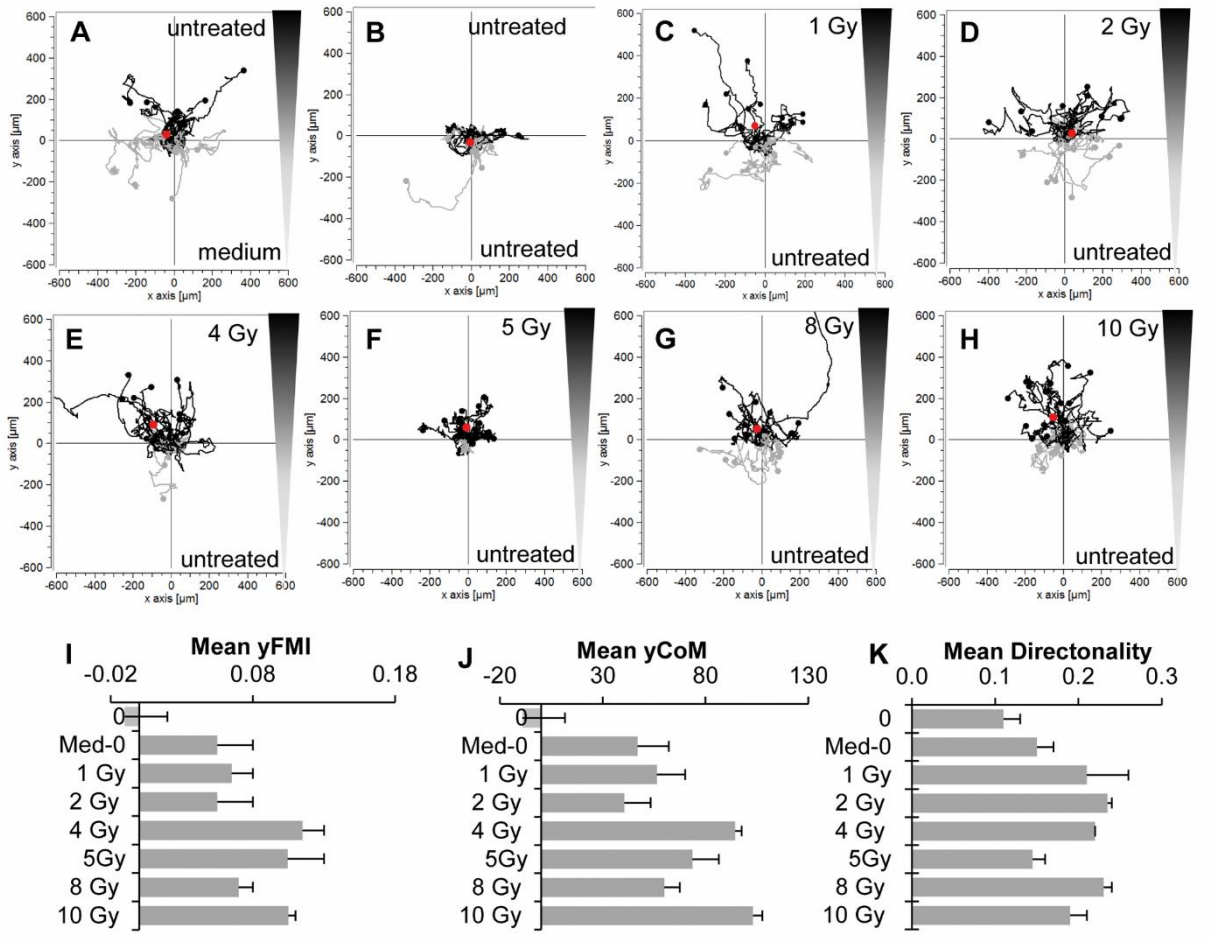

Fig. 3: *MSCs subjected to a gradient of isolated supernatants from nonirradiated and irradiated HuH7 cells (1-10 Gy) showed enhanced direct migration over 24 h* ***(C-H)*** *as compared to untreated HuH7 cells as controls, where only random chemokinesis was observed* ***(A-B)****. One representative image each is shown from two independent experiments. This was confirmed by quantification of chemotaxis*

parameters as yFMI, yCoM and directionality ***(I-K)****. yCoM is indicated by red dots* ***(J)****. Data are* represented as mean fold change ± SEM from two independent experiments.

This was further confirmed by testing primary MSCs, which were subjected to untreated supernatants from HuH7 cells and from cells, which were irradiated with 0, 1, 5 or 10 Gy (Fig. 4). Primary human bone marrow derived MSCs showed similar migratory behavior as seen in the immortalized MSCs (Fig. 3 and 4).

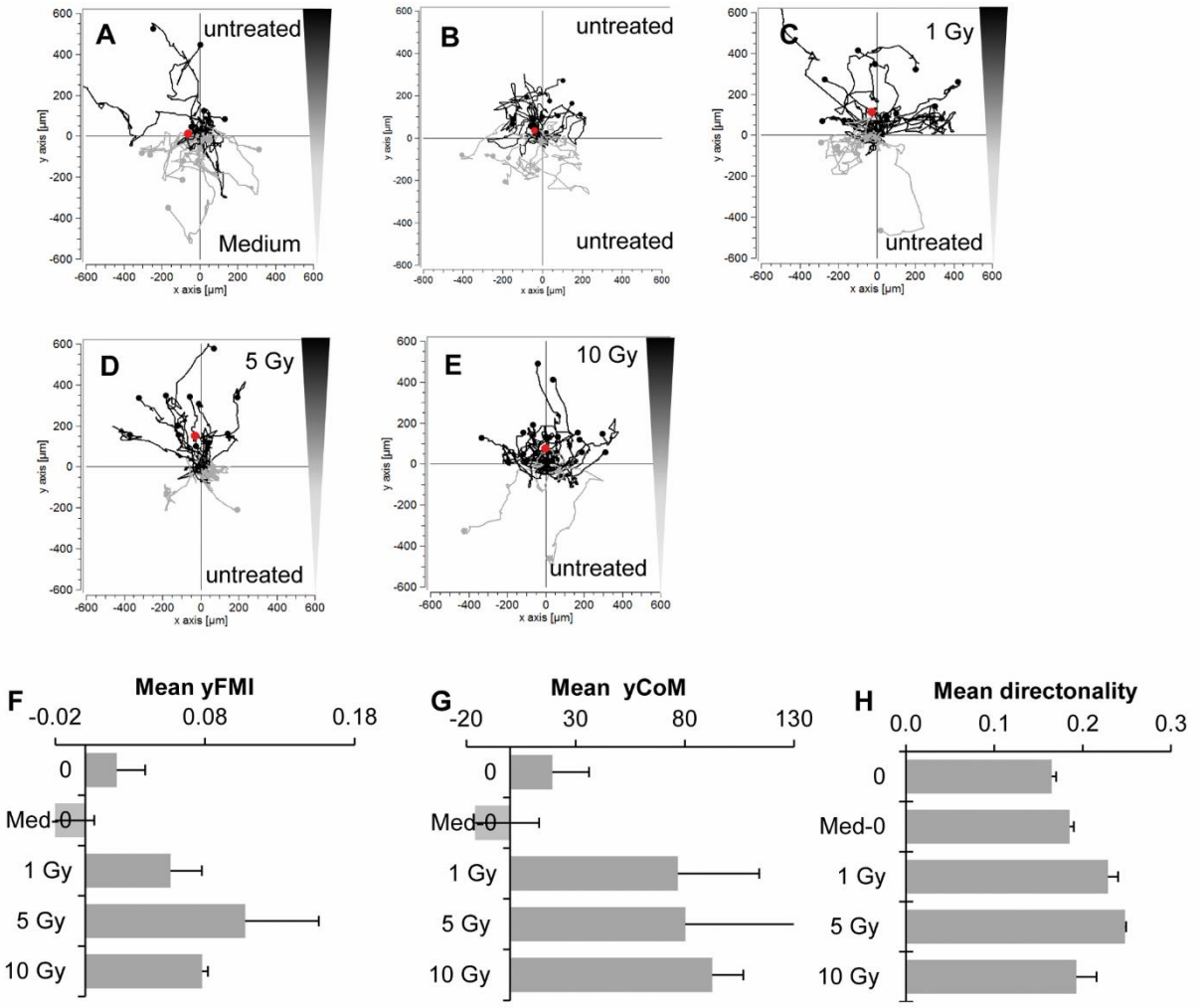

Fig. 4: *Chemotactic behavior of MSCs was further confirmed using primary human bone marrow derived MSCs* ***(A-H)****. Primary MSCs migrated along a gradient of supernatants from nonirradiated to irradiated HuH7 cells (1, 5 and 10 Gy) over 24 h* ***(C-E)*** *as compared to controls* ***(A-B)****. This was confirmed by quantification of chemotaxis parameters as yFMI, yCoM (red dots) and directionality* ***(F-H)****. Data are* represented as mean fold change ± SEM from two independent experiments.

Irradiation of MDA-MB-231 cells leads to enhanced chemokine and growth factor expression as well as directed MSC migration to cell supernatants

To demonstrate that the effects of irradiation on human tumor cells is not only seen in

HuH7 cells but also in other cancer cell lines, the human breast adenocarcinoma cell line MDA-MB-231 was irradiated *in vitro* using 0, 2, 5 or 10 Gy and mRNA expression was tested 0, 8, 24 and 48 h post radiation (Supplementary Fig. 1). MDA-MB-231 cells were evaluated for their steady state mRNA expression of CXCL8, CXCL12/SDF-1, TGFB1, TSP-1 and VEGF using qRT-PCR (Supplementary Fig. 1A-D). The mRNA expression for CXCL8, TGFB1, TSP-1 and VEGF was enhanced after radiation as compared to nonirradiated cells, but a variation in time course and response to radiation levels among the genes was observed (Supplementary Fig. 1A-D). No CXCL12/SDF-1 mRNA levels were detectable in MDA-MB-231 cells. CXCL8 mRNA expression levels showed a dose-dependent peak at 8 h but no increase at later time points (Supplementary Fig. 1A), whereas TGFB1 and VEGF mRNA expression showed a dose-dependent increase with a maximum at 24 h (Supplementary Fig. 1B, D). TSP-1 mRNA expression showed a dose-dependent increase with a maximum at 24 and 48 h post irradiation (Supplementary Fig. 1C).

To functionally validate the effect of MDA-MB-231 irradiation on the directed migration of MSCs, MSCs were subjected to a gradient generated between supernatants derived from nonirradiated and irradiated MDA-MB-231 cells as described above (Supplementary Fig. 2). Similar to the effects seen above with supernatants from HuH7 cells, MSCs showed directed chemotaxis towards irradiated supernatants. An increase of mean forward migration index (yFMI), mean center of mass (yCoM) and mean directionality of MSCs towards supernatants from irradiated as compared to nonirradiated MDA-MB-231 cells was observed (Supplementary Fig. 2F-H). While there was only a minor effect observed using 2 Gy and 10 Gy (Supplementary Fig. 2C, E, F-H), clearly enhanced MSC migration towards the supernatant isolated from 5 Gy irradiated cells was observed (yFMI: 0.121±0.036; Rayleigh values $p<0.01$, yCoM: 66.04±23.93 µm) (Supplementary Fig. 2D, F-H) as compared to controls (Supplementary Fig. 2A, B, F-H). Controls, in which MSCs were subjected to medium and supernatant from untreated MDA-MB-231 cells (yFMI: -0.061±0.012 yCoM: 34.02±0.78 µm) (Supplementary Fig. 2A, F-H) or to supernatant from untreated MDA-MB-231 cells in both chambers (yFMI: -0.01±0.01, yCoM: -0.28±0.21 µm) (Supplementary Fig. 2B, F-H), only showed random chemokinesis.

Radiation pretreatment of tumors enhances MSC recruitment in vivo

To validate radiation enhanced MSC recruitment in an *in vivo* setting, subcutaneous

HCC xenograft tumors implanted in nude mice were irradiated with 0, 2 or 5 Gy before systemic application of NIS-reporter engineered MSCs (Fig. 5). Using high precision image-guided SARRP, local tumor irradiation with CT guided imaging was performed (Fig. 5C). Isocenters were set in the tumor image to locate beams and calculate dose volume distribution within the tumors (Fig. 5A, C).

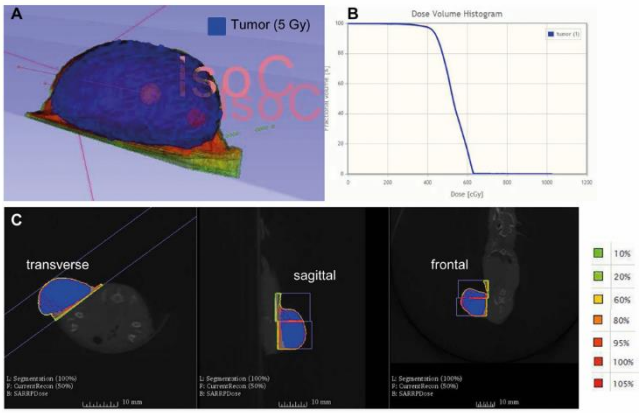

Fig. 5: *Irradiation was performed using SARRP. Upon radiation with 2 or 5 Gy, a CT was done allowing to mark and define the tumor (blue)* ***(A)****. CTs are shown in transversal, sagittal and frontal orientation* ***(C)****. Isocenters were set to locate the beams and to calculate the dose distribution within the tumor* ***(A, B)****. One representative image is shown from a subcutaneous HuH7 xenograft tumor irradiated with 5 Gy.*

After one i.v. injection of CMV-NIS-MSCs 24 h post radiation, MSC-mediated delivery of NIS expression into tumors was monitored by NIS reporter gene imaging using ^{123}I-scintigraphy (Fig. 6). Imaging studies revealed a significant tumor-specific accumulation of 7.9 ± 1.4 % and 9.2 ± 1.5 % of the total amount of applied ^{123}I dose per gram tumor (ID/g) in tumors pretreated with 2 or 5 Gy, respectively, as compared to 5.3 ± 0.8 % ID/g in nonirradiated tumors (Fig. 6A-D). A tumor-absorbed dose of 17.4 (nonirradiated), 27.6 (2 Gy) and 64.4 (5 Gy) mGy/MBq/g tumor ^{131}I with an effective half-life of 2.7 (nonirradiated), 2.3 (2 Gy) and 2.5 (5 Gy) h was determined. Endogenous NIS expression was also seen in the thyroid gland, the salivary glands (SG) as well as in the stomach and, due to renal excretion of radioiodide, in the urinary bladder (Fig. 6A-C).

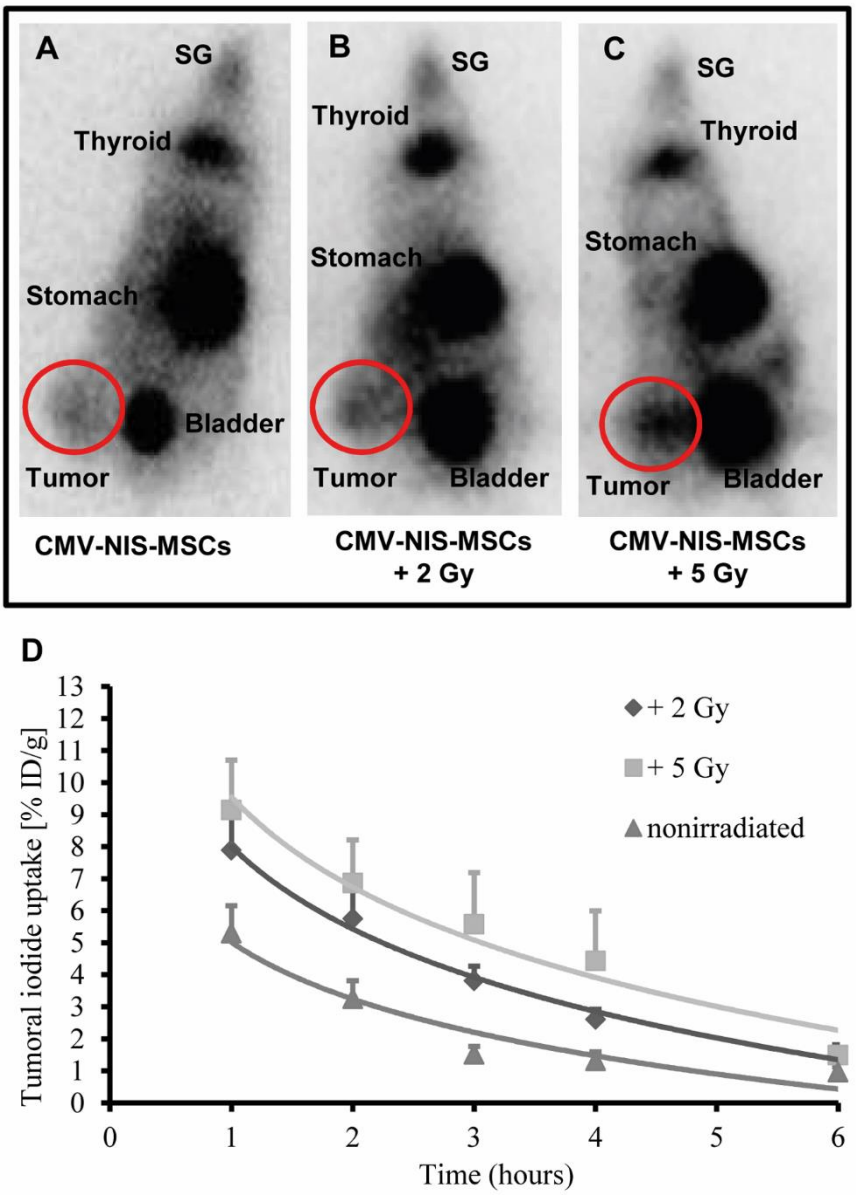

Fig. 6: *1 h after radioiodide injection, ^{123}I-scintigraphy* ***(A-D)*** *demonstrated enhanced radioiodide accumulation in radiation pretreated subcutaneous HCC tumors followed by systemic CMV-NIS-MSC application (n=4, each group). One representative image is shown per group* ***(A-C)****. Time course of radioiodide accumulation in tumors was determined by serial scanning* ***(D)****. Nonirradiated tumors showed a maximum ^{123}I uptake of 5.3 ± 0.8 % ID/g, whereas irradiated tumors revealed an accumulation of radioiodide up to 7.9 ± 1.4 % ID/g using 2 Gy or 9.2 ± 1.5 % ID/g using 5 Gy* ***(D)****. Results are respresented as mean ± SEM.*

After ^{123}I-scintigraphy, tissue sections of the tumors and non-target organs (liver, lung and spleen) were stained for NIS protein expression to determine the presence of MSCs by MSC-mediated NIS expression (Fig. 7). Nonirradiated tumors revealed only weak NIS expression in the tumors (Fig. 7A), whereas a pretreatment with 2 or 5 Gy led to higher levels of NIS expression, confirming a higher recruitment of MSCs to

irradiated tumors (Fig. 7E, I). No staining was observed in non-target organs (Fig. 7B-D, F-H, J-L).

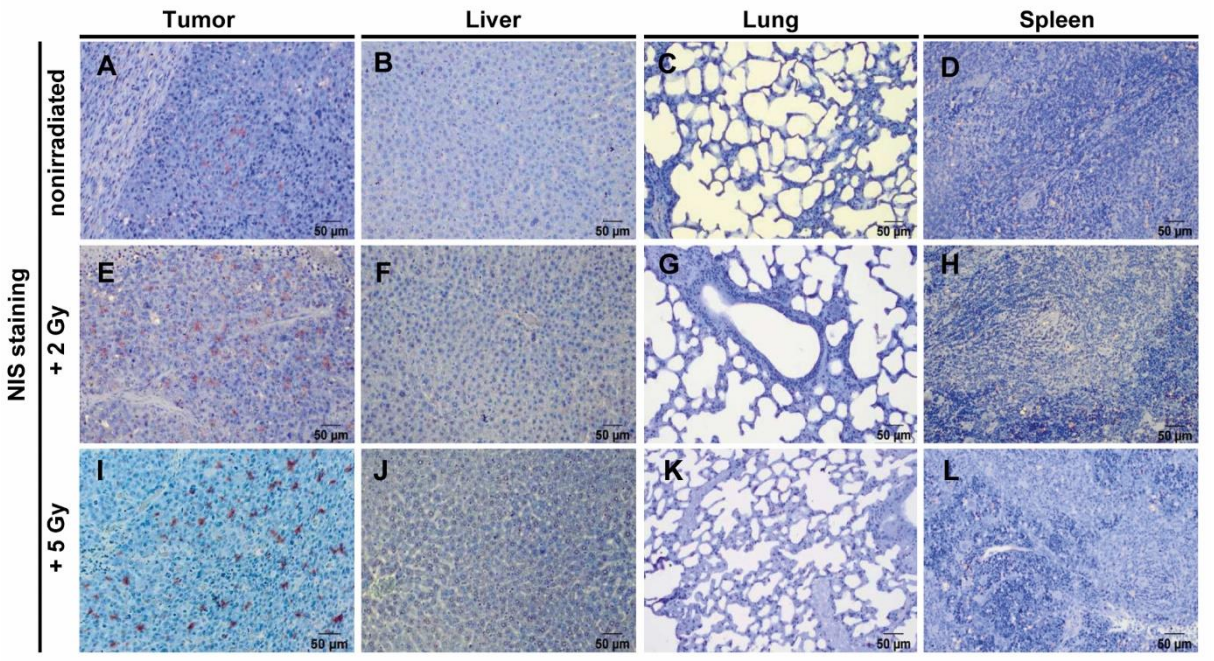

Fig. 7: *Compared to nonirradiated tumors* ***(A)****, higher NIS-specific immunoreactivity (red) was detected in tumors pretreated with external beam radiation therapy upon systemic MSC application* ***(E, I)****. For non-target organs, no NIS expression was detected* ***(B-D, F-H, J-L)****. One representative image is shown each. Scale bar = 50 µm.*

5.5 Discussion

Mesenchymal stem cells (MSCs) are currently under evaluation as tumor delivery vehicles based in part on their excellent tumor-homing properties. An important issue in the further development of this strategy is how well it could work when used in combination with existing tumor therapy. External beam radiotherapy is the most common form of cancer radiotherapy in use today. In the present study, we sought to evaluate the potential effects of radiation on the ability of MSCs, engineered to express the reporter gene NIS, to invade experimental tumors. The mechanisms underlying MSC recruitment to tumors have not been fully elucidated. The process is thought to mirror the mechanisms that are used by leukocytes during their recruitment to inflamed tissues, utilizing a cascade of events driven by cytokines, chemokines, integrins and selectins. A group of factors including PDGFB, VEGF and FGF2, chemokines/cytokines such as CXCL8 and CXCL12/SDF-1 and the pleotropic growth factor TGFB1/3 among others have been linked to MSC migration [47]. The homing of MSCs to tumor tissue can in some instances be enhanced by external beam radiation tumor pretreatment, potentially through increased secretion of chemokines and growth factors resulting from radiation injury [47]. Previous studies by Klopp *et al*. have shown improved engraftment of adoptively applied MSCs to irradiated murine mammary carcinoma as compared to nonirradiated tumors [65]. Similar results were also demonstrated in gliomas using hematopoietic progenitor cells (HPC), where increased migration was documented after gliomas were irradiated [118].

To test enhanced MSC homing following radiation treatment in a model of human hepatocellular cancer (HCC), we first addressed the question as to whether the expression and secretion of factors involved in the regulation of MSC migration were increased in the HCC cell line HuH7 following treatment [113, 114, 119]. The response to radiation differed between the genes tested with regards to level, time course and general response to radiation. The pleotropic cytokine TGFB1 is expressed in HCC and has been shown to promote tumorigenesis in established HCC tumors and to have an immunosuppressive effect [114]. In our study, irradiation of HuH7 cells revealed a dose-dependent increase in TGFB1 mRNA expression as well as enhanced protein secretion, though a slight decline in expression was observed when using high radiation doses (8 or 10 Gy). A similar effect was

observed for VEGF, a central regulator of angiogenesis [114]. Irradiated HuH7 cells also showed an increase in expression of another angiogenic factor, PDGFB. At the mRNA level, the highest increase was observed 12 h post radiation treatment, however PDGF-BB protein remained under the detection limit. Similar results were described in previous studies by Klopp et al., where a dose-dependent increase of TGFB1, PDGF-BB and VEGF protein expression was observed over a period of 48 h, when a murine mammary carcinoma cell line (4T1 cells) was irradiated with 0, 1 or 2 Gy [65]. In the HuH7 cell line, protein expression was not influenced by radiation before 48 h, whereas changes at the mRNA level appeared by 4 h post radiation treatment. In addition, we investigated FGF2, which is also known as a central regulator of the migratory potential of human MSCs [120]. Analysis of FGF2 revealed an increase on the mRNA level similar to PDGFB gene expression but remained below the detection limit for protein expression of irradiated HuH7 cells. Further investigation of the effect of radiation on HuH7 cells showed an increase of TSP-1 and the potent pro-inflammatory chemokines CXCL8 and CXCL12/SDF-1 on the mRNA and protein level. We observed an early effect of HuH7 cell radiation at the level of mRNA, where a wide range of chemokines and growth factors were increased as early as 4 h after irradiation and remained elevated until 24 h to 48 h post radiation treatment and for most factors an increase in protein secretion after 48 h. Thus, our data clearly demonstrate the ability of HuH7 cells to increase their expression of cytokines and growth factors directly involved in MSC recruitment after radiation treatment. These findings were further confirmed in another human cancer cell line derived from breast adenocarcinoma (MDA-MB-231). MDA-MB-231 showed a similar response to radiation as HuH7 by increasing mRNA expression levels of CXCL8, TGFB1, TSP-1 and VEGF in a dose-dependent manner using 0,2 ,5 or 10 Gy, but differed in regard to mRNA levels and time course (0, 8, 24 or 48 h).

An *in vitro* migration assay was then performed to corroborate that irradiation of tumor cells can cause an increased migration of MSCs. Those experiments confirmed enhanced direct chemotaxis of MSCs to supernatants isolated from irradiated HuH7 and MDA-MB-231 cells substantiating our hypothesis and formed the basis for an *in vivo* approach to improve the NIS-mediated iodide uptake in non-thyroidal tumors using MSCs as gene delivery vehicles by pretreating tumors with radiation. Previous studies demonstrated the excellent tumor-homing of MSCs into the microenvironment of different tumors [50-52, 57-60, 68]. The theranostic gene

NIS is used for noninvasive imaging of functional NIS expression by ^{123}I-scintigraphy, allowing efficient tracking of NIS engineered MSCs *in vivo* by dynamic radioiodide imaging. We and others have extensively investigated the capacity of NIS to induce radioiodide accumulation in non-thyroidal tumors using MSCs as NIS gene delivery vehicles [56-60]. The efficacy of MSCs to deliver the NIS gene deep into tumors has been shown in different approaches by our group [57-60]. Active MSC engraftment has been demonstrated in various tumor models, including subcutaneous and orthotopic HCC xenografts as well as a hepatic colon cancer metastases model [57-60]. These MSC-based NIS gene therapy approaches resulted in a significant delay in tumor growth and prolonged animal survival after radioiodine accumulation. We sought to build upon these results to improve the level and selectivity of MSC tumor homing, and to enhance the therapeutic efficacy of NIS-mediated ^{131}I treatment to further increase selectivity, efficacy and safety. Using a previously described subcutaneous HCC mouse model and reporter MSCs engineered with a CMV-NIS construct, significantly increased MSC recruitment was demonstrated into tumor sites that had been irradiated with low-doses (2 and 5 Gy). Francois *et al*. demonstrated enhanced MSC migration after treatment of tumors with high doses (26.5 Gy) of radiation [63]. Studies of Zielske *et al*. showed that more MSCs migrated to tumors irradiated with a minimum of 5 Gy [69]. Different tumor types, including breast, colon and head/neck tumors, were irradiated with 2, 5 or 9 Gy. Analysis of MSC recruitment showed enhanced recruitment in all tumors irradiated with 5 or 9 Gy, except in tumors established from UMSCC1 head/neck carcinoma cells [69]. On the other hand, Klopp *et al*. were able to efficiently attract MSCs to tumor sites of breast cancer using low-dose irradiation such as 1 and 2 Gy [65].

We examined if MSC recruitment is enhanced in tumors pretreated with low-dose irradiation (2 or 5 Gy) using NIS imaging (^{123}I-scintigraphy). Tumor-specific radioiodide uptake activity was observed in all groups (0, 2 and 5 Gy). Tumors locally treated with radiation revealed a significantly higher NIS-mediated iodide uptake after a single MSC application 24 h post radiation treatment compared to non-irradiated tumors. The maximum radioiodide uptake activity of tumors irradiated with 2 or 5 Gy was 7.9 and 9.2 % ID/g respectively, whereas nonirradiated tumors accumulated only 5.3 % ID/g. The enhanced recruitment of MSCs into irradiated HuH7 tumors was also verified *ex vivo* using NIS immunohistochemistry that showed increased recruitment of NIS-MSCs in tumors pretreated with low-dose radiation.

Importantly, the positive effects seen with low-dose irradiation (with lower toxicity and side effects on the normal surrounding tissues) effectively sets the stage for more detailed studies of the combined effects of enhanced delivery of therapy genes by MSCs with cancer radiation treatment. Radiotherapy has been also shown to have effects on the tumor stroma, which is comprised of tumor endothelial cells and cancer-associated fibroblasts (CAFs) as well as other cell types [121]. Radiation of tumors not only leads to enhanced stimulation of cytokine and growth factor secretion by tumor cells but is also responsible for radiation-induced dysfunction or even apoptosis of tumor endothelial cells, which in turn lead to hypoxia, increased permeability as well as an enhanced inflammatory response [121, 122]. Due to vascular depletion, the pro-angiogenic and pro-vasculogenic factors VEGF and CXCL12/SDF-1 are increased [121, 123, 124]. Radiation also drives activation of CAFs within the tumor stroma, which in turn increase growth factor secretion and the release of cytokines such as HGF, PDGF, CXCL12/SDF-1 and TGFβ [121]. Another aspect besides an increased inflammatory response, which was shown in this study to increase MSC recruitment *in vitro*, is a possible radiation-induced stimulation of tumor vascular permeability, which could be another important trigger for enhanced MSC recruitment *in vivo*. Using doses of 5-10 Gy, an initial increase of tumor blood flow after irradiation has been reported with a return to levels seen before irradiation 2-3 days post radiation [125]. Taking this into consideration, irradiation-induced enhanced MSC migration to tumors might be a combinatorial effect of stimulated secretion of cytokines and growth factors involved in the process of MSC tumor homing as well as increased tumor permeability allowing MSCs to passage the tumor stroma more easily. These complex effects of irradiation on tumor cells and their (micro-)environment not only enhances MSC tumor recruitment as demonstrated in our study, but may also foster MSC tumor engraftment and therefore, represents a highly promising tool to significantly stimulate MSC-driven gene therapy approaches. Taken together, our results show a dose-dependent increase of NIS-mediated accumulation of ^{123}I due to enhanced MSC recruitment to irradiated tumors using low-dose irradiation. Based on these findings an enhanced accumulation of the therapeutically active radioisotope ^{131}I is expected after combining EBRT and MSC gene delivery, which we will evaluate in future studies.

In summary, our study demonstrates that radiation of experimental HCC enhances the secretion of diverse inflammatory cytokines and growth factors involved in MSC

migration, which can be linked to enhanced migration of adoptively applied MSCs deep into tumor microenvironments. These data open the exciting prospect for a new therapy approach, in which HCC tumors are pretreated with low-dose radiation prior to systemic MSC application aiming at increasing the efficacy of MSC-mediated NIS gene therapy.

5.6 Supporting Information

5.6.1 Supplemental figures and tables

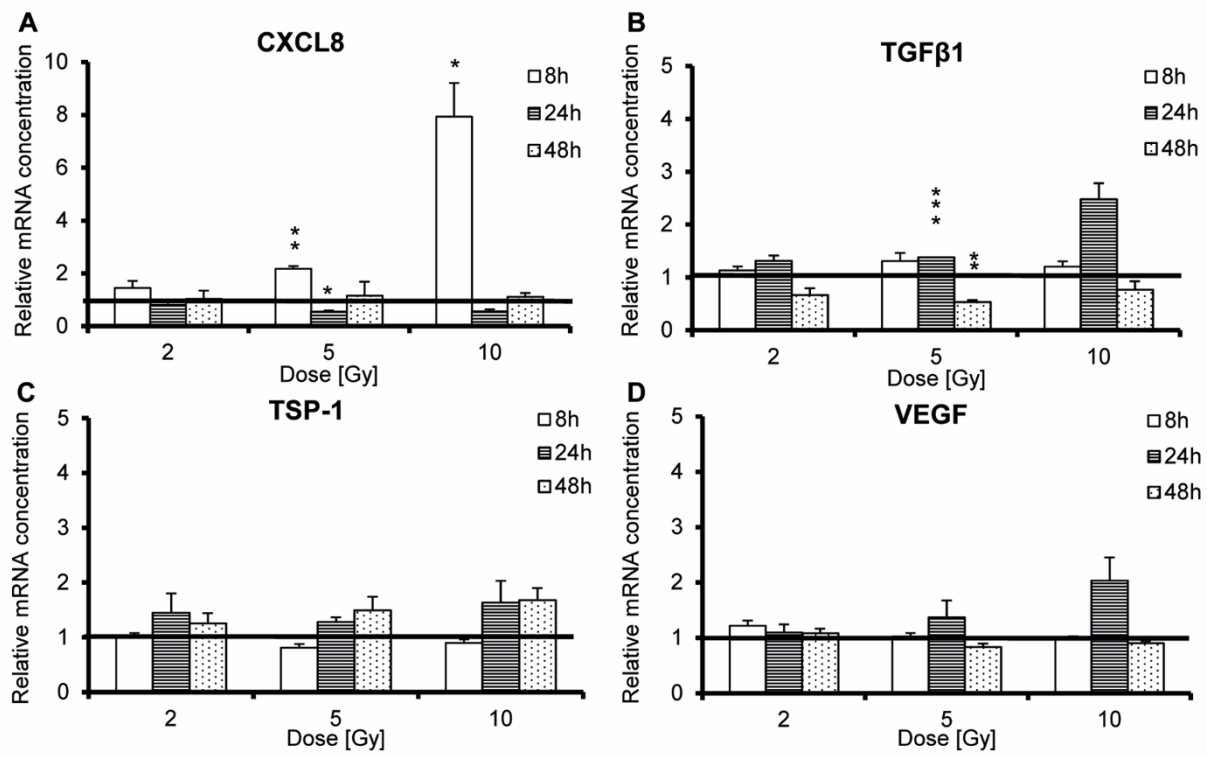

Supplementary Fig. 1: *Irradiation of MDA-MB-231 cells using 2, 5 or 10 Gy enhances gene expression of inflammatory cytokines and growth factors during a period of 8 to 48 h* ***(A-D)****. Data are represented as mean fold change ± SEM as compared to nonirradiated MDA-MB-231 cells (n=3; two-tailed Student's t-test: *P<0.05; **P<0.01, ***P<0.001).*

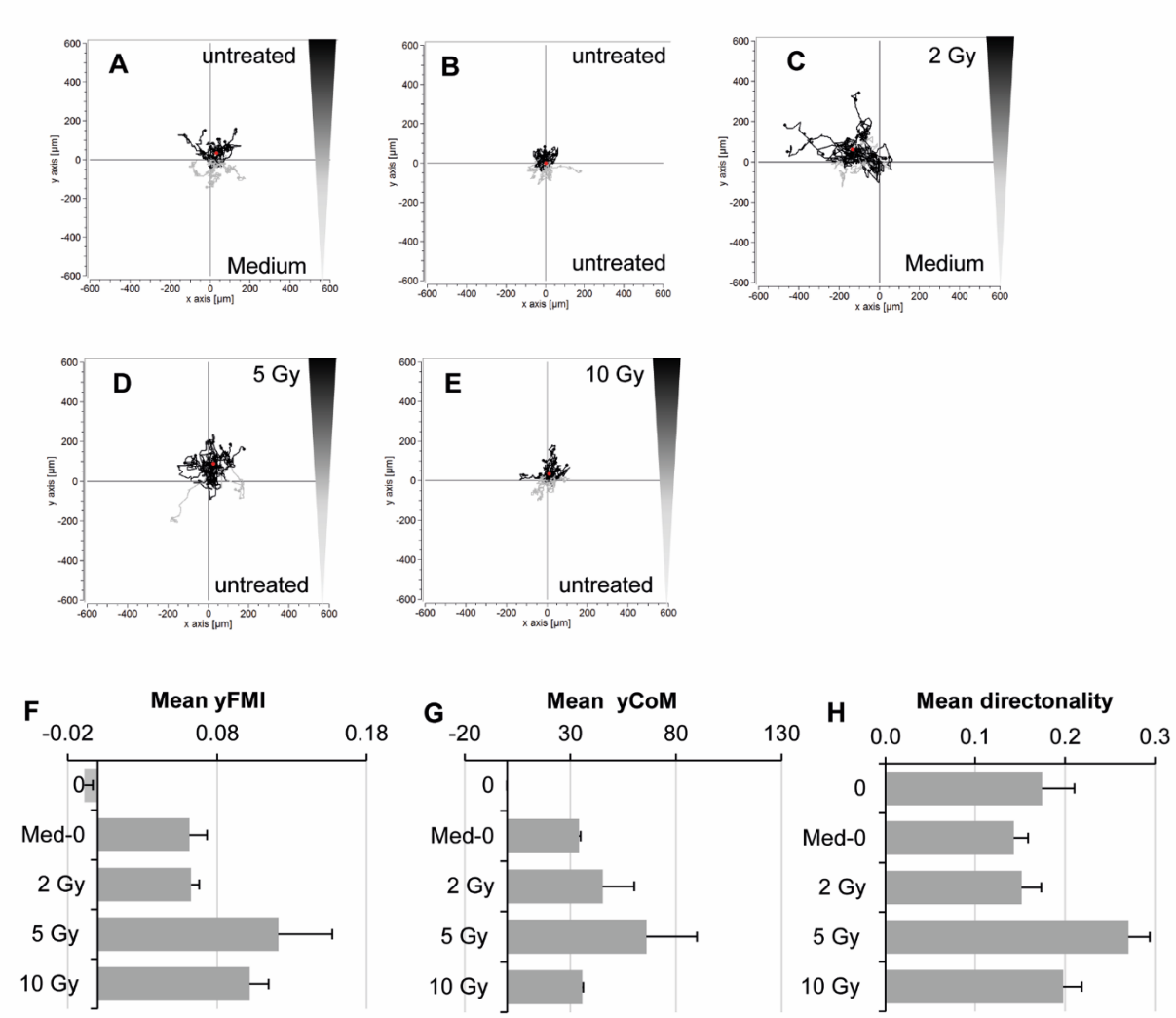

Supplementary Fig. 2: *MSCs subjected to a gradient of isolated supernatants from nonirradiated and irradiated MDA-MB-231 cells (2, 5 or 10 Gy) showed increased migration over 24 h* ***(C-E, F-H)*** *as compared to supernatants of untreated cells as controls, where only random chemokinesis was observed* ***(A, B, F-H)****. One representative image each is shown from two independent experiments. Quantification of chemotaxis parameters as yFMI, yCoM and directionality was done* ***(F-H)****. CoM is indicated by red dots* ***(G)****. Data are* represented as mean fold change ± SEM from two independent experiments.

5.7 Acknowledgements

We are grateful to Dr. S.M. Jhiang, Ohio State University, Columbus, OH, USA for supplying the full-length human NIS cDNA. We also thank Prof. Dr. K. Scheidhauer and Jakob Allmann, Department of Nuclear Medicine, Klinikum rechts der Isar der Technischen Universität München, Munich, Germany, for their assistance with the imaging studies. We thank Doris Mayr (Department of Pathology, Ludwig-Maximilians-University, Munich, Germany) for preparation of paraffin-embedded slides.

This work was supported by grants from the Deutsche Forschungsgemeinschaft within the Collaborative Research Center SFB 824 to C Spitzweg (project C8) and within the Priority Program SPP1629 to C Spitzweg and PJ Nelson (SP 581/6-1, SP 581/6-2, NE 648/5-2) as well as within a grant from the Wilhelm-Sander-Stiftung to C Spitzweg (2014.129.1).

6. Chapter 4: Radiation-induced Amplification of TGFB1-induced Mesenchymal Stem Cell-mediated *NIS* Gene ^{131}I Therapy

This chapter has been adapted from the submitted manuscript:

Schug C[1], Kitzberger C[1], Sievert W[2], Spellerberg R[1], Tutter M[1], Schmohl KA[1], Schwenk N[1], Christian Zach[3], Schwaiger M[4], Multhoff G[2], Wagner E[4], Nelson PJ[5] and Spitzweg C[1]. Radiation-induced Amplification of TGFB1-induced Mesenchymal Stem Cell-mediated *NIS* Gene ^{131}I Therapy. [submitted manuscript]

[1]Department of Internal Medicine IV, University Hospital of Munich, LMU Munich, Munich, Germany, [2]Center for Translational Cancer Research (TranslaTUM), Klinikum rechts der Isar, Radiation Immuno-Oncology group, Munich, Germany, [3]Department of Nuclear Medicine, University Hospital of Munich, Ludwig-Maximilian-University Munich, Munich, Germany, [4]Department of Nuclear Medicine, Klinikum rechts der Isar, Technische Universitaet Muenchen, Munich, Germany, [5]Department of Pharmacy, Center of Drug Research, Pharmaceutical Biotechnology, LMU Munich, Munich, Germany, [6]Clinical Biochemistry Group, Department of Internal Medicine IV, University Hospital of Munich, LMU Munich, Munich, Germany

6.1 Abstract

The sodium iodide symporter (NIS) is the operational molecule that has allowed the efficient treatment of thyroid malignancies by the administration of ^{131}I for over 70 years. Various vector-driven approaches are currently under investigation to introduce the *NIS* gene into non-thyroidal tumors in order to more broadly apply this effective anticancer therapy. One such system makes use of genetically engineered mesenchymal stem cells (MSC) as therapy vehicles for the delivery of *NIS* into solid tumors. MSCs show an innate ability to home to and invade tumor environments in response to the danger signals and inflammatory cytokines produced by the tumor milieu. We and others have demonstrated that tissue or signal-specific gene promoters are able to enhance the specificity of MSC-mediated *NIS* transgene expression in tumors. External beam radiation therapy (EBRT), a standard principal therapeutic modality for the treatment of cancer, results in tissue damage and hence enhanced recruitment of *NIS*-expressing MSCs into human hepatocellular carcinoma (HuH7). At the same time, the tumor-associated cytokine TGFB1 is strongly upregulated in HuH7 tumors in response to radiation pretreatment. In the current study, we show that combining EBRT with MSC-based NIS-mediated ^{131}I therapy dramatically enhances therapeutic efficacy when a synthetic TGFB1-inducible SMAD-responsive promoter, as opposed to a constitutive CMV-promoter, is used to drive *NIS* expression in MSCs. It is thought that the remarkable therapeutic effect seen is linked to the enhanced TGFB1 produced in this context, which leads to a highly selective and focused amplification of MSC-based *NIS* expression within the tumor milieu.

6.2 Introduction

The sodium iodide symporter (NIS) is an intrinsic transmembrane glycoprotein that actively transports iodide into the thyroid gland. NIS biology forms the basis for the efficient management of thyroid cancer patients through the use of radioiodine. NIS functions as a theranostic protein, allowing noninvasive imaging, such as ^{123}I-scintipgraphy and ^{124}I-PET imaging, as well as treatment by application of therapeutic radioiodine (^{131}I) [20, 21, 23, 126]. Diverse approaches are currently underway to investigate *NIS*-based therapy in non-thyroidal tumors using various delivery systems [20-23, 28, 30, 33, 34, 36-38, 41, 57-60]. Mesenchymal stem cells (MSCs) are attractive vehicles for the potential delivery of therapeutic genes into solid tumors. Adoptively applied, engineered versions of MSCs have been shown to allow the expression of therapeutic genes such as the *NIS* transgene deep within tumor environments [58-60]. The ability of MSCs to be recruited to tumor environments is due in large part to the release of various factors produced in response to the inflammation and hypoxic damage found in solid tumors [45-47]. The basic mechanisms underlying this recruitment are thought to parallel those seen in the recruitment of endogenous MSCs during tissue repair [45, 46].

While radiation in general represents one of the most common therapies for the treatment of carcinoma patients, external beam radiation therapy (EBRT) now allows an accurate delivery of radiation to tumors that effectively limits damage to the surrounding normal tissue [127]. EBRT can be combined with other therapeutic approaches to refine or enhance tumor targeting and patient outcome. Recent studies have shown that radiation pretreatment of tumors can enhance the tumor-homing properties of adoptively applied MSCs [63, 65, 69, 128]. Tumor irradiation leads to an increased inflammatory response and an enhanced secretion of factors involved in MSC recruitment [47, 65, 129].

Klopp *et al.* described enhanced MSC recruitment to irradiated murine mammary carcinoma [65]. A similar effect was also observed in irradiated gliomas using hematopoietic progenitor cells (HPC) [118]. Further, in a recent study our own group demonstrated enhanced secretion of various inflammatory factors involved in MSC tumor homing after irradiation of the human hepatocellular carcinoma (HCC) cell line HuH7. The increased expression of the chemokine (C-X-C motif) ligand 12/stromal cell-derived factor 1 (CXCL12/SDF-1), CXCL8, fibroblast growth factor 2 (FGF2),

platelet-derived growth factor (PDGF), transforming growth factor beta 1 (TGFB1), thrombospondin 1 (TSP-1) and vascular endothelial growth factor (VEGF) were linked to the enhanced migration of genetically engineered MSCs to the tumor stroma that in turn led to an increased expression of the theranostic *NIS* transgene under control of the constitutively active CMV-promoter [129]. Therefore, using radiation pretreatment to enhance the MSC tumor homing capability opens the exciting prospect of combining EBRT with MSC-mediated gene delivery strategies to improve transgene delivery to tumor environments.

Our group has previously shown that the use of tissue or signal-specific gene promoters, whose activation is linked to tumor-derived signals, allow a more selective activation of MSC-based transgenes such as *NIS* and thereby can improve the specificity of tumor treatment [58-60, 128]. As TGFB plays important roles in the biology of tumor growth and is expressed by most solid tumors, a synthetic TGFB1-inducible SMAD-responsive promoter, was tested in stably transfected engineered MSCs to control *NIS* transgene expression (SMAD-NIS-MSCs) within tumors. In our recent work we have reported that systemic application of SMAD-NIS-MSCs to mice harboring subcutaneous human hepatocellular carcinoma derived from the TGFB1-expressing HuH7 cell line resulted in a significant delay in tumor growth and prolonged survival of animals [128]. This proof-of-principle of using the TGFB1-inducible SMAD-responsive promoter as a tumor signal-responsive promoter in the setting of *NIS* gene therapy, together with the data from our previous work demonstrating stimulation of MSC recruitment by EBRT tumor pretreatment as well as identifying TGFB1 as a major tumor derived signals in response to EBRT treatment, suggested that EBRT may not only enhance the migratory behavior of MSCs but may also act to amplify promoter activation in SMAD-NIS-MSCs due to increased TGFB1 expression in irradiated tumors [128, 129]. We and others had previously speculated that gene promoters that are either directly or indirectly responsive to radiation-induced signals could potentially allow an amplification of therapy transgene expression when used in the setting of NIS-mediated radioiodine therapy. The accumulated radioiodine-induced tumor damage in association with an inflammatory response that effectively drives the activation of the radiation-responsive promoter could lead to more efficient *NIS* expression. Based on this hypothesis and the data described above, we combined in the present study EBRT treatment with MSC-mediated SMAD-promoter-driven *NIS* gene transfer to evaluate

potential additive effects. The therapeutic efficacy of engineered MSCs was tested by combining radiation pretreatment of tumors with the application of either SMAD- or CMV-NIS-MSC-mediated *NIS* gene delivery in mice harboring subcutaneous HuH7 tumors. MSCs were systemically injected 24 h after low-dose radiation pretreatment of the tumors. The subsequent effects on the tumoral TGFB1-induced, NIS-mediated radioiodide accumulation were examined using ^{123}I-scintigraphy. Therapeutic efficacy was then determined after pretreating tumors with radiation followed by SMAD- or CMV-NIS-MSC-mediated *NIS* transgene delivery and ^{131}I application. Pretreatment with low-dose external beam radiation of subcutaneous human HuH7 tumors, following systemic application of SMAD-NIS-MSCs resulted in an amazing reduction of tumor growth up to complete remission of tumors in a subset of animals and dramatically prolonged survival of animals as compared to animals receiving CMV-NIS-MSC treatment or controls.

6.3 Materials and methods

Cell culture

The human hepatocellular carcinoma cell line HuH7 used in the experiments were authenticated and purchased from JCRB Cell Bank (JCRB 0403, Osaka, Japan). DMEM (Sigma-Aldrich, St. Louis, Missouri, USA) supplemented with 10% FBS (FBS Superior, Biochrom/Merck Millipore, Berlin, Germany) and 100 U/ml penicillin/100 µg/ml streptomycin (Sigma-Aldrich) was used for cell culture. The human bone marrow derived, SV40 large T antigen immortalized MSC cell line was described and cultured as described previously [111]. An incubator at 37°C and 5% CO_2 was used for all cells.

SMAD-NIS-MSCs

The design of the pcDNA6-2ITRNEO-SMAD-NIS expression vector as well as the stable transfection of MSCs was performed as described previously [128]. SMAD-NIS-MSCs were cultured in RPMI medium containing 0.5 mg/ml geneticin (Invitrogen), 10% fetal bovine serum and 100 U/ml penicillin/100 µg/ml streptomycin.

^{125}I uptake assay

After starving cells overnight, SMAD-NIS-MSCs were stimulated with either only 10 ng/ml recombinant TGFB1 or in combination with HuH7-CM (irradiated or nonirradiated) or HuH7-CM only for a period of 24 h to validate promoter inducibility. NIS-mediated radioiodide uptake of SMAD-NIS-MSC was determined at steady-state conditions as described previously [66]. Results were normalized to cell viability.

Cell viability assay

Cell viability was determined using the commercially available MTT assay (Sigma-Aldrich) according to the manufacturer's recommendations as described previously [60].

Irradiation of HuH7 cells

Irradiation of HuH7 cells using 5 Gy was performed as described previously [129]. Supernatants of irradiated and non-irradiated HuH7 cells were removed 48 h after irradiation, centrifuged and stored at -80°C.

Immunohistochemical TGFB1 staining

Immunohistochemical TGFB1 staining were conducted as described previously [128].

Animals

5-week-old female CD1 nu/nu mice were purchased from Charles River (Sulzfeld, Germany) and housed under specific pathogen-free conditions. Mice had access to mouse chow and water *ad libitum*. Experiments were approved by the regional governmental commission for animals (Regierung von Oberbayern) and performed in accordance with institutional guidelines of the Klinikum rechts der Isar, Technische Universität München.

Establishment of HuH7 xenograft tumors

To establish HuH7 xenograft tumors in CD1 nu/nu mice, 5×10^6 HuH7 cells/100 µl PBS were injected subcutaneously into the right flank region as described previously [57]. Regular measurment and estimation of the tumor volume were done using the equation: length × width × height × 0.52. Exceeding a tumor size of 1500 mm^3 led to scarification of mice.

Irradiation of HuH7 xenograft tumors

The precise irradiation using 5 Gy was performed as described previously [129] after subcutaneous HuH7 tumors reached a diameter of approximately 5-10 mm for ^{123}I-scintigraphy or 1-5 mm for therapy.

Systemic SMAD-NIS-MSC application and in vivo ^{123}I-scintigraphy

5 mg/ml L-T4 (Sigma-Aldrich) was supplemented to the drinking water of mice to suppress thyroidal iodide uptake. 24 h after tumor irradiation 5×10^5 SMAD-NIS-MSCs in 500µl PBS were systemically applied. 72 h after SMAD-NIS-MSC injection, 18.5 MBq (0.5 mCi) of ^{123}I were applied peritoneally. Radioiodide biodistribution was assessed using ^{123}I-scintigraphy, a gamma camera provided with a low-energy high resolution collimator (e.cam, Siemens, Munich, Germany). Analysis of regions of

interests (ROIs) was done with the HERMES GOLD (Hermes Medical Solutions, Stockholm, Sweden) program. Quantified results were expressed as a fraction of the total amount of applied radionuclide per gram tumor tissue (% ID/g). The radionuclide retention time was determined by serial scanning within the tumors and dosimetric calculations were done as described previously [60].

Immunohistochemical stainings for NIS expression

After *in vivo* application of SMAD-NIS-MSCs, tumors and nontarget organs (liver, lung and spleen) were dissected. Paraffin-embedded tissues were immunohistochemically stained for NIS expression as described previously [130].

Radioiodine therapy study

10-days before therapy start, mice received drinking water supplemented with 5 mg/ml L-T4. For therapy, tumors were irradiated (5 Gy) followed by a single SMAD-NIS-MSCs application 24 h later. 72 h after the SMAD-NIS-MSC injection mice received 55.5 MBq ^{131}I (n=7; 5 Gy + SMAD-NIS-MSCs + ^{131}I). 24 h after ^{131}I application, the treatment cycle of radiation pretreatment and MSC application was repeated. For therapy completion, a last cycle as described was done without radiation pretreatment of tumors. As controls, a subset of mice received NaCl instead of radioiodide (n=8; SMAD-NIS-MSCs+NaCl) or saline only after radiation treatment (n = 6; 5 Gy + NaCl). For exact evaluation of the therapeutic effect, a subset of mice received no radiation therapy and only saline applications (n = 7; NaCl + NaCl). To illustrate the improved therapeutic effect of SMAD-NIS-MSCs, CMV-NIS-MSCs were applied instead for therapy (n=6; 5 Gy + SMAD-NIS-MSCs + ^{131}I). Tumor volume was measured regularly and mice were euthanized when a tumor volume of 1500 mm^3 was exceeded.

Indirect immunofluorescence assay

Frozen tissue sections of tumors from the radioiodine therapy study were used for indirect immunofluorescence analysis of Ki67 (cellular proliferation) and CD31 (blood vessel density) as described previously [60]. The percentage of positive cells for Ki67 and CD31-positive areas within the tumors was quantified by evaluation of 5 high-power fields per tumor (n=3, 5 Gy + SMAD-NIS-MSCs + ^{131}I; n=4, 5 Gy + CMV-NIS-MSCs + ^{131}I; n=6, 5 Gy + SMAD-NIS-MSCs + NaCl; n=5, 5 Gy + NaCl; n=7, NaCl +

NaCl) using ImageJ software (NIH, Bethesda, MD). Results are presented as means ± SEM. Statistical significance was calculated using students t-test.

Statistical methods

Results are expressed as mean ± SEM or percentage and statistical significance was tested by two-tailed Student´s *t*-test or one-way ANOVA for tumor volumes and log-rank test for survival plots for experiments. *P* values of < 0.05 were considered significant (*$p < 0.05$; **$p < 0.01$; ***$p < 0.001$).

6.4 Results

***In vitro* NIS-mediated radioiodide uptake in SMAD-NIS-MSCs**

To verify the selective response of SMAD-based synthetic gene promoter, SMAD-NIS-MSCs were stimulated *in vitro* with TGFB1 (10 ng/ml), which led to a 5.4 fold increase in NIS-mediated radioiodide ^{125}I accumulation (Fig. 1). No accumulation of ^{125}I was observed above background levels without TGFB1 stimulation. To further characterize the potential activation of this transgene response to tumor-radiation signals, SMAD-NIS-MSCs were additionally treated with irradiated and non-irradiated HuH7- CM. Whereas no accumulation of ^{125}I was observed after subjecting MSCs to HuH7-CM only, treatment with HuH7-CM together with TGFB1 resulted in an significant increase of radioiodide uptake of approximately 59 % in MSCs as compared to stimulation with TGFB1 only (Fig. 1). Radioiodide uptake activity in SMAD-NIS-MSCs stimulated with HuH7-CM from 5 Gy irradiated HuH7 cells (SMAD-NIS-MSCs + 5 Gy treated HuH7-CM) and TGFB1 resulted in an additional increase of about 12 % as compared to the stimulation with normal HuH7-CM and TGFB1 (Fig. 1). These findings corroborate with the analysis of a TGFB1 enzyme linked immunosorbent assay (ELISA), where no active but inactive TGFB1 protein was detected in HuH7-CM (data not shown).

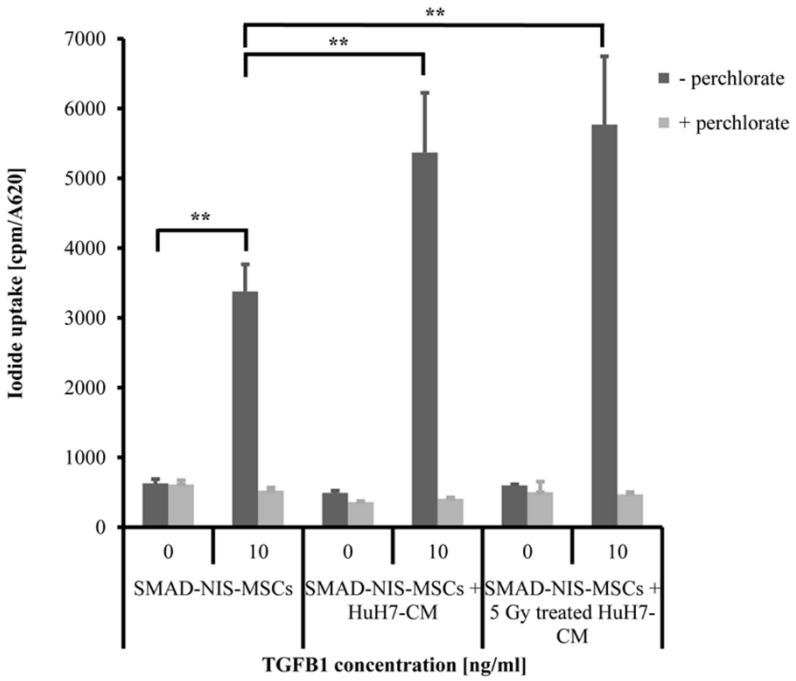

Fig. 1: *SMAD-NIS-MSCs stably expressing NIS under control of a SMAD-responsive promoter.* Iodide uptake studies demosntrated a 5.4-fold high NIS-specific, perchlorate-sensitive ^{125}I uptake in SMAD-NIS-MSCs stimulated with TGFB1 (10 ng/ml) as compared to unstimulated cells, where no radioiodide uptake above background levels was observed. Combined treatment of SMAD-NIS-MSCs with TGFB1 (10 ng/ml) and HuH7-CM led to further increased radioiodide uptake as compared to stimulated cells without HuH7-CM. This effect was even enhanced adding HuH7-CM from HuH7 cells, which were irradiated with 5 Gy. No radioiodide accumulation above background levels was observed treating SMAD-NIS MSCs with HuH7-CM (non-irradiated or irradiated) alone. Data are represented as means of three independent experiments ± SEM (n=3; two-tailed Student's t-test: *p<0.05; ** p <0.01, *** p <0.001).

TGFB1 expression in non-irradiated and irradiated HuH7 tumors

TGFB1 protein expression in subcutaneous HuH7 tumors was analyzed using immunohistochemistry (Fig. 2). Moderate TGFB1 expression was detected within the stroma of non-irradiated HuH7 tumors (Fig. 2a). Irradiation of tumors using a low-dose of 5 Gy led to an increase in TGFB1 protein expression within the tumor stroma (Fig. 2b).

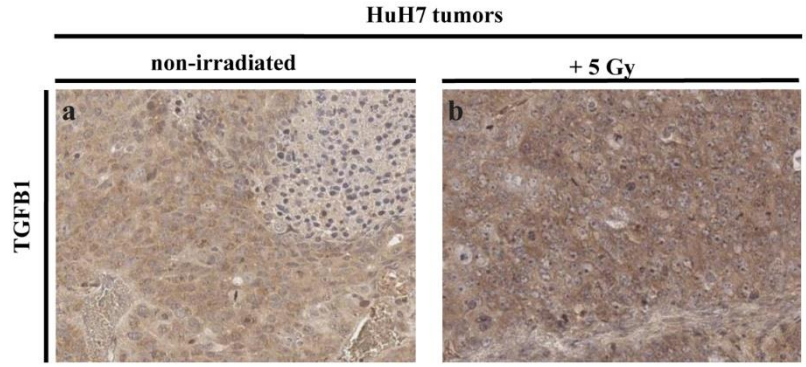

Fig. 2: *Tumor-specific TGFB1 protein expression. Dissected tumors showed TGFB1 protein expression (brown) in non-irradiated tumors* **(a)** *and an increased expression in tumors irradiated with low-dose radiation (5 Gy)* **(b)**. *One representative image at 20× magnification is shown each.*

In vivo ^{123}I-Scintigraphy

Nude mice with subcutaneous HCC xenograft tumors received a single SMAD-NIS-MSCs (0.5×10^6) injection via the tail vein (i.v.) 72 h prior to ^{123}I-scintigraphy (Fig. 3a, b). To monitor radioiodide biodistribution, 18.5 MBq ^{123}I were administered intraperitoneally. Non-irradiated HuH7 tumors revealed a radioiodide accumulation of approximately 7.0 % ID/g tumor and a biological half-life of 3.9 h with a tumor absorbed dose of 52.37 mGy/MBq ^{131}I (Fig. 3a, e). The stomach, salivary and thyroid gland as well as the urinary bladder, due to renal excretion, showed endogenous NIS-mediated radioiodide uptake. To demonstrate NIS-specificity, radioiodide uptake was blocked upon treatment with perchlorate 30 min prior to the radioiodide administration in a subset of mice (Fig. 3b). A second group of mice received tumor radiation pretreatment using 5 Gy 24 h prior to the single SMAD-NIS-MSCs application (Fig. 3c, d). The precise radiation of the subcutaneous tumors led to an increased NIS-specific radioiodide accumulation of approximately 9.8 % ID/g tumor as compared to non-irradiated tumors (7.0 % ID/g tumor) (Fig. 3a, e). A biological half-life of 3.0 h and a tumor absorbed dose of 56.72 mGy/MBq ^{131}I was calculated for the irradiated HuH7 tumors. Perchlorate treatment resulted in no accumulation of radioiodide in irradiated tumors (Fig. 3d).

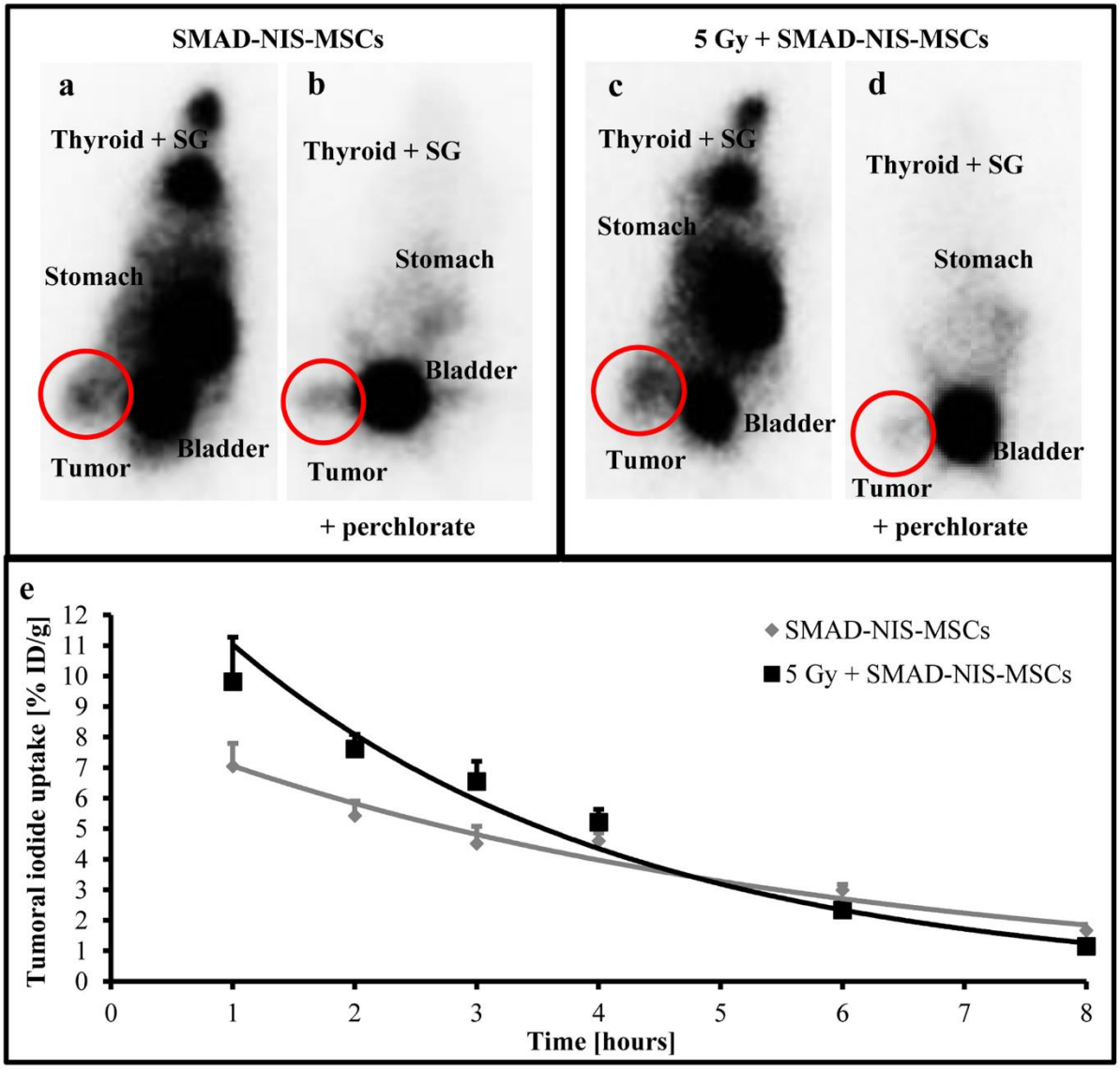

Fig. 3: *^{123}I-scintigraphy showed increased NIS-specific tumoral radioiodide uptake after radiation pretreatment of tumors. Subcutaneous HuH7 tumors were irradiated with 5 Gy. A single systemic injection of SMAD-NIS-MSCs 24 h after radiation pretreatment of tumors resulted in a maximum of approximately 9.8 % ID/g tumor as compared to non-irradiated tumors followed by SMAD-NIS-MSC injection (7.0 % ID/g tumor)* ***(a, c)****. Tumoral radioiodide uptake was blocked upon treatment with the NIS-specific inhibitor perchlorate* ***(b, d)****. Data are represented as mean values ± SEM.*

Ex vivo NIS protein expression in HuH7 tumors

NIS-immunohistochemistry was performed on non-irradiated as well as irradiated tumors after application of SMAD-NIS-MSCs showing high NIS-specific immunoreactivity throughout the tumor stroma (Fig. 4a, e). NIS protein expression was shown to be increased in the tumors receiving radiation pretreatment confirming an enhanced recruitment and activation of SMAD-NIS-MSCs in irradiated tumors

(Fig. 4e). No NIS protein expression was detected in non-target organs such as liver, lung and spleen (Fig. 4b-d, f-h).

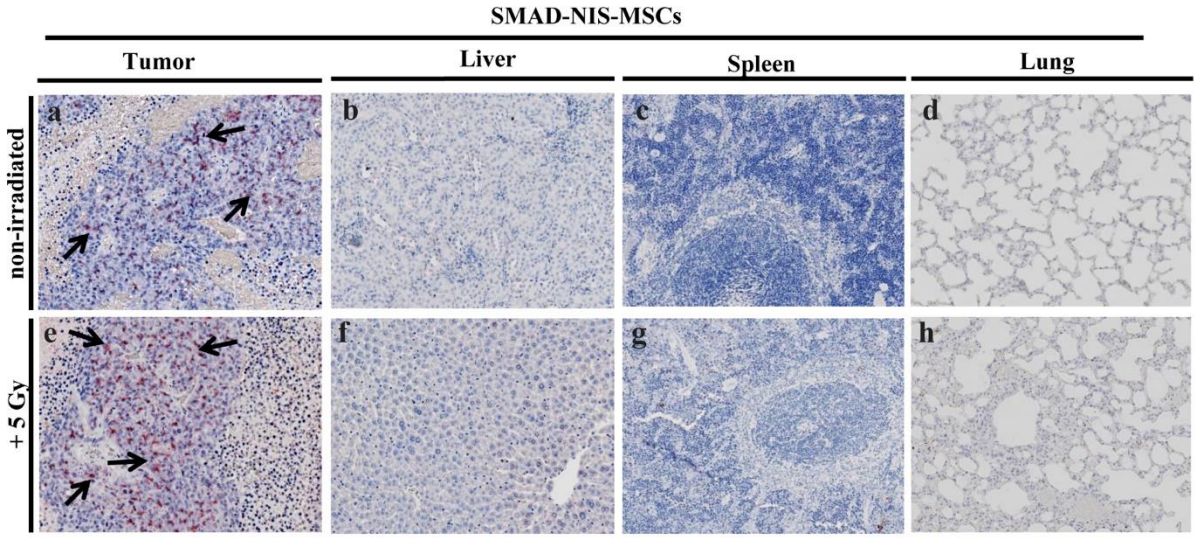

Fig. 4: *Tumor-specific NIS protein expression. After ^{123}I-scintigraphy, tumors were dissected and stained for NIS protein expression in SMAD-NIS-MSCs demonstrating high NIS-specific immunoreactivity (red) after receiving SMAD-NIS-MSCs* ***(a, e).*** *Tumor radiation pretreatment (5 Gy) led to increased NIS protein expression, thus confirming enhanced tumor homing of NIS-expressing MSCs to irradiated tumors* ***(a)****. No NIS protein expression was detected in non-target organs* ***(b-d)****. One representative image at 20× magnification is shown each.*

In vivo Radioiodine therapy studies

Therapeutic efficacy of the SMAD-NIS-MSC-based NIS-mediated ^{131}I therapy was then evaluated by systemically applying SMAD-NIS-MSCs in mice with subcutaneous HuH7 tumors, which were pretreated with 5 Gy (5 Gy + SMAD-NIS-MSCs + I-131) (Fig. 5). As controls, mice received radiation pretreatment followed by saline only (5 Gy + NaCl) or SMAD-NIS-MSCs followed by saline applications (5 Gy + SMAD-NIS-MSCs + NaCl). A further control group received saline only (NaCl + NaCl). To evaluate if there is an improved therapeutic effect due to the use of tumor signal-responsive promoter that is also activated by the response of radiation, a group of mice with irradiated tumors received MSCs stably transfected with the constitutive active CMV-promoter to control *NIS* transgene expression followed by radioiodine treatment (5 Gy + CMV-NIS-MSCs + I-131). Mice receiving NaCl only showed exponential tumor growth and had to be sacrificed within 35 days (Fig. 5a, b).

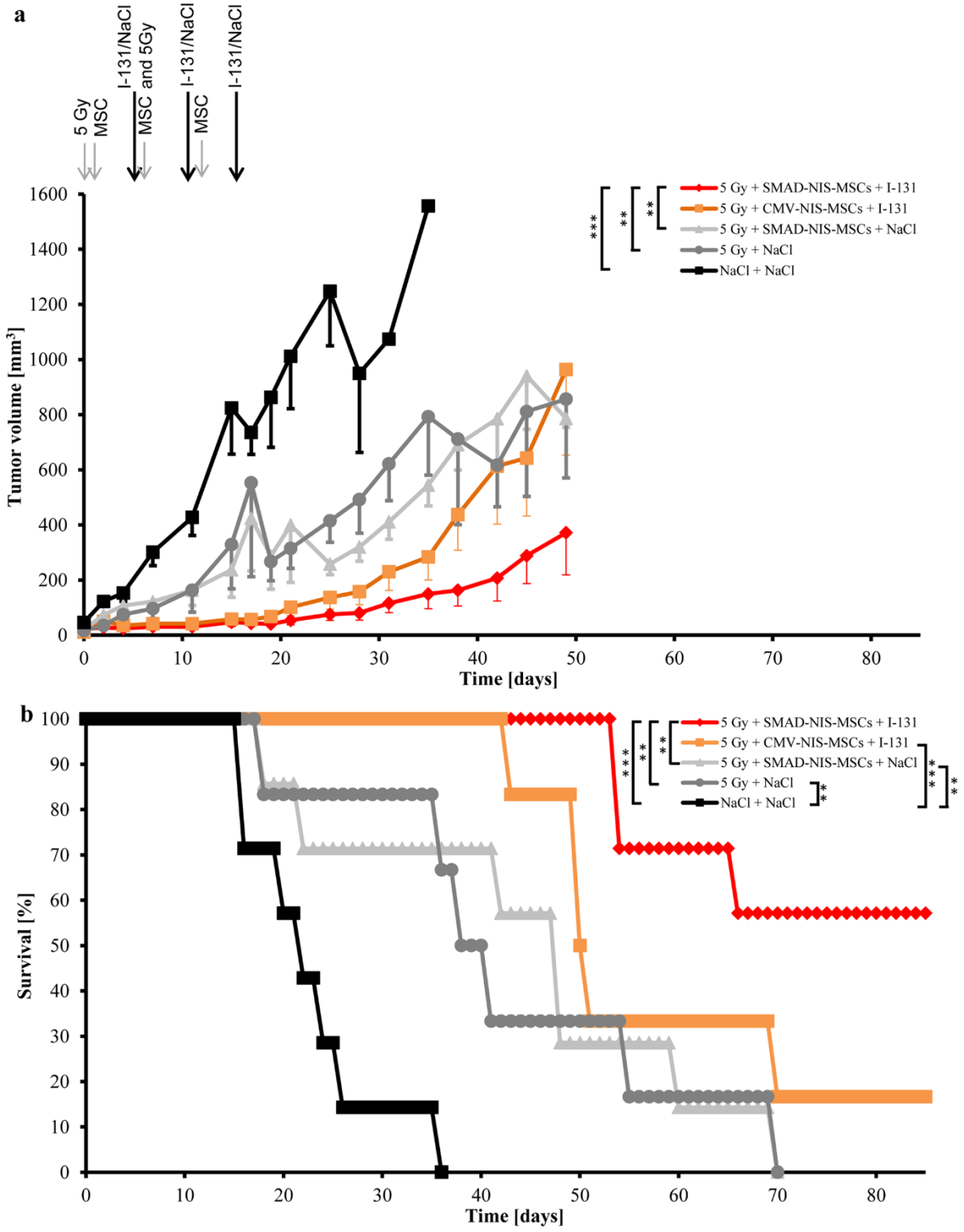

Fig. 5: *^{131}I therapy of subcutaneous HuH7 tumors led to a significant delay in tumor growth and improved survival. For an in vivo radionuclide therapy study, mice received radiation pretreatment followed by a single SMAD-NIS-MSC application and 55.5 MBq ^{131}I 48 h afterwards. This cycle was repeated, followed by a final cycle of a single SMAD-NIS-MSC application and ^{131}I (5 Gy + SMAD-NIS-MSC + I-131)* ***(a)****. Therapy of mice harboring HuH7 tumors resulted in a significant delay in tumor growth as compared to irradiated controls (5 Gy + NaCl (day 19-35, **p < 0.01) and 5 Gy + SMAD-*

*NIS-MSC + NaCl (day 25-38, **p < 0.01 and day 39-49, *p < 0.05)) or mice receiving NaCl only (NaCl + NaCl (day 2-17, ***p < 0.001 and day 18-21, **p < 0.01))* ***(a)****. Another therapy group received CMV-NIS-MSCs instead of SMAD-NIS-MSCs (5 Gy + CMV-NIS-MSCs + I-131) to evaluate the therapeutic efficacy of the tumor signal-responsive promoter. Both therapy groups demonstrated halted tumor growth at first, but CMV-NIS-treated mice developed fast tumor progression after 20 days with nearly no difference in tumor growth as compared to irradiated controls* ***(a)****. Therapy using radiation treatment in combination with SMAD-NIS-MSCs illustrated only slow tumor progression including two mice with complete tumor regression. Further, therapy mice (5 Gy + SMAD-NIS-MSC + I-131) demonstrated significantly improved overall survival after an observation period of 85 days as compared to all controls* ***(b)****.*

Radiation pretreated tumors of control mice (5 Gy + NaCl and 5 Gy + SMAD-NIS-MSCs + NaCl) led to significantly slower tumor growth as compared to the saline group (Fig. 5a) and prolonged survival up to 69 days (Fig. 5b). The therapy mice (5 Gy + SMAD-NIS-MSCs + I-131 and 5 Gy + CMV-NIS-MSCs + I-131) demonstrated significantly reduced tumor growth over that seen with radiation alone up to 20 days (Fig. 5a). After 20 days, tumors of the 5 Gy + CMV-NIS-MSCs + I-131 group started growing and nearly no difference in tumor growth was observed as compared to irradiated control groups (Fig. 5a). By contrast, 5 Gy + SMAD-NIS-MSCs + I-131 mice showed dramatically slower tumor progression after 20 days (Fig. 5a). Two mice in this group showed complete tumor regression. Therapy mice (5 Gy + SMAD-NIS-MSCs + I-131) demonstrated significantly prolonged survival as compared to all controls (Fig. 5b). Survival of the therapy groups was recorded until day 85 and observation was still ongoing at the time of this report. At this stage, 4 of 7 SMAD-NIS-MSCs-treated therapy mice (5 Gy + SMAD-NIS-MSCs + I-131) are still alive (2 mice with no tumor and 2 mice with small tumors of about 150-500 mm^3). By comparison, 1 of 6 mice from the CMV-NIS-MSC therapy group was still alive at day 85. Dissected tumors were also stained for the proliferation marker Ki67 (green) and the blood vessel marker CD31 (red) using immunofluorescence analysis (Fig. 6). In this instance, no difference was seen between the therapy groups (5 Gy + SMAD-NIS-MSCs + I-131 and 5 Gy + CMV NIS-MSCs + I-131) and mice of the controls (NaCl + NaCl, 5 Gy + NaCl or 5 Gy + SMAD-NIS-MSCs + NaCl) (Fig 6a, b, c).

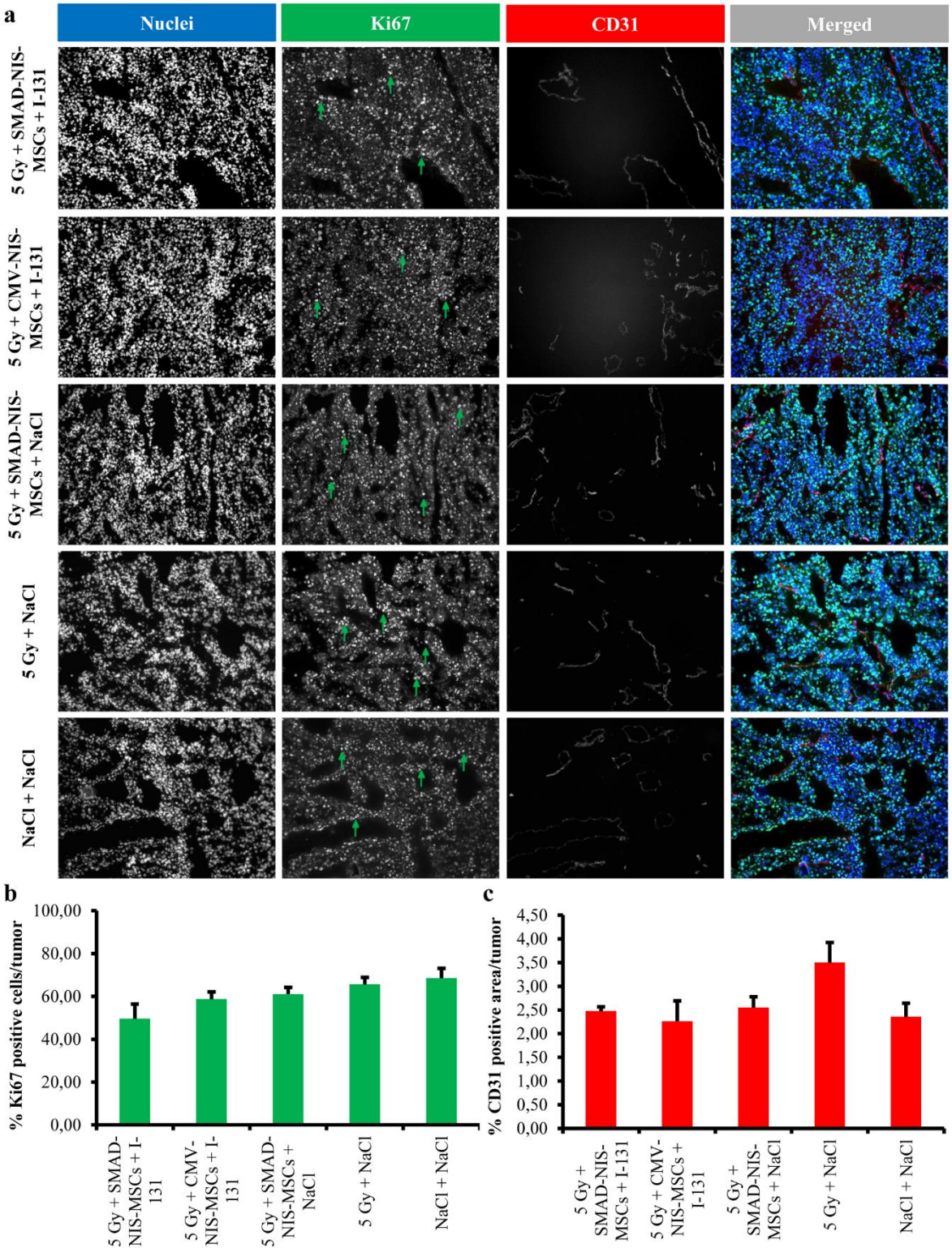

Fig. 6: *Immunofluorescence staining of proliferating cells (Ki67) and blood vessels (CD31). Immunofluorescence analysis for Ki67 (green) and CD31 (red) showed no difference in proliferation as well as blood vessel density in resected tumors of mice treated with radiation and SMAD-NIS-MSC followed by ^{131}I treatment as compared to therapy mice receiving CMV-NIS-MSCs or irradiated tumors of mice injected with SMAD-NIS-MSCs and NaCl or non-irradiated tumors receiving NaCl only* ***(a-c)****.*

Slides of tumors were counterstained with Hoechst nuclear stain and one representative image is shown each (20× magnification) ***(a)****.*

6.5 Discussion

Mesenchymal stem cells (MSCs) represent a promising tool for the delivery of therapeutic genes into tumor environments based on their strong tumor homing properties. The mechanisms underlying MSC migration to the tumor are thought to be driven by the inflammatory response of the tumor [46]. Key mediators in this scenario include inflammatory chemokines and growth factors such as the epidermal growth factor (EGF), PDGF, VEGF, CXCL12/SDF-1 and TGFB1/3 among others, which have been shown to attract MSCs [5, 47]. Irradiation of tumors has been shown to lead to an enhanced inflammatory response resulting in increased secretion of growth factors and chemokines, which in turn is associated with enhanced recruitment of MSCs [64, 65]. In a recent proof-of-principle study, our group has shown that recruitment of MSCs expressing *NIS* under control of the CMV-promoter was strongly enhanced towards subcutaneous HuH7 tumors after tumor pretreatment with low-dose radiation [129]. Radiation treatment (1-10 Gy) of HuH7 cells showed a dose-dependent increase in expression of CXCL8, CXCL12/SDF-1, FGF2, PDGFB, VEGF, TSP-1 as well as TGFB1 [129]. In addition, the combination of tumor radiation pretreatment and MSC-mediated *NIS* transgene delivery was found to result in enhanced NIS-mediated tumor-specific radioiodide accumulation as compared to non-irradiated tumors [129]. Besides the combination of a MSC-based *NIS*-mediated gene therapy approach with conventional therapies such as EBRT, a major focus of our group has been to evaluate the use of tumor-derived signal-specific promoters for *NIS* transgene activation to enhance tumor-specificity and variability regarding tumor heterogeneity. *NIS* driven by the RANTES/CCL5-promoter has been evaluated in various tumor mouse models and demonstrated improved survival of the animals as compared to the use of the unspecific CMV-promoter [57-59]. In a recent study we have shown that using tumor hypoxia for driving *NIS* transgene expression resulted in a prolonged survival of animals and a significant delay in tumor growth in an orthotopic HCC mouse model [60]. Our most recent approach of individually designed promoters, which become activated by signals of the tumor micromilieu, was the use of a TGFB1-inducible SMAD-responsive promoter [128]. In most HCC the pleiotropic factor TGFB1 is upregulated by different cells of the tumor stroma and tumor cells and is an important factor for tumor micromilieu-associated signaling [102, 107, 114]. The TGFB signaling pathway can be used to activate *NIS* transgene

expression through the TGFB1-inducible SMAD-responsive promoter in MSCs (SMAD-NIS-MSCs), where it resulted in a robust tumor-specific therapy response [128]. In parallel, we have described radiation-enhanced MSC tumor (HuH7) homing as well as increased TGFB1 expression in response to radiation [129]. Combining of enhancing MSC-mediated *NIS* gene delivery and amplifying TGFB1-inducible *NIS* expression by radiation pretreatment of tumors offers great potential to improve tumoral NIS-mediated radioiodide accumulation by taking advantage of these additive effects. *In vitro*, SMAD-NIS-MSCs demonstrated a robust and significant radioiodine uptake activity upon TGFB1 stimulation, which was significantly enhanced upon concomitant treatment with conditioned medium from HuH7 cells. A further stimulating effect was seen when conditioned medium from radiation pretreated (5 Gy) HuH7 cells was used. Further, immunohistology showed that non-irradiated HuH7 tumors had moderate TGFB1 protein expression throughout the tumor, whereas even low-dose irradiation (5 Gy) of HuH7 tumors led to increased TGFB1-specific immunoreactivity in tumors. These findings correlate with our recent data showing an enhanced and dose-dependent TGFB1 expression on mRNA as well as protein level in irradiated HuH7 cells *in vitro* [129]. Based on these results, SMAD-NIS-MSC biodistribution in irradiated subcutaneous HuH7 tumors was investigated *in vivo* using *NIS* as reporter gene. External beam radiation was used to enhance TGFB1 expression and thus increase promoter activation in SMAD-NIS-MSCs as well as to enhance their migratory potential. Tumors treated with 5 Gy radiation followed by a single application of SMAD-NIS-MSCs showed enhanced tumor-selective, TGFB1-driven induction of *NIS* that was demonstrated by high radioiodide accumulation of approximately 9.8 % ID/g tumor as compared to non-irradiated tumors (7.0 % ID/g tumor) using ^{123}I-scintigraphy. Parallel studies using the constitutively active CMV-promoter in combination with tumor irradiation revealed similar results with approximately 9.2 % ID/g tumor using 5 Gy and 5.3 % ID/g tumor in non-irradiated tumors [129]. As a next step towards clinical application, the therapeutic efficacy of combining EBRT with MSC-based, NIS-mediated radioiodine therapy was evaluated. Radiation pretreatment itself demonstrated therapeutic efficacy in control mice (5 Gy + NaCl; 5 Gy + SMAD-NIS-MSCs + NaCl) as compared to the saline only group (NaCl + NaCl). External beam radiation therapy in combination with the biologically targeted, NIS-mediated therapy (5 Gy + SMAD-NIS-MSCs + I-131) illustrated a robust therapeutic effect. Therapy mice demonstrated a

halt in tumor growth for 20-30 days with some tumors growing very slowly afterwards. Tumors of two mice within this group showed complete remission after approximately 40-50 days with no regrowth within the observation period of 85 days. The combination of external beam radiation therapy and SMAD-NIS-MSCs-mediated, NIS-induced ^{131}I therapy demonstrated significantly reduced tumor growth in therapy mice as well as significantly improved survival as compared to controls or therapy using CMV-NIS-MSCs, which at first demonstrated halted tumor growth for 3 to 4 weeks but showed tumor growth afterwards. The therapeutic effect seen was dramatically improved as compared to a ^{131}I therapy approach using SMAD-NIS-MSCs without radiation pretreatment as well as compared to all former studies of our group using MSCs as *NIS* transgene delivery vehicles [57-60, 128]. However, no difference was seen between the groups in staining proliferating cells (Ki67) or blood vessels (CD31). An explanation might be the time point at which tumors are resected and stained. The respective tumor is dissected and stained when the mouse had to be sacrificed, because the tumor has exceeded a critical volume. In the present study, mice from the therapy group as well as radiation control groups lived very long and the time between treatment and tumor resection may have been too long, allowing recovery of the tumors and rebuilding of the tumoral vasculature. To investigate the direct effects of therapy on the proliferative behavior of tumor cells and vascularization of the tumors, tumors will have to be resected and stained at earlier time points, which has to be addressed in future studies.

A critical aspect in the differences seen between the SMAD- and CMV-NIS-MSCs therapy might be the different characteristics of promoter activation. As the CMV-promoter is constitutively active, application of radioiodine effectively eliminates all MSCs present within the tumor environment that sufficiently express NIS. However, SMAD-NIS-MSCs upregulate *NIS* expression based on direct signaling from the TGFB-based tumor signal that they receive from the micromilieu and thus are at different stages of promoter activation and therefore *NIS* transgene expression at the time radioiodine is applied. So only a subset of SMAD-NIS-MSCs may become activated by TGFB1 while others remain inactivated, thus surviving the first therapy round. The SMAD-NIS-MSCs surviving the first ^{131}I course are then available to be activated in the second round of EBRT or radioiodine application, leading to a situation where SMAD-NIS-MSCs might accumulate from round to round, thus leading to the dramatic therapeutic effect seen in this study. Radiation-inducible

promoters are currently under investigation as a means to efficiently combine gene therapy with radiation treatment. These promoters normally regulate gene expression as response to the stress seen during radiation treatment and contain what can be thought of as radio-responsive elements [131]. The TGFB1-inducible SMAD-responsive promoter used in the current study makes use of an inflammatory response induced through radiation treatment leading to enhanced promoter activation and thus can be seen as an indirect but powerful radiation-inducible promoter.

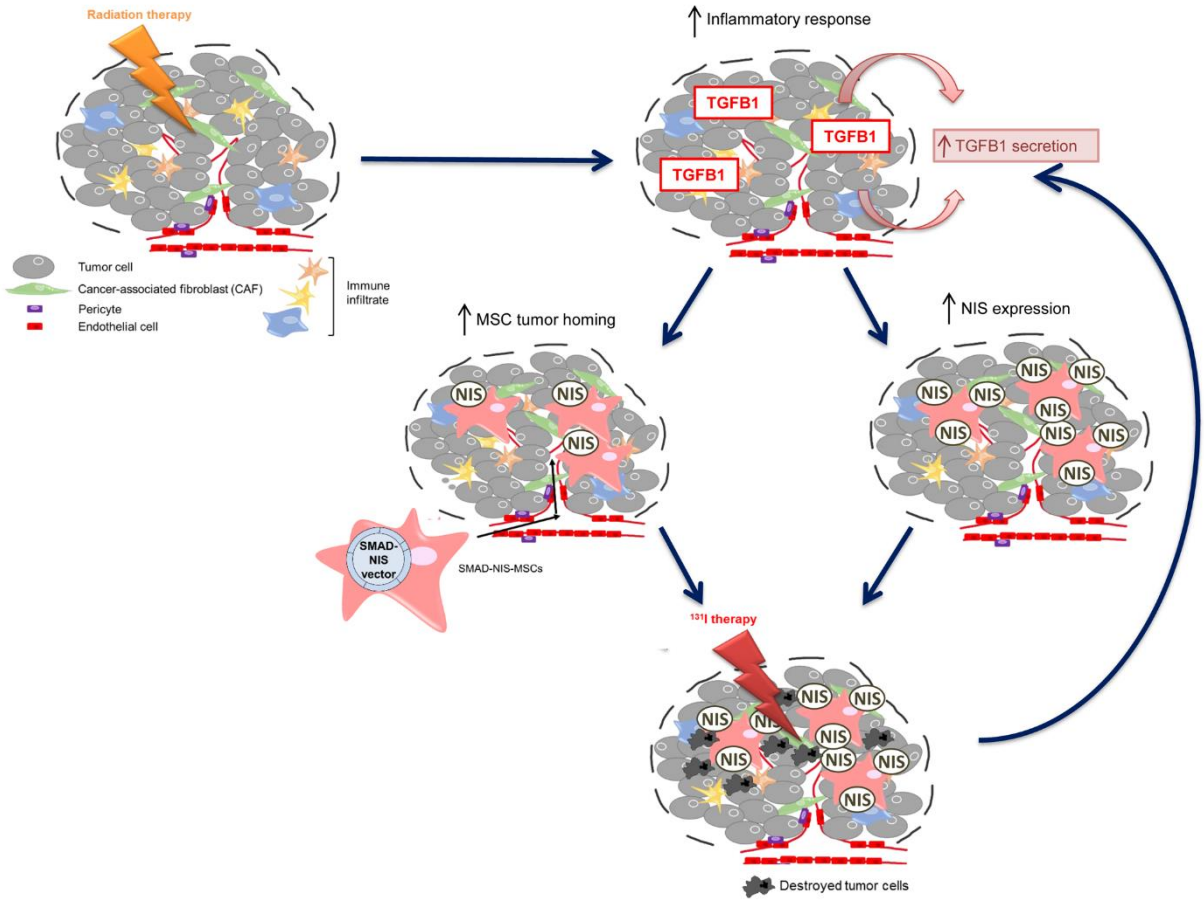

Fig. 7: *Activation cycle of SMAD-NIS-MSCs after radiation pretreatment and radioiodine therapy. Radiation pretreatment of tumors leads to an enhanced inflammatory response resulting in a strong increase of TGFB1 expression within the tumor environment. Due to this response, SMAD-NIS-MSCs show enhanced recruitment to the tumor stroma as well as increased NIS expression based on high TGFB1 levels. Radioiodine treatment then results in SMAD-NIS-MSCs-induced tumor cell destruction eliciting an inflammatory response by itself and thereby amplifying the downstream effects and leading to an even stronger effect than seen with radiation alone. The combination of repeated radiation pretreatment and SMAD-NIS-MSCs-mediated radioiodine therapy becomes a self-energizing cycle leading to the improved therapeutic efficacy of NIS-based gene therapy seen in this study.*

The radiation effect induced by application of radioiodine is also thought to enhance the inflammatory response. Thus, NIS-based radioiodine therapy could by itself lead to enhanced MSC recruitment as well as increased activation of the TGFB1, and the subsequent TGFB1-induced SMAD-promoter activity in MSCs results in prolonged *NIS* transgene expression due to repeated EBRT and radioiodine applications eventually leading to a self-energizing therapy cycle (Fig. 7).

Improved biologically-targeted and tumor-selective radioiodine accumulation demonstrated a dramatic therapeutic response by combining radiation pretreatment and NIS-mediated ^{131}I therapy. The tremendous therapeutic effect of this novel combination is based on taking advantage of the more than additive effects of radiation-induced tumor signals and tumor signal-responsive promoter activation that allows a significant amplification of tumor signal-specific *NIS* transgene expression.

The results presented here demonstrate the great potential of the TGFB1-inducible SMAD-responsive promoter to be used as a tumor-specific and radiation-inducible promoter in the context of *NIS* cancer gene therapy to both selectively control therapeutic transgene expression within the tumor environment and amplify therapeutic efficacy. These data provide exciting preclinical evidence and open the prospect of clinical translation of this highly promising combination therapy approach for highly effective TGFB1-inducible *NIS* cancer gene therapy taking advantage of the increased understanding of the tumor homing capacity of MSCs as one of the most promising and flexible systemic gene delivery approaches available to date.

6.6 Acknowledgements

We are grateful to Dr. S.M. Jhiang, Ohio State University, Columbus, OH, USA for supplying the full-length human NIS cDNA. We also thank Prof. Dr. K. Scheidhauer and Jakob Allmann, Department of Nuclear Medicine, Klinikum rechts der Isar der Technischen Universität München, Munich, Germany, for their assistance with the imaging studies. We thank Doris Mayr (Department of Pathology, LMU Munich, Munich, Germany) for preparation of paraffin-embedded slides and Marion Mielke (Department of Pathology and Comparative Experimental Pathology, Klinikum rechts der Isar der Technischen Universitaet Muenchen) for performing the immunohistochemistry. This work was supported by grants from the Deutsche Forschungsgemeinschaft within the Collaborative Research Center SFB 824 to C Spitzweg (project C8) and within the Priority Program SPP1629 to C Spitzweg and PJ Nelson (SP 581/6-1, SP 581/6-2, NE 648/5-2) as well as within a grant from the Wilhelm-Sander-Stiftung to C Spitzweg (2014.129.1).

7. Summary

The use of the theranostic sodium iodide symporter (NIS) for image-guided radioiodine therapy in non-thyroidal tumors has been extensively investigated in various tumor mouse models. The proof-of-principle of using *NIS* as a novel reporter and therapy gene has been convincingly demonstrated using different strategies for *NIS* transgene delivery, including systemic gene transfer targeting tumor metastases. The focus hereby lies in a safe application of the vectors followed by efficient transduction of tumor cells with a maximum of tumor selectivity and a minimum of off-target toxicity.

Mesenchymal stem cells (MSCs) have been developed as potent tumor therapy gene transfer vehicles based on their excellent active recruitment to both solid tumors and metastases. MSC-based NIS-mediated radioiodide therapy approaches have shown promising results in different studies, including our own work. As a next generation in the development of this system, we sought to improve the general strategy by enhancing both tumor-specificity and therapeutic efficacy.

In the course of this thesis, the potential for clinical translation of MSC-mediated *NIS* gene transfer was demonstrated by making use of an advanced clinically highly relevant tumor mouse model, by characterizing more selective tumor-associated gene promoters for driving transgene expression in engineered MSCs and finally, by combining NIS-mediated radioiodide therapy with external beam radiation therapy.

The evaluation of MSC-mediated *NIS* transgene delivery using a clinically highly relevant genetically engineered mouse model of pancreatic ductal adenocarcinoma (PDAC) helped to demonstrate the prominent preclinical efficacy of the general approach. These mice develop genetically induced aggressive pancreatic tumors and are well characterized to reliably reflect the human disease and present an ideal preclinical model for the evaluation of novel therapy approaches. In this study, we investigated the general tumor homing properties and tumor specificity of murine MSCs transfected with *NIS* linked to the constitutively active cytomegalovirus (CMV) promoter (NIS-MSCs) as well as NIS-induced radioiodide accumulation in PDAC. NIS-MSCs demonstrated high radioiodide uptake activity *in vitro* and imaging studies *in vivo* using ^{123}I-scintigraphy and ^{124}I-PET imaging revealed active MSC recruitment to tumor sites and a strong NIS-induced radioiodide accumulation specifically in PDAC. The approximate uptake of 16 % injected dose per gram tumor (ID/g) was significantly higher than that seen in earlier studies and supports the potential

efficacy of MSCs as gene delivery vehicles in more advanced tumor mouse models. The therapeutic potential was investigated by application of NIS-MSCs followed by ^{131}I, which resulted in reduced tumor growth in therapy animals, which is highly significant considering the aggressiveness of the tumor model. Further, slightly reduced tumor growth was observed in tumors receiving NIS-MSCs and saline only. Immunohistochemical analysis demonstrated differences within the stroma of tumors containing NIS-MSCs as compared to tumors without MSCs. In this setting, the presence of NIS-MSCs led to an increased activation of fibroblasts and their proliferative behavior as well as to a reconstruction of collagen within the tumor stroma, suggesting that the presence of MSCs in PDAC influences the stromal compartment in an antitumor way. This study demonstrates the enormous potential of MSC-based *NIS* transgene delivery in PDAC to monitor tumoral radioiodine accumulation by radioiodine imaging using *NIS* as reporter gene as well as a NIS-mediated ^{131}I-based therapy in PDAC.

As a next step, a novel tumor signal-specific promoter was investigated for *NIS* transgene expression in human MSCs to enhance tumor specificity and targeting variability. As the cytokine TGFB is a major player in tumorigenesis and is overexpressed in most tumors, the effect of *NIS* expression controlled by a TGFB1-inducible SMAD-responsive promoter (SMAD-NIS-MSCs) was evaluated. After *in vitro* establishment and characterization of SMAD-NIS-MSCs, which revealed high TGFB1 dose-dependent induction of radioiodide uptake, the biodistribution of SMAD-NIS-MSCs *in vivo* was determined by ^{123}I-scintigraphy monitoring. SMAD-NIS-MSCs showed effective tumor homing and *NIS* activation resulting in high tumoral radioiodide uptake in subcutaneous HuH7 tumors. These findings were confirmed by NIS-immunohistochemistry, which demonstrated tumor-specific NIS protein expression and no detection of NIS immunostaining in nontarget organs (liver, spleen, lung). Furthermore, SMAD-NIS-MSCs-mediated ^{131}I therapy resulted in strongly reduced tumor growth and prolonged survival of therapy animals. Tumor growth reduction was further confirmed by immunofluorescence analysis of Ki67 and CD31 expression showing decreased proliferating tumor cells as well as reduced density of blood vessels in therapy-treated mice. These data established a novel and effective approach for tumor-specific *NIS* gene expression taking advantage of tumor-derived signals using MSCs as gene delivery vehicles.

To study, if it would be possible to enhance the general tumor homing properties of MSCs, the effect of pretreating tumors with external beam radiation therapy (EBRT) was investigated. Extensive *in vitro* analysis by qPCR and ELISA revealed a strong increase in the secretion of factors involved in MSC tumor recruitment after tumor cell irradiation. Radiation of the human hepatocellular carcinoma cell line HuH7 using increasing doses (0-10 Gy) and at increasing time points (0-48h) showed a largely dose-dependent increase in the steady state mRNA expression of *CXCL8, CXCL12, FGF2, PDGFB, VEGF, THBS-1* as well as *TGFB1* varying in dose response and time. These results were further confirmed for most of the factors on protein level. The functional consequences of this increased cytokine production on the directed migration of MSCs was evaluated using a live cell tracking migration assay used to track changes in MSC migration after exposure to supernatants from untreated and irradiated HuH7 cells. An increase in mean forward migration index (yFMI), mean center of mass (yCoM) and mean directionality showed an enhanced chemotactic behavior of MSCs in response to irradiated supernatants. Analysis of the human breast adenocarcinoma cell line (MDA-MB-231) revealed similar results after radiation treatment. For proof-of-principle *in vivo*, subcutaneous HuH7 xenograft tumors were pretreated with radiation (0, 2 or 5 Gy) followed by a single CMV-NIS-MSC (*NIS* under control of the CMV promoter) application prior to ^{123}I-scintigraphy. ^{123}I-scintigraphy demonstrated a dose-dependent increase in NIS-mediated tumoral radioiodide accumulation in the irradiated tumors, which was further confirmed by NIS immunohistochemistry. These results highlight the enormous potential of using radiation tumor pretreatment to enhance MSC-mediated *NIS* gene transfer to tumors, which may be a powerful tool to improve therapeutic efficacy.

In the final project, taking advantage of the results of the two former studies, EBRT was combined with the SMAD-NIS-MSC-mediated therapy approach. This therapy strategy offered the possibility to apply radiation not only to improve MSC homing to tumors, but also to enhance promoter activation in SMAD-NIS-MSCs by stimulated release of TGFB1 due to radiation treatment of HuH7 cells. SMAD-NIS-MSCs demonstrated enhanced radioiodide uptake activity *in vitro* after stimulation with conditioned medium from irradiated HuH7 cells and TGFB1. Further, *ex vivo* analysis of HuH7 tumors using immunohistochemistry showed increased TGFB1 protein expression within the tumor stroma after radiation treatment as compared to nonirradiated tumors. Evaluation by ^{123}I-scintigraphy revealed a strong and improved

increase in radioiodide accumulation in subcutaneous HuH7 tumors after radiation pretreatment with 5 Gy followed by a single SMAD-NIS-MSC application. For therapy, mice received cycles of tumor radiation pretreatment followed by SMAD-NIS-MSC and ^{131}I applications. Therapy mice demonstrated significantly reduced tumor growth up to complete remission in a subset of tumors and remarkably improved survival as compared to controls, which received radiation followed by SMAD-NIS-MSCs and saline applications, radiation and saline, or saline only as treatment. In addition, the therapeutic efficacy of NIS-mediated radioiodine therapy in combination with EBRT was directly compared in mice receiving SMAD-NIS-MSCs or CMV-NIS-MSCs. Systemic application of the tumor-specific SMAD-NIS-MSCs demonstrated vastly improved therapeutic efficacy in comparison to the strong constitutive CMV-promoter used to drive *NIS* expression. The characteristics of promoter activation may have played a critical role in the therapeutic success seen in this study. MSCs transfected with the constitutive active CMV-promoter are presumably eliminated with the first application of radioiodine as these MSCs strongly express NIS. In contrast to that, SMAD-NIS-MSCs depend on the TGFB1 present in the tumor and thus may not show promoter activation (and *NIS* expression) at the time ^{131}I is applied. As a consequence, a subset of SMAD-NIS-MSCs not activated in the first therapy round survive, allowing further recruitment and accumulation of SMAD-NIS-MSCs in the tumor stroma from round to round leading to an an even more dramatic therapy effect in the following rounds. This may help explain the drastic therapeutic effect seen in SMAD-NIS-MSCs-treated mice as compared to using CMV-NIS-MSCs. Another possibility is that radioiodine application leads to an enhanced inflammatory response within the tumor. This results in a self-energizing cycle of inflammatory response (enhancing MSC recruitment) and increasing TGFB1 production (leading to an activation of the SMAD-promoter) following every round of EBRT and also NIS-mediated radioiodine therapy, resulting in the tremendous therapy effect seen. This hypothesis and the findings outlined above demonstrate the enormous potential and importance of using tumor-stroma specific promoters for *NIS* transgene expression in MSCs. The TGFB1-inducible SMAD-responsive promoter represents a powerful radiation-responsive promoter, activated by secondary events caused by radiotherapy.

In conclusion, the studies performed in this thesis dramatically refined and improved the use of genetically engineered MSCs as tumor-specific *NIS* transgene delivery

vehicles. The great potential of a MSC-driven, image-guided NIS-mediated radioiodine therapy was successfully demonstrated in an advanced genetically engineered mouse model of PDAC. This concept was further improved using a highly tumor-relevant gene promoter targeting the TGFB signaling pathway as well as combining the MSC-based *NIS* gene therapy approach with radiation therapy, which demonstrated greatly enhanced therapeutic efficacy. Ultimately, the combination of EBRT, with its effects on improved MSC tumor homing and stimulation of tumoral TGFB1 release, and TGFB1-inducible SMAD-NIS-MSCs tremendously improved the efficacy of the MSC-mediated *NIS* gene therapy approach including an amplification of MSC homing and SMAD-promoter activation induced by an additional inflammatory response triggered in the tumor by NIS-delivered radioiodine. These data open the exciting prospect for clinical translation of MSC-mediated *NIS* gene radionuclide therapy for nonthyroidal tumors and their metastases, especially in combination with external beam radiation therapy.

8. Publications

8.1 Original papers

Schug C, Kitzberger C, Sievert W, Spellerberg R, Tutter M, Schmohl KA, Schwenk N, Zach C, Schwaiger M, Multhoff G, Wagner E, Nelson PJ and Spitzweg C. Radiation-induced Amplification of TGFB1-induced Mesenchymal Stem Cell-mediated *NIS* Gene ^{131}I Therapy. [Submitted manuscript]

Schug C, Sievert W, Urnauer S, Müller AM, Schmohl KA, Wechselberger A, Schwenk N, Lauber K, Schwaiger M, Multhoff G, Nelson PJ, Spitzweg C. External beam radiation therapy enhances mesenchymal stem cell-mediated sodium iodide symporter gene delivery. Human Gene Therapy. 2018 May. [Epub ahead of print]

Schug C, Gupta A, Urnauer S, Schmohl KA, Steiger K, Trajkovic-Arsic M, Schwenk N, Schwaiger M, Nelson PJ, Siveke JT, Spitzweg C. A Novel Approach for Image-guided ^{131}I Therapy of Pancreatic Ductal Adenocarcinoma Using Mesenchymal Stem Cell-mediated NIS Gene Delivery. Molecular Cancer Research. 2018 Aug. [Epub ahead of print]; SC and AG contributed equally to this work

Schug C, Urnauer S, Jaeckel C, Schmohl KA, Tutter M, Steiger K, Schwenk N, Schwaiger M, Wagner E, Nelson PJ and Spitzweg C, TGFB1-driven induction of tumor-selective NIS transgene expression using mesenchymal stem cell-mediated gene delivery. Endocrine-Related Cancer. 2018 Aug. [Epub ahead of print]

Urnauer S, Schmohl KA, Tutter M, **Schug C**, Schwenk N, Morys S, Ziegler S, Bartenstein P, Clevert DA, Wagner E, Spitzweg C. Dual-targeting strategy for improved nonviral gene transfer of the theranostic sodium iodide symporter. [Submitted manuscript]

Schmohl KA, Dolp P, **Schug C**, Knoop K, Klutz K, Schwenk N, Bartenstein P, Nelson PJ, Ogris M, Wagner E, Spitzweg C. Reintroducing the Sodium-Iodide Symporter to Anaplastic Thyroid Carcinoma. Thyroid. 2017 Dec;27(12):1534-1543.

Urnauer S, Müller AM, **Schug C**, Schmohl KA, Tutter M, Schwenk N, Rödl W, Morys S, Ingrisch M, Bertram J, Bartenstein P, Clevert DA, Wagner E, Spitzweg C. EGFR-targeted nonviral NIS gene transfer for bioimaging and therapy of disseminated colon cancer metastases. Oncotarget. 2017 Sep 16;8(54):92195-92208.

Müller AM, Schmohl KA, Knoop K, **Schug C**, Urnauer S, Hagenhoff A, Clevert DA, Ingrisch M, Niess H, Carlsen J, Zach C, Wagner E, Bartenstein P, Nelson PJ, Spitzweg C. Hypoxia-targeted 131I therapy of hepatocellular cancer after systemic mesenchymal stem cell-mediated sodium iodide symporter gene delivery. Oncotarget. 2016 Aug 23;7(34):54795-54810.

Urnauer S, Morys S, Krhac Levacic A, Müller AM, **Schug C**, Schmohl KA, Schwenk N, Zach C, Carlsen J, Bartenstein P, Wagner E, Spitzweg C. Sequence-defined cMET/HGFR-targeted polymers as gene delivery vehicles for the theranostic sodium iodide symporter (NIS) gene. Mol Ther. 2016 Aug;24(8):1395-404.

8.2 Oral presentations

61th Annual Meeting of the German Society of Endocrinology, Bonn, Germany, March 2018. **Schug C**, Gupta A, Urnauer S, Steiger K, Cheung PFY, Neander C, Savvatakis K, Schmohl KA, Trajkovic-Arsic M, Schwenk N, Schwaiger M, Nelson PJ, Siveke JT and Spitzweg C, Mesenchymal stem cell-mediated NIS gene delivery – a novel approach for imaging-guided ^{131}I therapy of pancreatic ductal adenocarcinoma

87th Annual Meeting of the American Thyroid Association Trainee Grant Program, Victoria, Canada, October 2017. **Schug C**, Urnauer S, Schmohl KA, Tutter M, Schwenk N, Nelson PJ and Spitzweg C. TGFB1-induced radioiodine therapy of hepatocellular cancer after mesenchymal stem cell (MSC)-mediated sodium iodide symporter (NIS) gene delivery

60th Annual Meeting of the German Society of Endocrinology, Würzburg, Germany, March 2017. **Schug C**, Sievert W, Urnauer S, Müller AM, Schmohl KA, Wechselberger A, Schwenk N, Lauber K, Schwaiger M, Multhoff G, Nelson PJ, Spitzweg C. External beam radiation therapy: a promising tool to enhance mesenchymal stem cell migration towards tumors.

Gentianum Medizinische Klinik und Poliklinik IV, Fraueninsel am Chiemsee, Germany, April 2017. **Schug C**, Gupta A, Urnauer S, Schmohl KA, Steiger K, Trajkovic-Arsic M, Schwenk N, Schwaiger M, Nelson PJ, Siveke JT, Spitzweg C. Mesenchymal stem cell-mediated sodium iodide symporter (NIS) gene delivery in a mouse model of pancreatic ductal adenocarcinoma using NIS as reporter gene

15th International Thyroid Congress, Orlando, Florida, USA, October 2015. **Schug C**, Gupta A, Urnauer S, Schmohl KA, Steiger K, Trajkovic-Arsic M, Schwenk N, Schwaiger M, Nelson PJ, Siveke JT, Spitzweg C. Mesenchymal stem cell-mediated sodium iodide symporter (NIS) gene delivery in a mouse model of pancreatic ductal adenocarcinoma using NIS as reporter gene

8.3 Poster presentations

Annual Meeting of the European Society of Gen & Cell Therapy (ESGCT), Florence, Italy, October 2016 **Schug C**, Gupta A, Urnauer S, Schmohl KA, Steiger K, Trajkovic-Arsic M, Schwenk N, Schwaiger M, Nelson PJ, Siveke JT, Spitzweg C. Mesenchymal stem cell-mediated sodium iodide symporter (NIS) gene delivery in a mouse model of pancreatic ductal adenocarcinoma using NIS as reporter gene

59th Annual Meeting of the German Society of Endocrinology, Munich, Germany, May 2016. **Schug C**, Sievert W, Urnauer S, Müller AM, Schmohl KA, Wechselberger A, Schwenk N, Lauber K, Schwaiger M, Multhoff G, Nelson PJ, Spitzweg C. External beam radiation therapy: a promising tool to enhance mesenchymal stem cell migration towards tumors.

18th Congress of European Endocrinology, Munich, Germany, May 2016. **Schug C**, Sievert W, Urnauer S, Müller AM, Schmohl KA, Wechselberger A, Schwenk N, Lauber K, Schwaiger M, Multhoff G, Nelson PJ, Spitzweg C. External beam radiation therapy: a promising tool to enhance mesenchymal stem cell migration towards tumors.

8.4 Awards

Travel grant, German Society of Endocrinology
61th Annual Meeting of the German Society of Endocrinology, Bonn, Germany, March 2018. **Schug C**, Gupta A, Urnauer S, Steiger K, Cheung PFY, Neander C, Savvatakis K, Schmohl KA, Trajkovic-Arsic M, Schwenk N, Schwaiger M, Nelson PJ, Siveke JT and Spitzweg C, Mesenchymal stem cell-mediated NIS gene delivery – a novel approach for imaging-guided ^{131}I therapy of pancreatic ductal adenocarcinoma

Participation at the 87th Annual Meeting of the American Thyroid Association Trainee Grant Program, Victoria, Canada, October 2017

Travel grant, German Society of Endocrinology
87th Annual Meeting of the American Thyroid Association, Victoria, Canada, October 2017. **Schug C**, Urnauer S, Schmohl KA, Tutter M, Schwenk N, Nelson PJ and Spitzweg C. TGFB1-induced radioiodine therapy of hepatocellular cancer after mesenchymal stem cell (MSC)-mediated sodium iodide symporter (NIS) gene delivery.

Travel grant, German Society of Endocrinology
60th Annual Meeting of the German Society of Endocrinology, Würzburg, Germany, March 2017. **Schug C**, Sievert W, Urnauer S, Müller AM, Schmohl KA, Wechselberger A, Schwenk N, Lauber K, Schwaiger M, Multhoff G, Nelson PJ, Spitzweg C. External beam radiation therapy: a promising tool to enhance mesenchymal stem cell migration towards tumors.

Travel grant, German Society of Endocrinology
15th International Thyroid Congress, Orlando, Florida, USA, October 2015. **Schug C**, Gupta A, Urnauer S, Schmohl KA, Steiger K, Trajkovic-Arsic M, Schwenk N, Schwaiger M, Nelson PJ, Siveke JT, Spitzweg C. Mesenchymal stem cell-mediated sodium iodide symporter (NIS) gene delivery in a mouse model of pancreatic ductal adenocarcinoma using NIS as reporter gene

9. References

1. Siegel RL, Miller KD, Jemal A. Cancer Statistics, 2017. CA Cancer J Clin. 2017; 67: 7-30. doi: 10.3322/caac.21387.

2. Stewart BWW, C. P. World Cancer Report 2014. International Agency for Research on Cancer. 2014: 1-632. doi:

3. Hanahan D, Weinberg RA. Hallmarks of cancer: the next generation. Cell. 2011; 144: 646-74. doi: 10.1016/j.cell.2011.02.013.

4. Dvorak HF. Tumors: wounds that do not heal. Similarities between tumor stroma generation and wound healing. N Engl J Med. 1986; 315: 1650-9. doi: 10.1056/nejm198612253152606.

5. Droujinine IA, Eckert MA, Zhao W. To grab the stroma by the horns: from biology to cancer therapy with mesenchymal stem cells. Oncotarget. 2013; 4: 651-64. doi: 10.18632/oncotarget.1040.

6. Li H, Fan X, Houghton J. Tumor microenvironment: the role of the tumor stroma in cancer. J Cell Biochem. 2007; 101: 805-15. doi: 10.1002/jcb.21159.

7. Bremnes RM, Dønnem T, Al-Saad S, Al-Shibli K, Andersen S, Sirera R, Camps C, Marinez I, Busund L-T. The Role of Tumor Stroma in Cancer Progression and Prognosis: Emphasis on Carcinoma-Associated Fibroblasts and Non-small Cell Lung Cancer. Journal of Thoracic Oncology. 2011; 6: 209-17. doi: https://doi.org/10.1097/JTO.0b013e3181f8a1bd.

8. Balkwill FR, Capasso M, Hagemann T. The tumor microenvironment at a glance. J Cell Sci. 2012; 125: 5591-6. doi: 10.1242/jcs.116392.

9. Erez N, Truitt M, Olson P, Arron ST, Hanahan D. Cancer-Associated Fibroblasts Are Activated in Incipient Neoplasia to Orchestrate Tumor-Promoting Inflammation in an NF-kappaB-Dependent Manner. Cancer Cell. 2010; 17: 135-47. doi: 10.1016/j.ccr.2009.12.041.

10. Orimo A, Gupta PB, Sgroi DC, Arenzana-Seisdedos F, Delaunay T, Naeem R, Carey VJ, Richardson AL, Weinberg RA. Stromal fibroblasts present in invasive human breast carcinomas promote tumor growth and angiogenesis through elevated SDF-1/CXCL12 secretion. Cell. 2005; 121: 335-48. doi: 10.1016/j.cell.2005.02.034.

11. Urruticoechea A, Alemany R, Balart J, Villanueva A, Vinals F, Capella G. Recent advances in cancer therapy: an overview. Curr Pharm Des. 2010; 16: 3-10. doi:

12. Cross D, Burmester JK. Gene therapy for cancer treatment: past, present and future. Clin Med Res. 2006; 4: 218-27. doi:

13. Eccles SA. The epidermal growth factor receptor/Erb-B/HER family in normal and malignant breast biology. Int J Dev Biol. 2011; 55: 685-96. doi: 10.1387/ijdb.113396se.

14. Touchefeu Y, Harrington KJ, Galmiche JP, Vassaux G. Review article: gene therapy, recent developments and future prospects in gastrointestinal oncology. Aliment Pharmacol Ther. 2010; 32: 953-68. doi: 10.1111/j.1365-2036.2010.04424.x.

15. Fillat C, Carrio M, Cascante A, Sangro B. Suicide gene therapy mediated by the Herpes Simplex virus thymidine kinase gene/Ganciclovir system: fifteen years of application. Curr Gene Ther. 2003; 3: 13-26. doi:

16. Wang J, Lu XX, Chen DZ, Li SF, Zhang LS. Herpes simplex virus thymidine kinase and ganciclovir suicide gene therapy for human pancreatic cancer. World J Gastroenterol. 2004; 10: 400-3. doi:

17. Nayerossadat N, Maedeh T, Ali PA. Viral and nonviral delivery systems for gene delivery. Adv Biomed Res. 2012; 1: 27. doi: 10.4103/2277-9175.98152.

18. Alotaibi H, Tuzlakoglu-Ozturk M, Tazebay UH. The Thyroid Na+/I- Symporter: Molecular Characterization and Genomic Regulation. Mol Imaging Radionucl Ther. 2017; 26: 92-101. doi: 10.4274/2017.26.suppl.11.

19. Ravera S, Reyna-Neyra A, Ferrandino G, Amzel LM, Carrasco N. The Sodium/Iodide Symporter (NIS): Molecular Physiology and Preclinical and Clinical Applications. Annu Rev Physiol. 2017; 79: 261-89. doi: 10.1146/annurev-physiol-022516-034125.

20. Spitzweg C, Morris JC. The sodium iodide symporter: its pathophysiological and therapeutic implications. Clin Endocrinol (Oxf). 2002; 57: 559-74. doi:

21. Penheiter AR, Russell SJ, Carlson SK. The sodium iodide symporter (NIS) as an imaging reporter for gene, viral, and cell-based therapies. Curr Gene Ther. 2012; 12: 33-47. doi:

22. Baril P, Martin-Duque P, Vassaux G. Visualization of gene expression in the live subject using the Na/I symporter as a reporter gene: applications in biotherapy. Br J Pharmacol. 2010; 159: 761-71. doi: 10.1111/j.1476-5381.2009.00412.x.

23. Hingorani M, Spitzweg C, Vassaux G, Newbold K, Melcher A, Pandha H, Vile R, Harrington K. The biology of the sodium iodide symporter and its potential for targeted gene delivery. Curr Cancer Drug Targets. 2010; 10: 242-67. doi:

24. Dai G, Levy O, Carrasco N. Cloning and characterization of the thyroid iodide transporter. Nature. 1996; 379: 458-60. doi: 10.1038/379458a0.

25. Shimura H, Haraguchi K, Miyazaki A, Endo T, Onaya T. Iodide uptake and experimental 131I therapy in transplanted undifferentiated thyroid cancer cells expressing the Na+/I- symporter gene. Endocrinology. 1997; 138: 4493-6. doi: 10.1210/endo.138.10.5571.

26. Portulano C, Paroder-Belenitsky M, Carrasco N. The Na+/I- symporter (NIS): mechanism and medical impact. Endocr Rev. 2014; 35: 106-49. doi: 10.1210/er.2012-1036.

27. Spitzweg C, Dietz AB, O'Connor MK, Bergert ER, Tindall DJ, Young CY, Morris JC. In vivo sodium iodide symporter gene therapy of prostate cancer. Gene Ther. 2001; 8: 1524-31. doi: 10.1038/sj.gt.3301558.

28. Klutz K, Willhauck MJ, Wunderlich N, Zach C, Anton M, Senekowitsch-Schmidtke R, Goke B, Spitzweg C. Sodium iodide symporter (NIS)-mediated radionuclide ((131)I, (188)Re) therapy of liver cancer after transcriptionally targeted intratumoral in vivo NIS gene delivery. Hum Gene Ther. 2011; 22: 1403-12. doi: 10.1089/hum.2010.158.

29. Trujillo MA, Oneal MJ, McDonough S, Qin R, Morris JC. A probasin promoter, conditionally replicating adenovirus that expresses the sodium iodide symporter (NIS) for radiovirotherapy of prostate cancer. Gene Ther. 2010; 17: 1325-32. doi: 10.1038/gt.2010.63.

30. Grunwald GK, Klutz K, Willhauck MJ, Schwenk N, Senekowitsch-Schmidtke R, Schwaiger M, Zach C, Goke B, Holm PS, Spitzweg C. Sodium iodide symporter (NIS)-mediated radiovirotherapy of hepatocellular cancer using a conditionally replicating adenovirus. Gene Ther. 2013; 20: 625-33. doi: 10.1038/gt.2012.79.

31. Dingli D, Peng KW, Harvey ME, Greipp PR, O'Connor MK, Cattaneo R, Morris JC, Russell SJ. Image-guided radiovirotherapy for multiple myeloma using a recombinant measles virus expressing the thyroidal sodium iodide symporter. Blood. 2004; 103: 1641-6. doi: 10.1182/blood-2003-07-2233.

32. Goel A, Carlson SK, Classic KL, Greiner S, Naik S, Power AT, Bell JC, Russell SJ. Radioiodide imaging and radiovirotherapy of multiple myeloma using VSV(Delta51)-NIS, an attenuated vesicular stomatitis virus encoding the sodium iodide symporter gene. Blood. 2007; 110: 2342-50. doi: 10.1182/blood-2007-01-065573.

33. Grunwald GK, Vetter A, Klutz K, Willhauck MJ, Schwenk N, Senekowitsch-Schmidtke R, Schwaiger M, Zach C, Wagner E, Goke B, Holm PS, Ogris M, Spitzweg C. Systemic image-guided liver cancer radiovirotherapy using dendrimer-coated adenovirus encoding the sodium iodide symporter as theranostic gene. J Nucl Med. 2013; 54: 1450-7. doi: 10.2967/jnumed.112.115493.

34. Grunwald GK, Vetter A, Klutz K, Willhauck MJ, Schwenk N, Senekowitsch-Schmidtke R, Schwaiger M, Zach C, Wagner E, Goke B, Holm PS, Ogris M, Spitzweg C. EGFR-Targeted Adenovirus Dendrimer Coating for Improved Systemic Delivery of the Theranostic NIS Gene. Mol Ther Nucleic Acids. 2013; 2: e131. doi: 10.1038/mtna.2013.58.

35. Raper SE, Chirmule N, Lee FS, Wivel NA, Bagg A, Gao GP, Wilson JM, Batshaw ML. Fatal systemic inflammatory response syndrome in a ornithine transcarbamylase deficient patient following adenoviral gene transfer. Mol Genet Metab. 2003; 80: 148-58. doi:

36. Klutz K, Russ V, Willhauck MJ, Wunderlich N, Zach C, Gildehaus FJ, Goke B, Wagner E, Ogris M, Spitzweg C. Targeted radioiodine therapy of neuroblastoma tumors following systemic nonviral delivery of the sodium iodide symporter gene. Clin Cancer Res. 2009; 15: 6079-86. doi: 10.1158/1078-0432.ccr-09-0851.

37. Klutz K, Willhauck MJ, Dohmen C, Wunderlich N, Knoop K, Zach C, Senekowitsch-Schmidtke R, Gildehaus FJ, Ziegler S, Furst S, Goke B, Wagner E, Ogris M, et al. Image-guided tumor-selective radioiodine therapy of liver cancer after systemic nonviral delivery of the sodium iodide symporter gene. Hum Gene Ther. 2011; 22: 1563-74. doi: 10.1089/hum.2011.041.

38. Klutz K, Schaffert D, Willhauck MJ, Grunwald GK, Haase R, Wunderlich N, Zach C, Gildehaus FJ, Senekowitsch-Schmidtke R, Goke B, Wagner E, Ogris M, Spitzweg C. Epidermal growth factor receptor-targeted (131)I-therapy of liver cancer following systemic delivery of the sodium iodide symporter gene. Mol Ther. 2011; 19: 676-85. doi: 10.1038/mt.2010.296.

39. Schmohl KA, Gupta A, Grunwald GK, Trajkovic-Arsic M, Klutz K, Braren R, Schwaiger M, Nelson PJ, Ogris M, Wagner E, Siveke JT, Spitzweg C. Imaging and targeted therapy of pancreatic ductal adenocarcinoma using the theranostic sodium iodide symporter (NIS) gene. Oncotarget. 2017. doi: 10.18632/oncotarget.16499.

40. Urnauer S, Muller AM, Schug C, Schmohl KA, Tutter M, Schwenk N, Rodl W, Morys S, Ingrisch M, Bertram J, Bartenstein P, Clevert DA, Wagner E, et al. EGFR-

targeted nonviral NIS gene transfer for bioimaging and therapy of disseminated colon cancer metastases. Oncotarget. 2017; 8: 92195-208. doi: 10.18632/oncotarget.21028.

41. Urnauer S, Morys S, Krhac Levacic A, Muller AM, Schug C, Schmohl KA, Schwenk N, Zach C, Carlsen J, Bartenstein P, Wagner E, Spitzweg C. Sequence-defined cMET/HGFR-targeted Polymers as Gene Delivery Vehicles for the Theranostic Sodium Iodide Symporter (NIS) Gene. Mol Ther. 2016; 24: 1395-404. doi: 10.1038/mt.2016.95.

42. Uchibori R, Tsukahara T, Ohmine K, Ozawa K. Cancer gene therapy using mesenchymal stem cells. Int J Hematol. 2014; 99: 377-82. doi: 10.1007/s12185-014-1537-7.

43. Li Z, Fan D, Xiong D. Mesenchymal stem cells as delivery vectors for anti-tumor therapy. Stem Cell Investig. 2015; 2: 6. doi: 10.3978/j.issn.2306-9759.2015.03.01.

44. Wong RS. Mesenchymal stem cells: angels or demons? J Biomed Biotechnol. 2011; 2011: 459510. doi: 10.1155/2011/459510.

45. Hagenhoff A, Bruns CJ, Zhao Y, von Luttichau I, Niess H, Spitzweg C, Nelson PJ. Harnessing mesenchymal stem cell homing as an anticancer therapy. Expert Opin Biol Ther. 2016; 16: 1079-92. doi: 10.1080/14712598.2016.1196179.

46. Melzer C, Yang Y, Hass R. Interaction of MSC with tumor cells. Cell Commun Signal. 2016; 14: 20. doi: 10.1186/s12964-016-0143-0.

47. Spaeth E, Klopp A, Dembinski J, Andreeff M, Marini F. Inflammation and tumor microenvironments: defining the migratory itinerary of mesenchymal stem cells. Gene Ther. 2008; 15: 730-8. doi: 10.1038/gt.2008.39.

48. Tang C, Russell PJ, Martiniello-Wilks R, Rasko JE, Khatri A. Concise review: Nanoparticles and cellular carriers-allies in cancer imaging and cellular gene therapy? Stem Cells. 2010; 28: 1686-702. doi: 10.1002/stem.473.

49. Studeny M, Marini FC, Champlin RE, Zompetta C, Fidler IJ, Andreeff M. Bone marrow-derived mesenchymal stem cells as vehicles for interferon-beta delivery into tumors. Cancer Res. 2002; 62: 3603-8. doi:

50. Conrad C, Husemann Y, Niess H, von Luettichau I, Huss R, Bauer C, Jauch KW, Klein CA, Bruns C, Nelson PJ. Linking transgene expression of engineered mesenchymal stem cells and angiopoietin-1-induced differentiation to target cancer angiogenesis. Ann Surg. 2011; 253: 566-71. doi: 10.1097/SLA.0b013e3181fcb5d8.

51. Niess H, Bao Q, Conrad C, Zischek C, Notohamiprodjo M, Schwab F, Schwarz B, Huss R, Jauch KW, Nelson PJ, Bruns CJ. Selective targeting of genetically engineered mesenchymal stem cells to tumor stroma microenvironments using tissue-specific suicide gene expression suppresses growth of hepatocellular carcinoma. Ann Surg. 2011; 254: 767-74; discussion 74-5. doi: 10.1097/SLA.0b013e3182368c4f.

52. Zischek C, Niess H, Ischenko I, Conrad C, Huss R, Jauch KW, Nelson PJ, Bruns C. Targeting tumor stroma using engineered mesenchymal stem cells reduces the growth of pancreatic carcinoma. Ann Surg. 2009; 250: 747-53. doi: 10.1097/SLA.0b013e3181bd62d0.

53. von Einem JC, Peter S, Gunther C, Volk HD, Grutz G, Salat C, Stoetzer O, Nelson PJ, Michl M, Modest DP, Holch JW, Angele M, Bruns C, et al. Treatment of advanced gastrointestinal cancer with genetically modified autologous mesenchymal stem cells - TREAT-ME-1 - a phase I, first in human, first in class trial. Oncotarget. 2017; 8: 80156-66. doi: 10.18632/oncotarget.20964.

54. Li L, Guan Y, Liu H, Hao N, Liu T, Meng X, Fu C, Li Y, Qu Q, Zhang Y, Ji S, Chen L, Chen D, et al. Silica nanorattle-doxorubicin-anchored mesenchymal stem cells for tumor-tropic therapy. ACS Nano. 2011; 5: 7462-70. doi: 10.1021/nn202399w.

55. Sadhukha T, O'Brien TD, Prabha S. Nano-engineered mesenchymal stem cells as targeted therapeutic carriers. J Control Release. 2014; 196: 243-51. doi: 10.1016/j.jconrel.2014.10.015.

56. Dwyer RM, Ryan J, Havelin RJ, Morris JC, Miller BW, Liu Z, Flavin R, O'Flatharta C, Foley MJ, Barrett HH, Murphy JM, Barry FP, O'Brien T, et al. Mesenchymal Stem Cell-mediated delivery of the sodium iodide symporter supports radionuclide imaging and treatment of breast cancer. Stem Cells. 2011; 29: 1149-57. doi: 10.1002/stem.665.

57. Knoop K, Kolokythas M, Klutz K, Willhauck MJ, Wunderlich N, Draganovici D, Zach C, Gildehaus FJ, Boning G, Goke B, Wagner E, Nelson PJ, Spitzweg C. Image-guided, tumor stroma-targeted 131I therapy of hepatocellular cancer after systemic mesenchymal stem cell-mediated NIS gene delivery. Mol Ther. 2011; 19: 1704-13. doi: 10.1038/mt.2011.93.

58. Knoop K, Schwenk N, Dolp P, Willhauck MJ, Zischek C, Zach C, Hacker M, Goke B, Wagner E, Nelson PJ, Spitzweg C. Stromal targeting of sodium iodide

symporter using mesenchymal stem cells allows enhanced imaging and therapy of hepatocellular carcinoma. Hum Gene Ther. 2013; 24: 306-16. doi: 10.1089/hum.2012.104.

59. Knoop K, Schwenk N, Schmohl K, Muller A, Zach C, Cyran C, Carlsen J, Boning G, Bartenstein P, Goke B, Wagner E, Nelson PJ, Spitzweg C. Mesenchymal stem cell-mediated, tumor stroma-targeted radioiodine therapy of metastatic colon cancer using the sodium iodide symporter as theranostic gene. J Nucl Med. 2015; 56: 600-6. doi: 10.2967/jnumed.114.146662.

60. Muller AM, Schmohl KA, Knoop K, Schug C, Urnauer S, Hagenhoff A, Clevert DA, Ingrisch M, Niess H, Carlsen J, Zach C, Wagner E, Bartenstein P, et al. Hypoxia-targeted 131I therapy of hepatocellular cancer after systemic mesenchymal stem cell-mediated sodium iodide symporter gene delivery. Oncotarget. 2016. doi: 10.18632/oncotarget.10758.

61. Garcia MG, Bayo J, Bolontrade MF, Sganga L, Malvicini M, Alaniz L, Aquino JB, Fiore E, Rizzo MM, Rodriguez A, Lorenti A, Andriani O, Podhajcer O, et al. Hepatocellular carcinoma cells and their fibrotic microenvironment modulate bone marrow-derived mesenchymal stromal cell migration in vitro and in vivo. Mol Pharm. 2011; 8: 1538-48. doi: 10.1021/mp200137c.

62. Day CP, Merlino G, Van Dyke T. Preclinical mouse cancer models: a maze of opportunities and challenges. Cell. 2015; 163: 39-53. doi: 10.1016/j.cell.2015.08.068.

63. Francois S, Bensidhoum M, Mouiseddine M, Mazurier C, Allenet B, Semont A, Frick J, Sache A, Bouchet S, Thierry D, Gourmelon P, Gorin NC, Chapel A. Local irradiation not only induces homing of human mesenchymal stem cells at exposed sites but promotes their widespread engraftment to multiple organs: a study of their quantitative distribution after irradiation damage. Stem Cells. 2006; 24: 1020-9. doi: 10.1634/stemcells.2005-0260.

64. Kim SM, Oh JH, Park SA, Ryu CH, Lim JY, Kim DS, Chang JW, Oh W, Jeun SS. Irradiation enhances the tumor tropism and therapeutic potential of tumor necrosis factor-related apoptosis-inducing ligand-secreting human umbilical cord blood-derived mesenchymal stem cells in glioma therapy. Stem Cells. 2010; 28: 2217-28. doi: 10.1002/stem.543.

65. Klopp AH, Spaeth EL, Dembinski JL, Woodward WA, Munshi A, Meyn RE, Cox JD, Andreeff M, Marini FC. Tumor irradiation increases the recruitment of circulating

mesenchymal stem cells into the tumor microenvironment. Cancer Res. 2007; 67: 11687-95. doi: 10.1158/0008-5472.can-07-1406.

66. Spitzweg C, Zhang S, Bergert ER, Castro MR, McIver B, Heufelder AE, Tindall DJ, Young CY, Morris JC. Prostate-specific antigen (PSA) promoter-driven androgen-inducible expression of sodium iodide symporter in prostate cancer cell lines. Cancer Res. 1999; 59: 2136-41. doi:

67. Kim HJ, Jeon YH, Kang JH, Lee YJ, Kim KI, Chung HK, Jeong JM, Lee DS, Lee MC, Chung JK. In vivo long-term imaging and radioiodine therapy by sodium-iodide symporter gene expression using a lentiviral system containing ubiquitin C promoter. Cancer Biol Ther. 2007; 6: 1130-5. doi:

68. Schmohl KA, Muller AM, Wechselberger A, Ruhland S, Salb N, Schwenk N, Heuer H, Carlsen J, Goke B, Nelson PJ, Spitzweg C. Thyroid hormones and tetrac: new regulators of tumour stroma formation via integrin alphavbeta3. Endocr Relat Cancer. 2015; 22: 941-52. doi: 10.1530/erc-15-0245.

69. Zielske SP, Livant DL, Lawrence TS. Radiation increases invasion of gene-modified mesenchymal stem cells into tumors. Int J Radiat Oncol Biol Phys. 2009; 75: 843-53. doi: 10.1016/j.ijrobp.2008.06.1953.

70. Singh M, Lima A, Molina R, Hamilton P, Clermont AC, Devasthali V, Thompson JD, Cheng JH, Bou Reslan H, Ho CC, Cao TC, Lee CV, Nannini MA, et al. Assessing therapeutic responses in Kras mutant cancers using genetically engineered mouse models. Nat Biotechnol. 2010; 28: 585-93. doi: 10.1038/nbt.1640.

71. Narayanan V, Weekes CD. Molecular therapeutics in pancreas cancer. World J Gastrointest Oncol. 2016; 8: 366-79. doi: 10.4251/wjgo.v8.i4.366.

72. Siegel RL, Miller KD, Jemal A. Cancer statistics, 2016. CA Cancer J Clin. 2016; 66: 7-30. doi: 10.3322/caac.21332.

73. Hingorani SR, Petricoin EF, Maitra A, Rajapakse V, King C, Jacobetz MA, Ross S, Conrads TP, Veenstra TD, Hitt BA, Kawaguchi Y, Johann D, Liotta LA, et al. Preinvasive and invasive ductal pancreatic cancer and its early detection in the mouse. Cancer Cell. 2003; 4: 437-50. doi:

74. Izeradjene K, Combs C, Best M, Gopinathan A, Wagner A, Grady WM, Deng CX, Hruban RH, Adsay NV, Tuveson DA, Hingorani SR. Kras(G12D) and Smad4/Dpc4 haploinsufficiency cooperate to induce mucinous cystic neoplasms and invasive adenocarcinoma of the pancreas. Cancer Cell. 2007; 11: 229-43. doi: 10.1016/j.ccr.2007.01.017.

75. Mazur PK, Siveke JT. Genetically engineered mouse models of pancreatic cancer: unravelling tumour biology and progressing translational oncology. Gut. 2012; 61: 1488-500. doi: 10.1136/gutjnl-2011-300756.

76. Siveke JT, Schmid RM. Chromosomal instability in mouse metastatic pancreatic cancer--it's Kras and Tp53 after all. Cancer Cell. 2005; 7: 405-7. doi: 10.1016/j.ccr.2005.04.025.

77. Bardeesy N, Aguirre AJ, Chu GC, Cheng KH, Lopez LV, Hezel AF, Feng B, Brennan C, Weissleder R, Mahmood U, Hanahan D, Redston MS, Chin L, et al. Both p16(Ink4a) and the p19(Arf)-p53 pathway constrain progression of pancreatic adenocarcinoma in the mouse. Proc Natl Acad Sci U S A. 2006; 103: 5947-52. doi: 10.1073/pnas.0601273103.

78. Schneider G, Siveke JT, Eckel F, Schmid RM. Pancreatic cancer: basic and clinical aspects. Gastroenterology. 2005; 128: 1606-25. doi:

79. Siveke JT, Einwachter H, Sipos B, Lubeseder-Martellato C, Kloppel G, Schmid RM. Concomitant pancreatic activation of Kras(G12D) and Tgfa results in cystic papillary neoplasms reminiscent of human IPMN. Cancer Cell. 2007; 12: 266-79. doi: 10.1016/j.ccr.2007.08.002.

80. Trajkovic-Arsic M, Heid I, Steiger K, Gupta A, Fingerle A, Worner C, Teichmann N, Sengkwawoh-Lueong S, Wenzel P, Beer AJ, Esposito I, Braren R, Siveke JT. Apparent Diffusion Coefficient (ADC) predicts therapy response in pancreatic ductal adenocarcinoma. Sci Rep. 2017; 7: 17038. doi: 10.1038/s41598-017-16826-z.

81. Von Luttichau I, Notohamiprodjo M, Wechselberger A, Peters C, Henger A, Seliger C, Djafarzadeh R, Huss R, Nelson PJ. Human adult CD34- progenitor cells functionally express the chemokine receptors CCR1, CCR4, CCR7, CXCR5, and CCR10 but not CXCR4. Stem Cells Dev. 2005; 14: 329-36. doi: 10.1089/scd.2005.14.329.

82. Kawaguchi Y, Cooper B, Gannon M, Ray M, MacDonald RJ, Wright CV. The role of the transcriptional regulator Ptf1a in converting intestinal to pancreatic progenitors. Nat Genet. 2002; 32: 128-34. doi: 10.1038/ng959.

83. Marino S, Vooijs M, van Der Gulden H, Jonkers J, Berns A. Induction of medulloblastomas in p53-null mutant mice by somatic inactivation of Rb in the external granular layer cells of the cerebellum. Genes Dev. 2000; 14: 994-1004. doi:

84. Spitzweg C, Baker CH, Bergert ER, O'Connor MK, Morris JC. Image-guided radioiodide therapy of medullary thyroid cancer after carcinoembryonic antigen promoter-targeted sodium iodide symporter gene expression. Hum Gene Ther. 2007; 18: 916-24. doi: 10.1089/hum.2007.081.

85. Rahib L, Smith BD, Aizenberg R, Rosenzweig AB, Fleshman JM, Matrisian LM. Projecting cancer incidence and deaths to 2030: the unexpected burden of thyroid, liver, and pancreas cancers in the United States. Cancer Res. 2014; 74: 2913-21. doi: 10.1158/0008-5472.CAN-14-0155.

86. Von Hoff DD, Ervin T, Arena FP, Chiorean EG, Infante J, Moore M, Seay T, Tjulandin SA, Ma WW, Saleh MN, Harris M, Reni M, Dowden S, et al. Increased survival in pancreatic cancer with nab-paclitaxel plus gemcitabine. N Engl J Med. 2013; 369: 1691-703. doi: 10.1056/NEJMoa1304369.

87. Conroy T, Desseigne F, Ychou M, Bouche O, Guimbaud R, Becouarn Y, Adenis A, Raoul JL, Gourgou-Bourgade S, de la Fouchardiere C, Bennouna J, Bachet JB, Khemissa-Akouz F, et al. FOLFIRINOX versus gemcitabine for metastatic pancreatic cancer. N Engl J Med. 2011; 364: 1817-25. doi: 10.1056/NEJMoa1011923.

88. Cousin B, Ravet E, Poglio S, De Toni F, Bertuzzi M, Lulka H, Touil I, Andre M, Grolleau JL, Peron JM, Chavoin JP, Bourin P, Penicaud L, et al. Adult stromal cells derived from human adipose tissue provoke pancreatic cancer cell death both in vitro and in vivo. PLoS One. 2009; 4: e6278. doi: 10.1371/journal.pone.0006278.

89. Khakoo AY, Pati S, Anderson SA, Reid W, Elshal MF, Rovira, II, Nguyen AT, Malide D, Combs CA, Hall G, Zhang J, Raffeld M, Rogers TB, et al. Human mesenchymal stem cells exert potent antitumorigenic effects in a model of Kaposi's sarcoma. J Exp Med. 2006; 203: 1235-47. doi: 10.1084/jem.20051921.

90. Kidd S, Caldwell L, Dietrich M, Samudio I, Spaeth EL, Watson K, Shi Y, Abbruzzese J, Konopleva M, Andreeff M, Marini FC. Mesenchymal stromal cells alone or expressing interferon-beta suppress pancreatic tumors in vivo, an effect countered by anti-inflammatory treatment. Cytotherapy. 2010; 12: 615-25. doi: 10.3109/14653241003631815.

91. Nakamura K, Ito Y, Kawano Y, Kurozumi K, Kobune M, Tsuda H, Bizen A, Honmou O, Niitsu Y, Hamada H. Antitumor effect of genetically engineered mesenchymal stem cells in a rat glioma model. Gene Ther. 2004; 11: 1155-64. doi: 10.1038/sj.gt.3302276.

92. Ozdemir BC, Pentcheva-Hoang T, Carstens JL, Zheng X, Wu CC, Simpson TR, Laklai H, Sugimoto H, Kahlert C, Novitskiy SV, De Jesus-Acosta A, Sharma P, Heidari P, et al. Depletion of carcinoma-associated fibroblasts and fibrosis induces immunosuppression and accelerates pancreas cancer with reduced survival. Cancer Cell. 2014; 25: 719-34. doi: 10.1016/j.ccr.2014.04.005.

93. Rhim AD, Oberstein PE, Thomas DH, Mirek ET, Palermo CF, Sastra SA, Dekleva EN, Saunders T, Becerra CP, Tattersall IW, Westphalen CB, Kitajewski J, Fernandez-Barrena MG, et al. Stromal elements act to restrain, rather than support, pancreatic ductal adenocarcinoma. Cancer Cell. 2014; 25: 735-47. doi: 10.1016/j.ccr.2014.04.021.

94. Waghray M, Yalamanchili M, Dziubinski M, Zeinali M, Erkkinen M, Yang H, Schradle KA, Urs S, Pasca Di Magliano M, Welling TH, Palmbos PL, Abel EV, Sahai V, et al. GM-CSF Mediates Mesenchymal-Epithelial Cross-talk in Pancreatic Cancer. Cancer Discov. 2016; 6: 886-99. doi: 10.1158/2159-8290.Cd-15-0947.

95. von Ahrens D, Bhagat TD, Nagrath D, Maitra A, Verma A. The role of stromal cancer-associated fibroblasts in pancreatic cancer. J Hematol Oncol. 2017; 10: 76. doi: 10.1186/s13045-017-0448-5.

96. Ahn SJ, Jeon YH, Lee YJ, Lee YL, Lee SW, Ahn BC, Ha JH, Lee J. Enhanced anti-tumor effects of combined MDR1 RNA interference and human sodium/iodide symporter (NIS) radioiodine gene therapy using an adenoviral system in a colon cancer model. Cancer Gene Ther. 2010; 17: 492-500. doi: 10.1038/cgt.2010.3.

97. Dwyer RM, Bergert ER, O'Connor MK, Gendler SJ, Morris JC. Adenovirus-mediated and targeted expression of the sodium-iodide symporter permits in vivo radioiodide imaging and therapy of pancreatic tumors. Hum Gene Ther. 2006; 17: 661-8. doi: 10.1089/hum.2006.17.661.

98. Huang R, Zhao Z, Ma X, Li S, Gong R, Kuang A. Targeting of tumor radioiodine therapy by expression of the sodium iodide symporter under control of the survivin promoter. Cancer Gene Ther. 2011; 18: 144-52. doi: 10.1038/cgt.2010.66.

99. Mansfield DC, Kyula JN, Rosenfelder N, Chao-Chu J, Kramer-Marek G, Khan AA, Roulstone V, McLaughlin M, Melcher AA, Vile RG, Pandha HS, Khoo V, Harrington KJ. Oncolytic vaccinia virus as a vector for therapeutic sodium iodide symporter gene therapy in prostate cancer. Gene Ther. 2016; 23: 357-68. doi: 10.1038/gt.2016.5.

100. Niu G, Gaut AW, Ponto LL, Hichwa RD, Madsen MT, Graham MM, Domann FE. Multimodality noninvasive imaging of gene transfer using the human sodium iodide symporter. J Nucl Med. 2004; 45: 445-9. doi:

101. Peerlinck I, Merron A, Baril P, Conchon S, Martin-Duque P, Hindorf C, Burnet J, Quintanilla M, Hingorani M, Iggo R, Lemoine NR, Harrington K, Vassaux G. Targeted radionuclide therapy using a Wnt-targeted replicating adenovirus encoding the Na/I symporter. Clin Cancer Res. 2009; 15: 6595-601. doi: 10.1158/1078-0432.ccr-09-0262.

102. Neuzillet C, Tijeras-Raballand A, Cohen R, Cros J, Faivre S, Raymond E, de Gramont A. Targeting the TGFbeta pathway for cancer therapy. Pharmacol Ther. 2015; 147: 22-31. doi: 10.1016/j.pharmthera.2014.11.001.

103. Derynck R, Akhurst RJ, Balmain A. TGF-beta signaling in tumor suppression and cancer progression. Nat Genet. 2001; 29: 117-29. doi: 10.1038/ng1001-117.

104. Massague J. TGF-beta signal transduction. Annu Rev Biochem. 1998; 67: 753-91. doi: 10.1146/annurev.biochem.67.1.753.

105. Wrana JL, Attisano L, Wieser R, Ventura F, Massague J. Mechanism of activation of the TGF-beta receptor. Nature. 1994; 370: 341-7. doi: 10.1038/370341a0.

106. Breuhahn K, Longerich T, Schirmacher P. Dysregulation of growth factor signaling in human hepatocellular carcinoma. Oncogene. 2006; 25: 3787-800. doi: 10.1038/sj.onc.1209556.

107. Lopez-Novoa JM, Nieto MA. Inflammation and EMT: an alliance towards organ fibrosis and cancer progression. EMBO Mol Med. 2009; 1: 303-14. doi: 10.1002/emmm.200900043.

108. Massague J. TGFbeta in Cancer. Cell. 2008; 134: 215-30. doi: 10.1016/j.cell.2008.07.001.

109. Abou-Shady M, Baer HU, Friess H, Berberat P, Zimmermann A, Graber H, Gold LI, Korc M, Buchler MW. Transforming growth factor betas and their signaling receptors in human hepatocellular carcinoma. Am J Surg. 1999; 177: 209-15. doi:

110. Bedossa P, Peltier E, Terris B, Franco D, Poynard T. Transforming growth factor-beta 1 (TGF-beta 1) and TGF-beta 1 receptors in normal, cirrhotic, and neoplastic human livers. Hepatology. 1995; 21: 760-6. doi:

111. Thalmeier K, Huss R. Highly efficient retroviral gene transfer into immortalized CD34(-) cells and organ distribution after transplantation into NOD/SCID mice. Cytotherapy. 2001; 3: 245-51. doi: 10.1080/146532401317070871.

112. Jackel C, Nogueira MS, Ehni N, Kraus C, Ranke J, Dohmann M, Noessner E, Nelson PJ. A vector platform for the rapid and efficient engineering of stable complex transgenes. Sci Rep. 2016; 6: 34365. doi: 10.1038/srep34365.

113. Capece D, Fischietti M, Verzella D, Gaggiano A, Cicciarelli G, Tessitore A, Zazzeroni F, Alesse E. The inflammatory microenvironment in hepatocellular carcinoma: a pivotal role for tumor-associated macrophages. Biomed Res Int. 2013; 2013: 187204. doi: 10.1155/2013/187204.

114. Yang JD, Nakamura I, Roberts LR. The tumor microenvironment in hepatocellular carcinoma: current status and therapeutic targets. Semin Cancer Biol. 2011; 21: 35-43. doi: 10.1016/j.semcancer.2010.10.007.

115. Papageorgis P, Stylianopoulos T. Role of TGFbeta in regulation of the tumor microenvironment and drug delivery (review). Int J Oncol. 2015; 46: 933-43. doi: 10.3892/ijo.2015.2816.

116. Biswas S, Guix M, Rinehart C, Dugger TC, Chytil A, Moses HL, Freeman ML, Arteaga CL. Inhibition of TGF-beta with neutralizing antibodies prevents radiation-induced acceleration of metastatic cancer progression. J Clin Invest. 2007; 117: 1305-13. doi: 10.1172/jci30740.

117. Schug C, Wechselberger A, Urnauer S, Schmohl K, Muller AM, Schwenk N, Lauber K, Nelson PJ, Spitzweg C. (2016). External beam radiation therapy: a promising tool to enhance mesenchymal stem cell migration towards tumors. (Endocrine Abstracts.

118. Tabatabai G, Frank B, Mohle R, Weller M, Wick W. Irradiation and hypoxia promote homing of haematopoietic progenitor cells towards gliomas by TGF-beta-dependent HIF-1alpha-mediated induction of CXCL12. Brain. 2006; 129: 2426-35. doi: 10.1093/brain/awl173.

119. Gao Y, Zhou Z, Lu S, Huang X, Zhang C, Jiang R, Yao A, Sun B, Wang X. Chemokine CCL15 Mediates Migration of Human Bone Marrow-Derived Mesenchymal Stem Cells Toward Hepatocellular Carcinoma. Stem Cells. 2016; 34: 1112-22. doi: 10.1002/stem.2275.

120. Schmidt A, Ladage D, Schinkothe T, Klausmann U, Ulrichs C, Klinz FJ, Brixius K, Arnhold S, Desai B, Mehlhorn U, Schwinger RH, Staib P, Addicks K, et al. Basic

fibroblast growth factor controls migration in human mesenchymal stem cells. Stem Cells. 2006; 24: 1750-8. doi: 10.1634/stemcells.2005-0191.

121. Barker HE, Paget JT, Khan AA, Harrington KJ. The tumour microenvironment after radiotherapy: mechanisms of resistance and recurrence. Nat Rev Cancer. 2015; 15: 409-25. doi: 10.1038/nrc3958.

122. Langley RE, Bump EA, Quartuccio SG, Medeiros D, Braunhut SJ. Radiation-induced apoptosis in microvascular endothelial cells. Br J Cancer. 1997; 75: 666-72. doi:

123. Kioi M, Vogel H, Schultz G, Hoffman RM, Harsh GR, Brown JM. Inhibition of vasculogenesis, but not angiogenesis, prevents the recurrence of glioblastoma after irradiation in mice. J Clin Invest. 2010; 120: 694-705. doi: 10.1172/jci40283.

124. Lerman OZ, Greives MR, Singh SP, Thanik VD, Chang CC, Seiser N, Brown DJ, Knobel D, Schneider RJ, Formenti SC, Saadeh PB, Levine JP. Low-dose radiation augments vasculogenesis signaling through HIF-1-dependent and -independent SDF-1 induction. Blood. 2010; 116: 3669-76. doi: 10.1182/blood-2009-03-213629.

125. Park HJ, Griffin RJ, Hui S, Levitt SH, Song CW. Radiation-induced vascular damage in tumors: implications of vascular damage in ablative hypofractionated radiotherapy (SBRT and SRS). Radiat Res. 2012; 177: 311-27. doi:

126. Dingli D, Russell SJ, Morris JC, 3rd. In vivo imaging and tumor therapy with the sodium iodide symporter. J Cell Biochem. 2003; 90: 1079-86. doi: 10.1002/jcb.10714.

127. Bernier J, Hall EJ, Giaccia A. Radiation oncology: a century of achievements. Nat Rev Cancer. 2004; 4: 737-47. doi: 10.1038/nrc1451.

128. Schug C, Urnauer S, Jackel C, Schmohl KA, Tutter M, Steiger K, Schwenk N, Schwaiger M, Wagner E, Nelson PJ, Spitzweg C. TGFB1-driven mesenchymal stem cell-mediated NIS gene transfer. Endocr Relat Cancer. 2018. doi: 10.1530/erc-18-0173.

129. Schug C, Sievert W, Urnauer S, Muller AM, Schmohl KA, Wechselberger A, Schwenk N, Lauber K, Schwaiger M, Multhoff G, Wagner E, Nelson PJ, Spitzweg C. External Beam Radiation Therapy Enhances Mesenchymal Stem Cell-Mediated Sodium-Iodide Symporter Gene Delivery. Hum Gene Ther. 2018. doi: 10.1089/hum.2018.025.

130. Willhauck MJ, Sharif Samani BR, Gildehaus FJ, Wolf I, Senekowitsch-Schmidtke R, Stark HJ, Goke B, Morris JC, Spitzweg C. Application of 188rhenium

as an alternative radionuclide for treatment of prostate cancer after tumor-specific sodium iodide symporter gene expression. J Clin Endocrinol Metab. 2007; 92: 4451-8. doi: 10.1210/jc.2007-0402.

131. Ogawa R, Morii A, Watanabe A, Cui ZG, Kagiya G, Fukuda S, Kume K, Hasegawa T, Hatashita M, Izumi H, Ishimoto T, Feril LB, Jr. Development of a therapeutically important radiation induced promoter. Bioengineered. 2013; 4: 44-9. doi: 10.4161/bioe.21965.

10. Acknowledgments

It has been an intensive period of my life and I would like to reflect on all the people, who have supported me, and thank them for their great help throughout the last years.

First, I would like to express my sincere gratitude to my supervisor Prof. Dr. Christine Spitzweg for giving me the opportunity to work on these exciting projects and to be part of her research group. I am very grateful for providing me with all the equipment needed and for her excellent supervision as well as continuous scientific support during all these years. Without her guidance and persistent help this thesis would have not been possible.

I would also like to thank Prof. Dr. Ernst Wagner for accepting me as an external PhD student. I am very grateful for his helpful advices and insightful discussions. Also all his lab members are gratefully acknowledged for their help.

Further, I am very grateful to Prof. Dr. Peter J. Nelson for his persistent help and scientific support whenever needed. I am thankful for the great collaboration and all the fruitful discussions we had. Many thanks to all the members of his lab.

Many thanks to the whole Spitzweg lab for supporting me all these years and making me always smile. It was such a good time with many laughs, incredible travels and interesting discussions. Special thanks to Sarah for her continuous support and the time we had together. I would like to thank Mariella for all the fun we had during scintigraphy imagings. Many thanks to Katy for proof-reading everything and not being mad when I “lent” her calculator again. Additionally, I would like to express my deepest thankfulness to Nathalie for always helping me and providing me with my daily Milchschnitte. Also, I would like to thank Andrea for teaching me everything when I started. Furthermore, many thanks to our newest members Carolin, Rebekka and Yang for all the laughs we had in the last few months.

Further, I would like to thank the members of the department of Nuclear Medicine at the Klinikum rechts der Isar (director: Prof. Dr. Wolfgang Weber and former director:

Prof. Dr. Markus Schwaiger) for their great support and technical assistance during imaging and therapy studies.

Special thanks to Prof. Dr. Gabriele Multhoff and Dr. Wolfgang Sievert for the great collaboration, for helping me with my external beam radiation projects and making everything possible.

I would like to thank Prof. Dr. Jens T. Siveke and his group members for providing us with the PDAC mouse model and Aayush Gupta for performing all the MR imagings with me.

I am also very grateful to the members of the SFB824 for their great collaboration.

I want to thank all my friends for having an “open ear” and always being there when needed.

Finally, I owe my deepest gratitude to my family. Thank you, Mum, Gel and Dadi for your constant support, love and encouragement. Thank you, Frieder for being on my side, for helping me through stressful times and not letting me give up.
You all never stopped believing in me and my thesis would have not been possible without you.